NASA

INVESTIGATION OF CONTINUOUSLY TRAVERSING MICROPHONE SYSTEM FOR MODE MEASUREMENT

by

D.E. Cicon, T.G. Sofrin and D.C. Mathews

November 1982

Prepared for

1. REPORT NO. NASA-CR-168040	2. GOVERNMENT AGENCY	3. RECIPIENT'S CATALOG NO.
4. TITLE AND SUBTITLE INVESTIGATION OF CONTINUOUSLY TRAVERSING MICROPHONE SYSTEM FOR MODE MEASUREMENT		5. REPORT DATE November 1982
		6. PERFORMING ORG. CODE
7. AUTHOR(S) D.E. Cicon, T.G. Sofrin and D.C. Mathews		8. PERFORMING ORG. REPT. NO. PWA-5846-26
9. PERFORMING ORG. NAME AND ADDRESS UNITED TECHNOLOGIES CORPORATION Pratt & Whitney Aircraft Group Commercial Engineering East Hartford, CT 06108		10. WORK UNIT NO.
		11. CONTRACT OR GRANT NO. NAS3-23168
12. SPONSORING AGENCY NAME AND ADDRESS National Aeronautics and Space Administration Lewis Research Center 21000 Brookpark Road, Cleveland, Ohio 44135		13. TYPE REPT./PERIOD COVERED Final Report
		14. SPONSORING AGENCY CODE

16. ABSTRACT

The continuously Traversing Microphone System consists of a data acquisition and processing method for obtaining the modal coefficients of the discrete, coherent acoustic field in a fan inlet duct. The system would be used in fan rigs or full-scale engine installations where present measurement methods, because of the excessive number of microphones and long test times required, are not feasible. The purpose of the investigation reported here was to develop a method for defining modal structure by means of a continuously traversing microphone system and to perform an evaluation of the method, based upon analytical studies and computer-simulated tests. A variety of system parameters were examined, and the effects of deviations from ideal were explored. Effects of traverse speed, digitizing rate, run time, roundoff error, calibration errors, and random noise background level were determined.

For constant fan operating speed, the sensitivity of the method to normal errors and deviations was determined to be acceptable. Good recovery of mode coefficients was attainable. Fluctuating fan speed conditions received special attention, and it was concluded that by employing suitable time delay procedures, satisfactory information on mode coefficients can be obtained under realistic conditions.

A plan for further development, involving fan rig tests, was prepared.

17. KEY WORDS (SUGGESTED BY AUTHOR(S)) Fan Sound Mode Measurements Continuously Traversing Microphone Computer-Simulated Tests Analytical Evaluation	18. DISTRIBUTION STATEMENT Unclassified - Unlimited	
19. SECURITY CLASS THIS (REPT) Unclassified	20. SECURITY CLASS THIS (PAGE) Unclasified	21. NO. PGS 133	22. PRICE *

TABLE OF CONTENTS

TABLE OF CONTENTS (Cont'd)

LIST OF ILLUSTRATIONS

LIST OF TABLES

LIST OF TABLES (Cont'd)

INVESTIGATION OF CONTINUOUSLY TRAVERSING MICROPHONE SYSTEM
FOR MODE MEASUREMENT

by

D.E. Cicon, T.G. Sofrin and D.C. Mathews

United Technologies Corporation
Pratt & Whitney Aircraft Group
Commercial Engineering

1.0 SUMMARY

The continuously Traversing Microphone System consists of a novel data acquisition, data processing method for obtaining the modal coefficients of the discrete, coherent acoustic field in a fan inlet duct. The system is intended for use in fan rigs or full-scale engine installations where present measurement methods involving impractical numbers of microphones and long test times are not feasible.

The purpose of the investigation reported here was to develop a method for defining modal structure by means of a continuously traversing microphone system and to perform an evaluation of the method, based upon analytical studies and computer-simulated tests. A further requirement of the investigation was to prepare a plan for further development of the method that would lead to a practical operational method for full-scale engine use.

In the course of this program, a variety of system parameters were examined, and the effects of deviations from ideal operating conditions were explored by analytical methods and by running simulated tests using computer-generated data in place of actual test microphone data. Effects of traverse speed, digitizing rate, run time, roundoff error, calibration errors, and random noise background level were determined.

It was found that for constant fan operating speed, the sensitivity of the method to normal errors and deviations was acceptable. Good recovery of mode coefficients was attainable without imposing unrealistic requirements on the system operating characteristics.

The subject of operation under fluctuating fan speed conditions received special attention, since speed variations have long been recognized as a source of inaccuracy in all mode measurement systems. It was found that when highly propagating modes are measured close to their source, the effects of fan speed variation are negligible. For modes closer to cutoff and/or measured farther from their source, fan speed variations can seriously affect measurement of their strengths.

However, a relatively simple modification of the basic Traversing Microphone System was devised to counter the adverse effects of speed fluctuation. This modification involves using a time delay in the data processing phase of the system to match the acoustic time delay between the time when the rotor speed changes and when it is received at the microphone. Even though the acoustic delay time varies among the propagating modes, use of a single compensating average delay in the data processing results in marked improvement.

Based on results of these speed variation studies, it was concluded that the Traversing Microphone Method, employing suitable time delay procedures, can obtain satisfactory information on mode coefficients under realistic full-scale engine operating conditions.

In view of the favorable evaluation of the Traversing Microphone Method, based on results of these analytical and computer-simulated studies, an appropriate plan for further development was evolved. This plan includes refinement of the compensating time delay modification and details for guiding the selection of a fan rig and test program so that the system can be fabricated and checked out under actual test conditions.

2.0 INTRODUCTION

2.1 BACKGROUND

Knowledge of the modal structure of fan noise plays an important part in the development of quiet powerplants. For example, identification of the precise source of fan discrete tones in a new engine under development (which points the way to the appropriate design) is greatly enhanced if the associated mode can be defined. In another illustration, where engine modifications are tested, the effects of these modifications may be obscured unless changes in the appropriate modes are isolated. In the area of sound-absorbing fan duct liners, design of the liner is facilitated by knowledge of both frequency distribution and mode structure of the noise field to be attenuated.

Despite the importance of mode measurement capability and the duration of this requirement for over twenty years, no practical method for obtaining suitable mode measurements on full-scale engines has been demonstrated. On small, experimental fan rigs, on the other hand, where the number of propagating modes is limited, successful mode measurements have been made since the earliest fan noise investigations. Comparable success with full scale engines and large rigs has not been attained.

Many methods have been explored in pursuit of this goal, a sample of which may be found in ref. 1 through 10. The primary reason that these methods have been unsuccessful in full-scale applications is the very large number of microphones or microphone locations required to measure the corresponding high number of propagating modes. If only a limited number of such modes were of interest, the microphone requirement would still be excessive because of the need to isolate the limited modes from the total number present. To overcome this problem of impractically large quantity of microphones, procedures have been examined where a smaller number have been successively positioned in the duct at the larger number of required locations. Such procedures are prohibitively time-consuming for full-scale tests. Further problems arise when microphone-holding rakes penetrate the duct and generate wakes that interact with the rotor, creating spurious interaction noise.

The Traversing Microphone System was conceived as a method to overcome these problems. It consists, basically of a single radial rake, mounting a small number of microphones, which is rotated continuously at relatively slow speed during the data acquisition run. Tape recorded microphone data together with fan shaft and traverse shaft position data are then processed to give as many modal coefficients as are required. By this method, the number of microphones is reduced to a practical value and the test time is kept within feasible limits.

This report is an account of the development of the Traversing Microphone System and an analytical and computer-aided evaluation of the system.

3

2.2 PROGRAM DESCRIPTION

An account of the basic features of the Traversing Microphone System is given in Section 3. The section also presents an analysis of the extraneous noise generated when the wake of the microphone rake is cut by the fan and shows how this noise is isolated by the system so as to not contaminate the desired modal coefficients.

Section 4 gives the computing algorithms used in data reduction to generate the required mode coefficients. This program did not involve actual tests on a fan rig. Instead, data that would be generated by test were simulated for processing by the traverse system. The data to be analyzed were generated in a simulation program, which is also described in Section 4. This computer-simulated test procedure allows very close comparisons to be made between known modes that are used to make up the synthesized acoustic field and the corresponding values that result from application of the Traversing Microphone Method.

Sections 5 and 6 present a detailed account of the system characteristics, as determined by analytical studies and the computer-simulated tests. Section 5 deals with selection of design parameters and the effects of deviations from ideal operating conditions, such as measurement errors and random noise. These effects are examined under constant fan speed operating conditions. The effects of small variations in fan speed, a major problem in all fan noise measurements, are treated in Section 6.

The results reported and summarized in Sections 5 and 6, comprise an evaluation of the Traversing Microphone System. A plan for further development of the system is presented in Section 7.

The conduct of the work performed in this investigation was divided into contractual tasks as a logical means of describing and monitoring the course of the program. The format of this report, outlined above, was chosen to present as clear a picture as possible of the principles and features of the Traversing Microphone Method. In order to provide a bridge between the contract Statement of Work (S.O.W) task designation and the section in this report where the corresponding work is described, the following cross-reference listing is provided for convenience:

Contract (S.O.W.) Task Designation		Task Description	Report Section
Task 1,	Part 1	Development of Mode Coefficient Algorithm	4.1, 4.2, 4.3
	Part 2	Analytical Studies of System Characteristics	5, 6
	Part 3	Develop Computer Program for Mode Coefficients	4.1, 4.2 4.3, B
Task 2,	Part 1	Develop Computer Program to Simulate Test Data	4.4, B
	Part 2	Computer Simulated Test and Method Evaluation	5, 6
	Part 3	Plan for Further Development	7

4

3.0 PRINCIPLES OF THE CIRCUMFERENTIALLY TRAVERSING MICROPHONE METHOD

3.1 BASIS OF THE METHOD

There are several closely related ways of describing or interpreting the continuous circumferential traversing method for mode extraction. The viewpoint adopted here is, first, to recall the procedure used to obtain the amplitude spectrum of a particular class of coherent time signals and, second, to demonstrate that the time signal of a circumferentially traversing microphone is a function of the circumferential mode structure at the axial and radial location of the microphone in the fan duct. A final step, not unique to the traverse method, is needed to resolve the circumferential mode structure at each microphone radius into its radial mode constituents.

3.1.1 Analysis of a Class of Time Signals

Consider a general rotating machine having a drive shaft turning at speed Ω (rad/sec). Depending on details, a variety of vibration or acoustic signals can be generated at angular frequencies $\omega_1, \omega_2 \ldots \omega_k$. These components are constant, not necessarily integer, multiples of the single basic shaft frequency: $\omega_1 = g_1\Omega, \omega_2 = g_2\Omega \ldots \omega_k = g_k\Omega$, where the g_k are called "orders".

For such a machine, the vibratory or acoustic time signal at some location may be written

$$p(t) = \mathrm{Re}\sum_k C_k \, \mathrm{expi} -\omega_k t = \sum_k \frac{C_k}{2} \, \mathrm{expi} -\omega_k t + \sum_k \frac{C_k^\star}{2} \, \mathrm{expi}\, \omega_k t \qquad (3\text{-}1)$$

(The negative argument of the exponential is used here in anticipation of the conventional description of forward waves in an acoustic field.)

From a recording of $p(t)$ it is required to determine the complex (amplitude and phase) coefficients, C_k. Suppose that, in addition to $p(t)$, there is available on another channel a corresponding recording of drive shaft angle $\gamma = \Omega t$, and suppose we wish to first extract from $p(t)$ the specific "target" coefficient C_K corresponding to $k = K$.

This may be done by computing from the shaft angle signal, Ωt, a complex target signal $V_K(t) = \mathrm{expi}\,\omega_K t = \mathrm{expi}(g_K \Omega t)$, multiplying this by $p(t)$, and averaging over a time interval, T. The result will be a transform of $p(t)$ defined as

$$\mathrm{Tr}\{p(t)\} = \frac{1}{T}\int_0^T p(t)\,\mathrm{expi}(g_k \Omega t)dt \qquad (3\text{-}2)$$

On substituting the series representation for p(t)

$$Tr\left\{p(t)\right\} = \sum_k \frac{c_k}{2} \quad \frac{1}{T}\int_0^T expi\ [(g_K - g_k)\Omega t]dt + \tag{3-3}$$

$$\sum_k \frac{c_k^*}{2} \quad \frac{1}{T}\int_0^T expi\ [(g_K + g_k)\Omega t]dt$$

For the single component of p(t) corresponding to k = K, the target signal, the integrand in the first series is unity and the resulting time average is $c_K/2$. All other terms in both series have oscillatory integrands. The resulting integrals will vanish if the integration time corresponds to an integer number of cycles, but this feature is not essential. Because of the time-averaging feature, the contributions from such terms may be reduced to acceptably small levels by use of a suitably long averaging time, T. These extraneous contributions to the transform of p(t), called residual terms, are discussed in some detail later.

The result of this processing of the pressure signal is thus

$$Tr\left\{p(t)\right\} = \frac{1}{T}\int_0^T p(t)\ expi(g_K\Omega t)dt \tag{3-4}$$

$$= \frac{c_K}{2} + residual\ terms$$

With the understanding that the residual terms can be made as small as we please by taking T large enough, there follows the expressions for computing a typical target coefficient

$$c_K = 2Tr\left\{p(t)\right\} \tag{3-5}$$

By repeating this process for values of K corresponding to frequencies or orders of interest, the components of p(t) may be determined.

An important feature of this type of transform is that small variations in drive shaft speed, Ω, are accommodated since they are reflected in proportional changes of the p(t) components as well as the target signal. The integrand, expi $[(g_K-g_k)\Omega t]$ remains unity for k = K whether Ω is constant or not. For variable speed, Ωt is replaced by the measured shaft angle

$$\gamma(t) = \int_0^t \Omega(t)dt$$

6

To conform with the fact that the target signal, V, is formed from direct measurement of shaft angle, γ, rather than measurement of shaft speed, Ω, and since this distinction is an important, advantageous feature of the method, the transform, eq. (3-2), is better expressed in the more general form

$$Tr\{p(t)\} = \frac{1}{T} \int_0^T p(t) \exp i [g_K \gamma(t)] dt \tag{3-o}$$

For speed variations normally encountered in practice, as with the constant speed case, it is shown later that the "residual terms" can be reduced to satisfactory levels so that the coefficient, C_K is still given by eq. (3-5).

It will be recognized that the process defined by eq. (3-6) is analogous to a tracking filter where the tracking signal frequency is a selected multiple, g_K, of the shaft frequency. Because the process gives the coefficient corresponding to a selected multiple of shaft frequency rather than a specific fixed frequency, it may be called an "order" transform.

The foregoing gives the essentials of the procedure for analyzing a class of coherent time signals in general. It will now be shown how the acoustic mode structure of fan noise can be made to correspond to a time signal having properties that allow the order transform to be employed effectively.

3.1.2 Time Signal of Traversing Microphone

The expressions for the behavior of the coherent fan noise field in a duct are well known. However, for the purpose of introducing the basic features of the circumferentially traversing microphone system it is best to restrict attention to the acoustic pressure at a fixed radial location in a fixed transverse plane (perpendicular to the duct axis), and to describe the acoustic pressure there in terms of two variables: angular location, θ, and time, t. The resulting expression is simply

$$p(\theta, t) = \text{Re} \sum_m \sum_n C_m^n \exp i (m\theta - n\Omega t) \tag{3-7}$$

Here m is the circumferential wave number (with positive integer values corresponding to forward spinning modes and negative numbers indicating reverse spin). Ω is shaft speed (assumed constant initially), and n is an integer giving the harmonic or order with respect to shaft speed. n is restricted here to positive integer values, the most important by far corresponding to fan blade-passage harmonics: n = B, n = 2B, etc., where B is the number of fan blades.

The complex circumferential mode coefficient, C_m^n, gives amplitude and phase at order n of the m-mode pattern at the radial location and transverse plane of the microphone.

The traversing microphone system that will be used to measure the pressure field is shown schematically in Figure 3-1. Several microphones are disposed radially along a rake assembly that rotates in a circumferential direction at angular speed Γ. The expression for the pressure, eq. (3-7), applies to any one typical microphone radius.
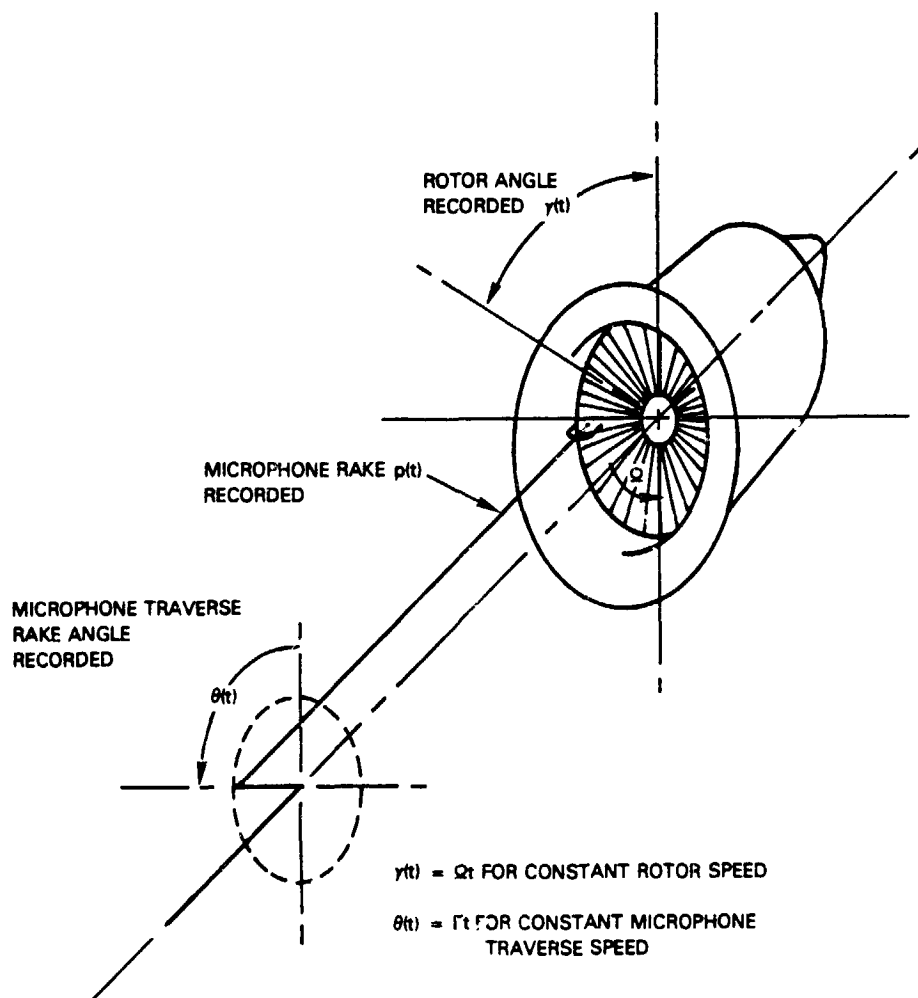
Figure 3-1   Schematic of Traversing Microphone System

The signal sensed by a typical microphone is obtained by replacing θ in eq. (3-7) by Γt to give

8

$$p(t) = p(\theta = \Gamma t, t) = Re \sum_m \sum_n C_m^n \, expi \, (m\Gamma - n\Omega)t \qquad (3-8)$$

$$\text{or} \quad p(t) = Re \sum_m \sum_n C_m^n \, expi \, -\omega_m^n t \qquad (3-9)$$

$$\text{where} \quad \omega_m^n = (n\Omega - m\Gamma) \qquad (3-10)$$

is the circular frequency, sensed by the rotating microphone, of the m-mode spinning pattern associated with the nth order fan shaft harmonic.

Thus, for each mode, m, associated with a shaft harmonic, n, there is a corresponding frequency, ω_m^n, in the time signal of the rotating microphone. This relation is illustrated in Figure 3-2, where a frequency component $\omega_n = n\Omega$ in fixed coordinates splits into a tone cluster with constituents spaced Γ radians/sec apart in the rotating microphone coordinate system. Reverse spinning modes (m negative) sweep past the moving microphone at higher relative speeds than corresponding forward modes (m positive) and generate slightly higher frequency signals in a way that transforms higher relative velocities into higher frequencies.
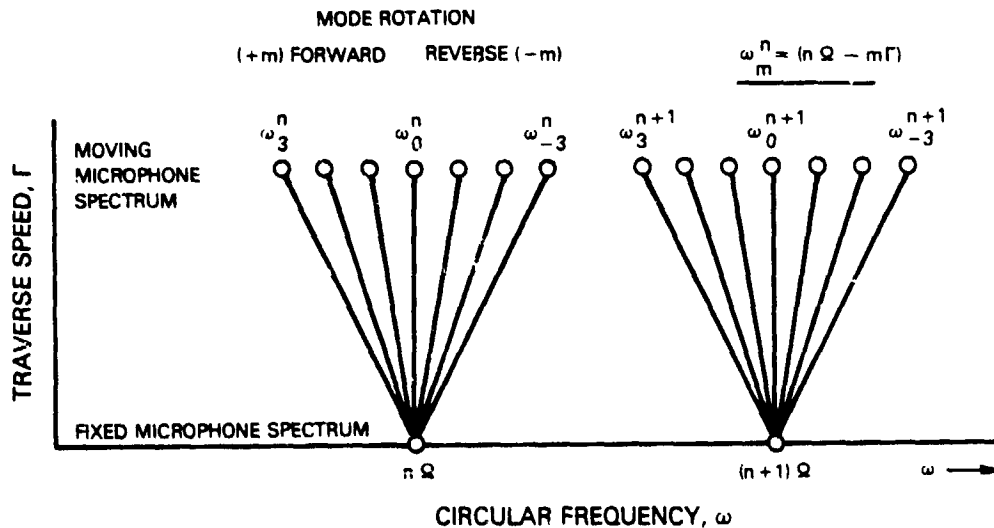
Figure 3-2   Frequency Separation Effect of Traverse Speed

If the microphone rotational speed is not too high the tone clusters from neighboring n-harmonics will not overlap, and there will be a one-to-one reciprocal mapping between the (m, nΩ) points in the modal-frequency spectrum

of the noise field and the frequency components, ω_m^n, in the traversing microphone time signal.

This relationship, illustrated in Figure 3-2, may also be interpreted in terms of the modal-frequency spectrum of the acoustic field, as shown in Figure 3-3. To simplify presentation, it is assumed that the only significant frequencies, ω, in the fixed-coordinate specification of the fan noise field, correspond to multiples of blade-passage harmonics: $\omega = B\Omega$, $2B\Omega$, etc. For each such harmonic, the circumferential modal structure can be represented by a set of delta functions of strength $|C_m^n|$ located at the appropriate modal coordinate, m. Thus the sound field in fixed coordinates can be represented by a two-dimensional spectrum in variables m and ω. The effect of microphone rotation, as given by eq. (3-10) is to transform each (m, ω) point in fixed coordinates into the frequency $\omega' = \omega_m^n = (n\Omega - m\Gamma)$ in the rotating microphone coordinate system. This transformation is shown in Figure 3-3 by connecting each (m, ω) point in the modal-frequency spectrum with a point $\omega' = \omega_m^n$ on the vertical frequency axis by means of a line with slope Γ.
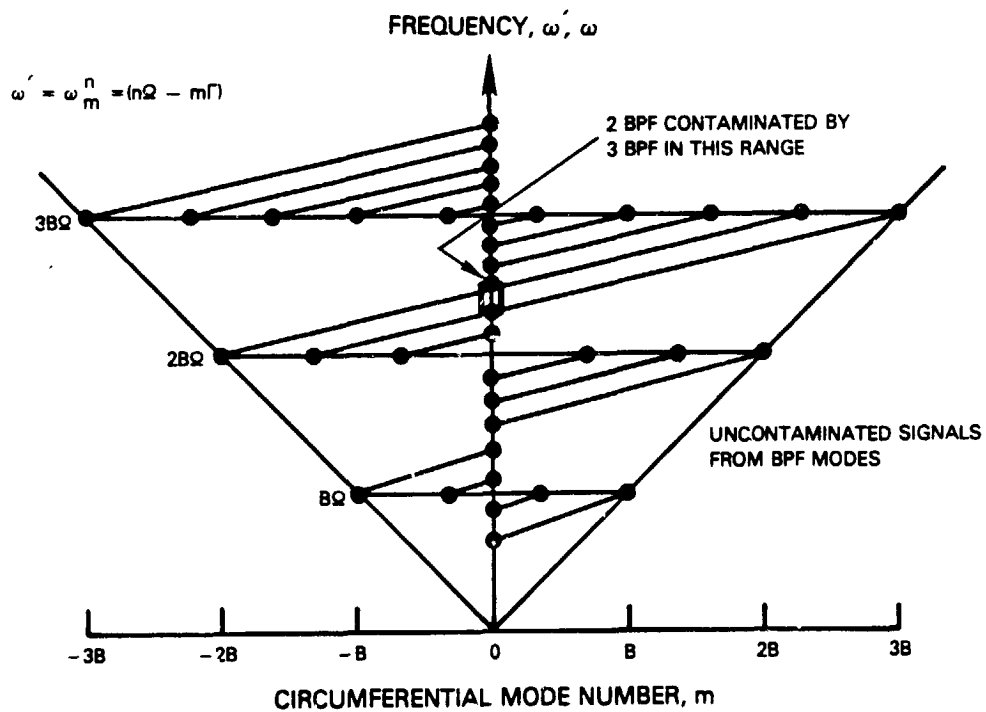
Figure 3-3   Modal Frequency Spectrum and Its Equivalent in Rotating Microphone Signal

Recovery of the modal coefficients C_m^n comprising the microphone time signal,

p(t), in eq. (3-8) is patterned after the procedure described previously for analysis of a time signal. In this case two parameters, m and n, are involved. By measuring both fan shaft angle, $\gamma = \Omega t$, and microphone angle, $\theta = \Gamma t$, a reference signal is formed for target mode $m = M$ and order $n = N$

$$V_M^N(t) = \text{expi} - (M\Gamma - N\Omega)t \tag{3-11}$$

$$\text{or} \quad = \text{expi} - [M\theta(t) - N\gamma(t)]$$

where, generally, $\theta(t) = \int \Gamma(t)dt$ and $\gamma(t) = \int \Omega(t)dt$.

Multiplying this target signal by the microphone signal and time-averaging gives the transform

$$\text{Tr}\left\{p(t)\right\} = \frac{1}{T}\int_0^T \left[\text{Re}\sum_m\sum_n \frac{C_m^n}{2}\text{expi }(m\theta - n\gamma)\right] \cdot V_M^N(t)dt \tag{3-12}$$

$$\text{Tr}\left\{p(t)\right\} = \frac{1}{T}\int_0^T \sum_m\sum_n \frac{C_m^n}{2}\text{expi }[(m - M)\theta(t) - (n - N)\gamma(t)]dt \tag{3-13}$$
$$+ \text{ conjugate terms involving } C_m^{n\star}$$

For the single component of p(t) corresponding to the target signal, that is, $m = M$ and $n = N$, the integrand is the constant, $(1/2)C_M^N$. All other integrands are oscillatory, including those for the conjugate terms. Therefore, their time-averages either vanish exactly or can be made as small as desired by use of a suitably long averaging time, T. Neglecting such residual terms, the transform reduces to

$$\text{Tr}\left\{p(t)\right\} = \frac{C_M^N}{2} \tag{3-14}$$

from which the modal coefficient is given by

$$C_M^N = 2\text{Tr}\left\{p(t)\right\} \tag{3-15}$$

For a harmonic, N, of fan shaft frequency (usually B, 2B, etc.) a succession of target signals $V_M^N(t)$, with $M = 0, \pm 1, \pm 2$, are used in the transform, eq. (3-12), to give all the coefficients of the propagating modes, in turn. In

this manner, all the C_M^N or, alternatively, only those of special interest may be computed.

Details of the process will be developed later, especially the reduction of residual terms. At this point i' is worth noting that for the target (m = M, n = N) mode the integrand in .. (3-12) is just the constant $(1/2)C_M^N$, whether or not the fan shaft and microphone speeds are constant, so that recovery of the coefficients C_M^N by eq. (3-15) would not seem to depend upon maintaining an ideally constant fan speed during the data-acquisition time. Further analysis of this question, which turns out to be more complicated, was a major subject of the investigation and is reported later.

3.1.3 Determination of Circumferential - Radial Mode Coefficients

The final step in the traversing microphone method utilizes the values of the circumferential modal coefficients, C_m^n, that have been calculated, as described above, at each microphone radial location, to determine the radial mode constituents, $C_{m\mu}^n$, of the pressure field corresponding to each (m,n) pair. This radial mode decomposition is not unique to the continuously traversing microphone method, but common to all mode measurement systems where the acoustic pressure is measured at a plurality of angular locations and radii in a common transverse plane of the fan duct.

For each microphone radius, $r=r_i$, the continuous microphone traverse method has generated, as previously described, a set of circumferential coefficients that depend on the microphone radius and can now be designated by $C_m^n(r_i)$ instead of just C_m^n to indicate their radial dependence. From the well-known properties of the acoustic field in a cylindrical duct each such $C_m^n(r_i)$ (the complex pressure at $r=r_i$ due to mode m, order n) can be expanded in a series of radial mode eigenfunctions, $E_{m\mu}$

$$C_m^n(r_i) = \sum_{\mu=0}^{\nu-1} C_{m\mu}^n E_{m\mu}(k_{m\mu}r_i) \qquad (i = 1,2, \ldots .I) \qquad (3-16)$$

$$\text{where } E_{m\mu}(k_{m\mu}r_i) = J_m(k_{m\mu}r_i) + Q_{m\mu}Y_m(k_{m\mu}r_i) \qquad (3-17)$$

Computer programs exist for calculating the eigenvalues $k_{m\mu}$ and $Q_{m\mu}$ and the resulting eigenfunctions $E_{m\mu}$ for circular or annular ducts in terms of the appropriate inner and outer radii. Therefore, eq. (3-16) is a set of linear equations in the unknown modal coefficients, $C_{m\mu}^n$, with known constant coefficients, $E_{m\mu}(k_{m\mu}r_i)$. There are U unknown quantities, $C_{m\mu}^n$, where U is the highest radial mode, corresponding to m, that can propagate at frequency nΩ. These linear equations can therefore be solved for the $C_{m\mu}^n$ provided that the number of equations, I, or radial locations at which the circumferential traverses have been made to give the $C_M^N(r_i)$, is at least equal to the greatest number, U, of radial modes that can propagate to the

plane of the microphones. Details of the method of solution are given in a later section of this report.

This concludes the basic description of the principles of the traversing microphone method. Detailed features of the method, and the effects of design parameters and departures from ideal operating conditions are the subjects of the remainder of this report.

3.2 SEPARATION OF TRAVERSE WAKE INTERACTION NOISE

The general concept of measuring fan noise modal structure by means of a plurality of microphones distributed across a section of the inlet duct has always been subject to criticism due to concern with the fact that the wakes from the microphone rakes or support structure are cut by the fan to create extraneous interaction noise modes. This extraneous noise makes it impossible to obtain accurate measurements of the primary noise mode structure present under normal operating conditions. Exceptions to this problem of noise contamination have existed under certain laboratory test conditions where the microphone wake interactions were ignorable due to extremely low inlet air velocities and/or small wake size. But, in practical, large scale fan rig or engine configurations, many microphones are needed to measure the large number of propagating modes, and since the inlet air velocity is substantial, wakes from the required microphones and their support structure are bound to produce significant levels of contaminating interaction noise. In fact, circumvention of this problem led to the concept of arrays of microphones confined to the wall surface of the inlet, as described in ref. 1 and 2. One problem with such wall-mounted microphone arrays is that an undesirably large number of microphones and/or long test times are usually required.

Because of the importance and prominence of this extraneous interaction noise problem, the continuously traversing microphone method was carefully examined from this standpoint before initiation of the detailed program of study which is the subject of this report.

In the first place, it is obvious that any radially oriented rake, bearing a set of microphones and spanning the inlet duct, will produce extraneous interaction modes of essentially all circumferential orders, m, at each harmonic of blade frequency. Minimizing dimensions of rake and microphones and streamlining may help, but due to the substantial inlet airspeeds present in practice, such measures may not be adequate. However, the modal structure of the wake interaction noise from the circumferential traversing microphone, differs in a crucial way from the mode structure that would be generated by the wake of a fixed radial rake. This distinction between the extraneous noise fields of a fixed radial rake and a circumferentially traversing radial rake allows the extraneous and primary interaction noise fields to be separated, and thus permits accurate measurements of the primary, uncontaminated noise field to be made by the traversing microphone system.

The general nature of this distinction is equally obvious: the wake of the fixed rake is fixed in space and time, whereas the wake of the traversing rake rotates slowly about the duct axis. It is this apparently small difference that matters, as is shown in the following analysis.

Consider the wake of a fixed radial obstruction in the inlet, and especially the ℓth circumferential spatial harmonic of this wake. When this distortion is cut by the rotor, the interaction noise field will be a superposition of frequency harmonics of the form

$$p_\ell^n(\theta,t) = \text{Re}\left\{C_\ell^n \exp i\,[(n \mp \ell)\theta - n\Omega t]\right\} \tag{3-18}$$

(For B evenly spaced fan blades, $n = B$, $2B$, etc.)

If, now, the radial obstruction turns slowly at Γ rad/sec the relative air velocity will not change magnitude, so that the wake defect and the modal coefficient amplitudes are unaffected. However, due to the wake rotation the frequency of wake cutting is changed. It can be shown, ref. 11, that the resulting pressure pattern becomes

$$p_\ell^n(\theta,t) = \text{Re}\left\{C_\ell^n \exp i\,[(n \overset{-}{_+} \ell)\theta - (n\Omega \overset{-}{_+} \ell\Gamma)t]\right\} \tag{3-19}$$

This states that two mode-frequency pairs are produced:

mode number, m	frequency, ω
$(n - \ell)$	$(n\Omega - \ell\Gamma)$
$(n + \ell)$	$(n\Omega + \ell\Gamma)$

and

Because of wake rotation, the $m = n-\ell$ mode is now present at frequency $(n\Omega - \ell\Gamma)$ instead of just $n\Omega$ in the fixed wake interaction, and the other mode with $m = n+\ell$ has a higher frequency, $n\Omega + \ell\Gamma$. (If the wake rotation is counter to that of the rotor a negative value of Γ is used.)

To obtain the corresponding time signal sensed by a microphone that also rotates at Γ, θ is replaced by $\theta = \Gamma t$ in eq. (3-19) just as was done for any fixed wake interaction in obtaining eq. (3-8). The result is extremely simple

$$p_\ell^n(t) = p_\ell^n(\theta = \Gamma t,\ t) = \text{Re}\left\{C_\ell^n \exp i - n(\Omega - \Gamma)t\right\} \tag{3-20}$$

As a result of the cancellation of the $\ell\Gamma t$ terms in eq. (3-19) when the $\theta = \Gamma t$ replacement is made, it is seen that the rotating microphone signal is completely free of any spectral component involving the wake harmonic, ℓ.

The actual wake will be a superposition of spatial harmonics, ℓ, so that the complete microphone signal associated with the nth frequency harmonic of rotor shaft speed is

$$p^n(t) = \sum_{\ell} p_{\ell}^n(t) = \text{Re}\left[\left(\sum_{\ell} c_{\ell}^n\right) \text{expi} - n(\Omega - T)t\right] \qquad (3-21)$$

$$\text{or} \quad p^n(t) = \text{Re}\left\{B^n \text{expi} - n(\Omega - T)t\right\} \qquad (3-22)$$

The extraordinary feature of this rotating microphone signal, as evident from eq. (3-22), is that for each harmonic of rotor shaft speed, n, there is but a single component in the rotating microphone spectrum instead of a cluster of tones. Regardless of the rake wake structure, the rotating microphone signal has a frequency of $n(\Omega - T)$ despite the existence of the plurality of mode pairs $(n \pm \ell)$ for $\ell = 1, 2$, etc. present in the duct acoustic field.

By comparison of this signal, eq. (3-22), with the more complicated signal sensed by the rotating microphone that corresponds to the unperturbed modal field, eq. (3-8) and (3-10), the extraneous wake-cutting signal frequency coincides with that of the single component of the unperturbed field mode having $m = n$.

Instead of the microphone wake noise contaminating all of the spectral components, the contamination is restricted to spectral lines corresponding only to those of the direct rotor field $(m = n)$ rather than the general interaction field having components corresponding to $m = 0, \pm 1, \pm 2$, etc. for each n.

For a rotor operating at subsonic tip speeds only those interaction noise modes having $|m|$ less than n can propagate. Thus, the presence of components in the rotating microphone signal at frequencies corresponding to the direct rotor field where $m = n$ are readily identified as due to the extraneous microphone wake cutting noise and are ignored. All other spectral components correspond to the primary interaction field to be measured and are uncontaminated by the wake of the traversing microphone system.

This ready separability of the "true" and "spurious" spectral components is illustrated in Figure 3-4, for a symmetric B-blade rotor operating at subsonic tip speeds. (At supersonic rotor speeds, where modes with m greater than B can propagate, the spurious wake cutting signal will contaminate only the $m = B$ mode.)
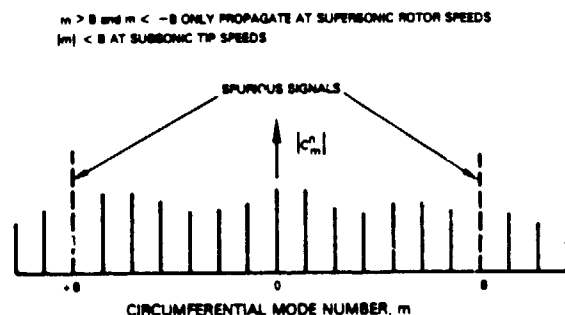
Figure 3-4   Spurious Signals Caused by Traverse Microphone Wake-Rotor Interaction

15

4.0 COMPUTING ALGORITHMS AND SIMULATED TEST PROCEDURES

4.1 INTRODUCTION

During this investigation a computer program was developed to extract the circumferential mode coefficients, $C_m^n(r_i)$, by transforms of the microphone signals as given in eq. (3-12) and (3-15). Resolution of these circumferential modes into radial mode constituents, $C_{m\mu}^n$, by solution of the simultaneous equations, eq. (3-16), comprised the next part of the computer program. These two subprograms form what is called the Analysis Program.

Computer-simulated tests were conducted to check out this program and study the overall operating characteristics of the traversing microphone system. These tests required writing a program to simulate the pressure signal that would be measured by the traversing microphone during the course of an actual test run on an engine or fan rig. This computer program is called the Synthesis Program. The Synthesis Program, obviously, would not be involved in processing of any actual fan noise test data.

This section discusses the algorithms used to perform the required calculations. The notation used here is consistent with that employed in the previous sections. The actual computer programs involve somewhat different notation to conform with standard practice. Consequently, to avoid problems with translation of notation and because programming details are of secondary interest, detailed descriptions of the computer notation, programming, and input-output format are relegated to Appendix B.

4.2 ALGORITHM FOR CIRCUMFERENTIAL MODE COEFFICIENTS: C_m^n

For purposes of digital computation, the integral transform, eq. (3-12), used to obtain the circumferential mode coefficients, C_m^n, from the microphone signals, must be replaced by a finite, discrete transform. The basic integral transform of eq. (3-12) can be expressed as

$$Tr\left\{p(t)\right\} = \frac{1}{T} \int_0^T p(t) \ V_M^N(t)dt$$

$$= \frac{1}{T} \int_0^T p(t) \ expi - [M\theta(t) - N\Upsilon(t)]dt \qquad (4-1)$$

The specific circumferential modal coefficient C_M^N is then given by eq. (3-15), i.e.

$$C_M^N = 2Tr\left\{p(t)\right\}$$

(For simplicity, the radial location dependence of $p(t)$ and M,N indices for the operator symbol $Tr\{ \ \}$ are suppressed.)

Because the orthogonal properties of the sine and cosine functions apply for finite summation as well as for integration, an effective discrete transform corresponding to eq. (4-1) is

$$Tr\left\{p(t_q)\right\} = \frac{1}{T}\sum_{q=0}^{Q-1} p(t_q)V_M^N(t_q)\Delta t$$

$$= \frac{1}{T}\sum_{q=0}^{Q-1} p(t_q)\,expi - [M\theta(t_q) - N\gamma(t_q)]\Delta t$$

For Q equal time increments, $\Delta t = T/Q$, this becomes

$$Tr\left\{p(t_q)\right\} = \frac{1}{Q}\sum_{q=0}^{Q-1} p(t_q)\,expi - [M\theta(t_q) - N\gamma(t_q)] \tag{4-2}$$

Values of $p(t)$, $\theta(t)$ and $\gamma(t)$ at the instants t_q are supplied to the computer by digitizing the pressure and angle analog signals generated by microphones and shaft angle transducers. The pressure signals must be prefiltered by low-pass analog filters and the digitizing rate (or sampling frequency) must be selected by Nyquist criterion to prevent aliasing. The normal calculation procedure is to select an order N (usually B or 2B) of interest, and to then execute eq. (4-2) for M = 0, +1, +2 . . . up to the maximum M that can propagate. This is done for each radially located microphone generating $p(t_q)$. (The corresponding circumferential mode coefficients C_M^N are just twice the transform, by eq. (3-15).)

This procedure under ideal operating conditions is sufficient to obtain accurate values of the C_M^N. In practice, however, a number of factors may lead to contamination of the result. These factors include the presence of broadband random noise in the $p(t)$ signals, and a combination of fan speed variations and source-to-microphone acoustic propagation time delays. These effects are treated in some detail in Sections 5 and 6. For the moment, it is sufficient to state that these contaminating effects can be reduced by modifying the transforms with a weighting function factor, $W(t)$ or $W(t_q)$, in the integrand. This is a standard signal analysis procedure, called weighting, tapering or windowing, employed to reduce the contamination ("leakage") from off-target frequency components in the signal.

Several standard weighting functions, $W(t_q)$, are in use. For the current traversing microphone study, two options were used:

Rectangular weighting: $W(t_q) \equiv 1$ (4-3)

(as implied by eq. (4-2))

Hamming weighting: $W(t_q) = \frac{1}{0.54} [0.54 - 0.46\cos(\frac{2\pi t_q}{T})]$ (4-4)

The generalized, weighted form of the transform eq. (4-2) is

$$Tr\left\{p(t_q)\right\} = \frac{1}{Q}\sum_{q=0}^{Q-1} p(t_q)W(t_q) \, \text{expi} - [M\theta(t_q) - N\gamma(t_q)]$$ (4-5)

This is the algorithm used in this study for computation of the coefficients C_M^N employing either eq. (4-3) or (4-4) for the $W(t_q)$ weighting function options.

4.3 ALGORITHM FOR CIRCUMFERENTIAL-RADIAL MODE COEFFICIENTS, $C_{m\mu}^n$

After the circumferential mode coefficients, $C_m^n(r_i)$ have been obtained at each of the microphone radii, r_i, a screening procedure should be used to eliminate circumferential m-modes judged to contribute comparatively negligible $C_m^n(r_i)$ at all r_i locations. This screening may be done manually by examination of a $C_m^n(r_i)$ printout table or by writing a computer screening program to bridge the circumferential and radial mode subprograms. If the number of propagating modes is sufficiently small, it will be simpler to compute all C_m^n without screening. (No such screening procedures were needed or used in the computer-simulated tests run in this program.)

Then, corresponding to each $C_m^n(r_i)$, a resolution into constituent circumferential-radial mode coefficients, $C_{m\mu}^n$, may be performed by solution of the previously given simultaneous equations that express each $C_m^n(r_i)$ in terms of the unknown coefficients, $C_{m\mu}^n$, and the known eigenfunctions, $E_{m\mu}(k_{m\mu}r_i)$, eq. (3-16), i.e.

$$C_m^n(r_i) = \sum_{\mu=0}^{U-1} C_{m\mu}^n E_{m\mu}(k_{m\mu}r_i) \qquad (i=1,2,\ldots I)$$

The known constants $E_{m\mu}(k_{m\mu}r_i)$ are computed from eq. (3-17).

U denotes the number of propagating radial (μ) modes associated with the circumferential mode index, m. The largest number of radial modes will exist for m=0, with progressively smaller numbers as m increases. Evidently the number of microphone locations, I, must be at least equal to U. This means that there will be more readings and equations available for obtaining the comparatively few $C_{m\mu}^n$ when m is large than when m is small.

Procedures for solving eq. (3-16) have been examined in some detail and reported in ref. 12. The procedure selected for use in this investigation was adopted on the basis of the ref. 12 study and for two other reasons that will

18

be now developed. It is worth remarking that the prime objective of this program was to study the properties and to refine the procedures of the circumferentially traversing microphone system. It is only after the circumferential mode coefficients $C_m^n(r_i)$ have been obtained by the traversing microphone method or any other fixed-microphone array method that procedures for extracting the radial constituents, $C_{m\mu}^n$, need be considered. A detailed study of radial mode extraction procedures, such as reported in ref. 12, is beyond the objectives of the program reported here.

For background purposes it is helpful to consider the hypothetical case where the circumferential mode coefficient, C_m^n, has been determined as a continuous function of r, so that eq. (3-16) becomes

$$C_m^n(r) = \sum_{\mu=0}^{U-1} C_{m\mu}^n E_{m\mu}(k_{m\mu}r) \qquad (4-6)$$

In this case, the $C_{m\mu}^n$ may be recovered by applying the Bessel transform as follows

$$\int_a^b C_m^n(r) \cdot r \cdot E_{m\nu}(k_{m\nu}r)dr = \sum_{\mu=0}^{U-1} C_{m\mu}^n \int_a^b r \, E_{m\mu}(k_{m\mu}r)E_{m\nu}(k_{m\nu}r)dr, \qquad (4-7)$$

where the range of integration is from $r = a$ at the hub or inner radius of the annular duct to $r = b$ at the tip or outer radius.

Because of the (r-weighted) orthogonality of the eigenfunctions

$$\int_a^b rE_{m\mu}(k_{m\mu}r)E_{m\nu}(k_{m\nu}r)dr = \begin{cases} \Lambda_m & \text{for} & \mu = \nu \\ \\ 0 & \text{for} & \mu \neq \nu \end{cases} \qquad (4-8)$$

where $$\Lambda_{m\nu} = \int_a^b rE_{m\nu}^2(k_{m\nu}r)dr,$$

only the diagonal terms on the right hand side of eq. (4-7) survive, thus giving the $C_{m\nu}^n$ coefficient explicitly

$$C_{m\nu}^n = \frac{1}{\Lambda_{m\nu}} \int_a^b C_m^n(r) \cdot r \cdot E_{m\nu}(k_{m\nu}r)dr \qquad (4-9)$$

This procedure and its result are closely analogous to the Fourier type integral transform used previously for circumferential mode analysis. However, unlike the Fourier integral transform, it does not translate exactly into a

discrete form because the orthogonality property, eq. (4-8) holds only for integration and not also for finite summation.

Since in practice the C_m^n (r_i) are available at only a finite number of radial locations, a discrete finite form for $C_{m\nu}^n$, corresponding to eq. (4-9), is not obtainable. There will always remain off-diagonal terms in the equivalent of eq. (4-7). It may be expected that these off-diagonal terms may be made small compared with the diagonal elements by employing small r-increments (more microphones), by judicious selection of the r_i locations in the annulus, by use of some higher order numerical integration (such as Simpson, etc.), or by employing some combination of these measures.

The procedure selected in this study was as follows:

i.   It was assumed that I equispaced microphones were employed to measure the U radial modes, with $I \geqslant U$.

ii. Then, each of the I equations of eq. (3-16) is multiplied by $r_i E_{m\nu}(k_{m\nu}r_i)$ and the results are summed over i to give a new set of equations

$$\sum_{i=1}^{I} C_m^n(r_i)r_i E_{m\nu}(k_{m\nu}r_i) = \sum_{\mu=0}^{U-1} C_{m\mu}^n \left[\sum_{i=1}^{I} r_i E_{m\mu}(k_{m\mu}r_i)E_{m\nu}(k_{m\nu}r_i) \right] \qquad (4-10)$$

iii. The above set of equations, eq. (4-10), is U simultaneous linear equations in the U unknowns, $C_{m\mu}^n$. The first equation is obtained by using the index $\nu = 0$, the second by $\nu = 1$, etc., ending with $\nu = U-1$. As described, there will be non-zero off-diagonal terms on the right hand side. However, these terms will be small compared with the diagonal elements if the number of microphones, I, is reasonable and will approach zero as I increases, because the finite summations are approximations to the integrals having properties of eq. (4-8).

iv. Eq. (4-10) is now in standard simultaneous equation form and can be solved by any appropriate subroutine available in the user's computer library.

Execution of this part of the analysis program completes the determination of the circumferential-radial mode coefficients. It may be shown that the procedure described above corresponds precisely to obtaining a best fit, in the least squares sense, of the U eigenfunctions to the I data points, $C_m^n(r_i)$. A further discussion of the procedure is presented in Section 5.

4.4 SIMULATION OF PRESSURE FIELD

As described in Section 4.1 a computer program was written to generate computer-simulated pressures that would be sensed by the traversing microphones in an actual test. The simulation program starts with a selectable number of modal coefficients having known, assumed values. It then computes the microphone pressure $p(t_q)$ at each instant of time as a superposition of the modal contributions.

20

At this point, a provision is made to modify the resulting pressure in a
variety of ways. These modifications may involve rounding or truncating the
pressure or may involve the addition of random broadband noise. If no
modifications are made, the computed pressures when used as input to the
previously described analysis program will obviously result in computed modal
coefficients that agree with the initial input selections. (Insufficiently
close agreement indicates programming error or computer roundoff error, either
of which requires immediate correction.) Depending on the nature of the
modification applied, this simulation-analysis loop provides an instructive
means for studying the effects of deviations from ideal operating conditions
upon the performance of the traversing microphone method.

For constant speed operation, the algorithms used for synthesizing the
pressure at a typical microphone location are

$$p(t_q) = \text{Re} \sum_m \sum_n C_m^n \text{ expi}[m\theta(t_q) - n\gamma(t_q)] \qquad (4\text{-}11)$$

where microphone angle $\qquad \theta(t_q) = \Gamma t_q \qquad\qquad\qquad (4\text{-}12)$

fan shaft angle $\qquad\qquad \gamma(t_q) = \Omega t_q \qquad\qquad\qquad (4\text{-}13)$

The pressure, $p(t_q)$, thus simulated by eq. (4-11) serves as input to the
analysis algorithm, eq. (4-5). The values of $\theta(t_q)$ and $\Gamma(t_q)$ obtained from
(4-12) and (4-13) are also used to formulate the target signals,

$$V_M^N(t_q) = \text{expi} - [M\theta(t_q) - N\gamma(t_q)], \qquad (4\text{-}14)$$

employed in the analysis transform, eq. (4-5).

In eq. (4-11), each C_m^n is a circumferential mode coefficient at the typical
microphone radius. The phase of this coefficient is defined as zero when the
microphone is at $\theta = 0$ and the shaft angle is at $\gamma = 0$ or any integral
multiple of 2π. This convention conforms with standard mode measurement
practice.

In the simulated tests performed here the number of modes employed to make up
the pressure was kept small to make the program more easily manageable and its
results clearer than if very many modes were used. Most "tests" employed only
1 or 2 shaft harmonics, $n = B$ and/or $n = 2B$. For each such n, frequently a
single m mode was used, and rarely were more than three modes present.

In the analysis part of the program, values of the target parameters, M and N,
included the m and n input values, together with other m and n for which there
was no input ($C_m^n = 0$). An ideal, perfect result of a "test" was to obtain
all the input mode C_m^n accurately and to obtain essentially zero output when
targeting other modes.

As mentioned at the beginning of this section, the ideal pressure signal, simulated by eq. (4-11), could be modified when desired in order to reflect rounding or truncating or to include the addition of a computer-generated random noise signal to simulate broadband noise. These options are discussed in Section 5.

It should be repeated that eq. (4-11), eq. (4-12), and eq. (4-13) apply only to constant rotor and traverse speeds. Variable speed operation requires different expressions and is discussed in Section 6.

Simulated tests for determination of the circumferential-radial mode coefficients, $C_{m\mu}^n$, in terms of the circumferential coefficients, $C_m^n(r_i)$, were performed separately from the circumferential traverse program for reasons given in Section 4.3.

The algorithm used to simulate the circumferential mode coefficient, $C_m^n(r_i)$ at a plurality of radii, r_i, is given by eq. (3-16), i.e.

$$C_m^n(r_i) = \sum_{\mu=0}^{U-1} C_{m\mu}^n \, E_{m\mu}(k_{m\mu} r_i)$$

For a fixed m and n, a set of $C_{m\mu}^n$ would be selected corresponding to $\mu = 0, 1, \ldots (U-1)$ and the $C_m^n(r_i)$ would be computed for each microphone radius. These simulated $C_m^n(r_i)$ could then be modified to incorporate truncation errors, for example, or other options. The modified $C_m^n(r_i)$ then served as input to the analysis algorithm, eq. (4-10). Comparison of input and output values of the $C_{m\mu}^n$ led to an evaluation of the radial mode decomposition process.

5.0 SYSTEM CHARACTERISTICS - CONSTANT SPEED OPERATION

At this point a prospective user of the traversing microphone method probably has two types of questions to be resolved:

1. How should design parameters of the system - traverse speed, traverse time, etc. - be selected to make measurements on a specific engine or rig?

2. How significant will deviations from ideal operating conditions, such as rig speed fluctuations, broadband fan noise, etc. be in affecting the accuracy of the results?

Both classes of questions are addressed in this Section 5 and in Section 6. Variable speed operation is discussed in Section 6 rather than in 5. Although it is but one form of deviation from ideal operation, its scope and impact on all mode measurements warrants special attention.

There is not always a clear boundary between the type 1 (design parameters) and type 2 (deviation) matters, but this categorization may nevertheless be helpful.

A listing of some topics in these categories follows:

Design Parameters to Be Selected

Traverse speed	τ
Traverse time	T
Traverse turns	$R \ (= (1/2\pi)\tau T)$
Digitizing rate	Q/T
Microphone radii	r_i
Number of microphones	I

Deviations and Errors

Error in pressure measurement
Error in rotor angle measurement
Error in microphone angle
Residual term errors in algorithm
Extraneous spectral components
Broadband noise contamination
Rotor speed deviations (Section 6)
Traverse speed deviations (Section 6)

Section 5.1 discusses the frequency response function of the system, which is basic to further study. Section 5.2 addresses questions that deal primarily with selection of design parameters, and Section 5.3 focuses on the effect of errors such as listed above. Because these matters are often related, there will be frequent cross-references between 5.2 and 5.3.

The characteristics discussed in Sections 5 and 6 were determined by means of analytical studies or computer-simulated tests, or by a combination of these methods.

Selection of design parameters and estimation of the effects of deviations from ideal operating conditions is based on the frequency response function of the system, which will now be examined.

5.1 SYSTEM FREQUENCY RESPONSE FUNCTIONS

A frequency response function of the traversing microphone system will be defined as the result of transforming a unit amplitude, complex pressure signal at arbitrary frequency, ω, by transforms of the type given in Section 3 for the continuous case and in Section 4 for the discrete analysis.

A unit weighting function, $W(t) \equiv 1$ is considered first. For the integral transforms of Section 3, the frequency response function, denoted by y, has the generic form

$$y = \frac{1}{T} \int_{t_a}^{t_a + T} \text{expi} (-\omega t) \cdot \text{expi} (\omega_0 t) dt \tag{5-1a}$$

$$y = \frac{1}{T} \int_{t_a}^{t_a + T} \text{expi} (\omega_0 - \omega) t \, dt \tag{5-1b}$$

$$y = \frac{1}{T} \int_{t_a}^{t_a + T} \text{expi} (\Delta\omega t) dt \tag{5-1c}$$

The factor expi $(-\omega t)$ represents any pure harmonic component in the signal $p(t)$. The target signal, under constant fan and traverse speeds, is given by expi $(\omega_0 t)$, and $\Delta\omega$ is the difference frequency. As is seen, y is a function of $\Delta\omega$ and also of the averaging time, T, and the initial time, t_a.

The integration in eq. (5-1c) is immediate, and after a little manipulation, the result can be expressed in a standard form

$$y = \frac{\sin \Delta\omega T/2}{\Delta\omega T/2} \text{expi} \, \Delta\omega(t_a + T/2) \tag{5-2a}$$

24

or, with $\Delta\omega = 2\pi\Delta f$,

$$y = \frac{\sin\Delta fT\pi}{\Delta fT\pi} \text{expi}[2\Delta f(t_a + T/2)\pi] \qquad (5\text{-}2b)$$

The amplitude of y indicates how well a signal is measured and is the well known "diffraction function"

$$\text{dif}(\Delta fT) = \frac{\sin(\Delta fT\pi)}{\Delta fT\pi} \qquad (5\text{-}3)$$

It is occasionally more convenient to denote this same quantity by the notation

$$\text{diff}(\Delta fT\pi) = \frac{\sin\Delta fT\pi}{\Delta ft\pi} = \frac{\sin \Delta\omega T/2}{\Delta\omega T/2} = \text{diff}(\Delta\omega T/2) \qquad (5\text{-}4)$$

This function is unity for $\Delta f = 0$ and has zeros where Δf is a multiple of 1/T. It is sketched in Figure 5-1. The height of the nearest side lobe is about -13.5 dB relative to the main lobe, and subsequent maxima vary inversely with Δf. Note that if the time origin is defined at the midpoint of the run, so that $t_a = -T/2$, the phase shift implied by the exponential factor in eq. (5-2b) vanishes for all Δf.
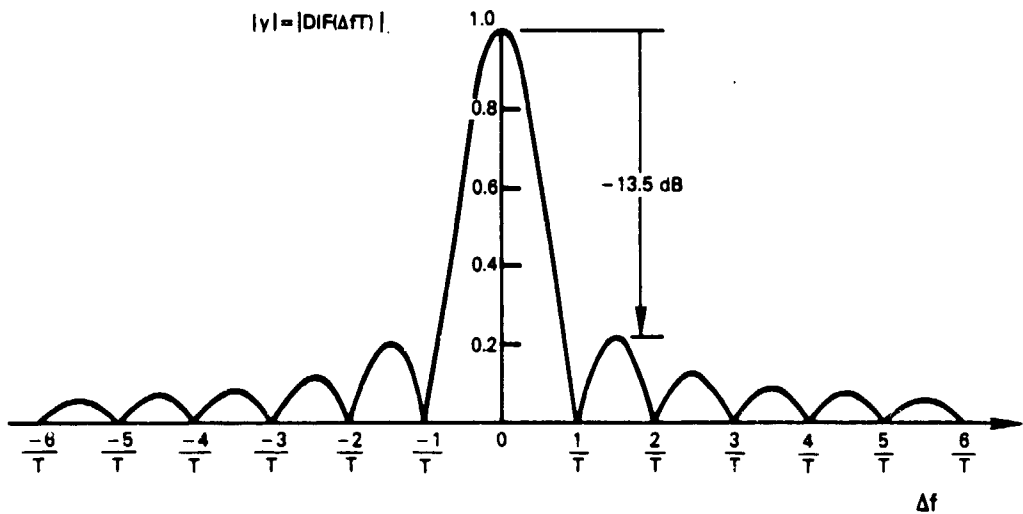
Figure 5-1   System Frequency Response Function Amplitude
                 $|y| = \text{dif}(\Delta fT) = \sin(\Delta fT\pi)/(\Delta fT\pi)$
                 (Uniform Weighting, W = 1)

25

Before applying the properties of the response function to the traversing microphone system, the response functions for the discrete form of the transform and for the weighted transforms will be described.

The discrete analog of the response function, eq. (5-1c), corresponding to the response function for the discrete transform, eq. (4-2), is

$$y_d = \frac{1}{Q} \sum_{q=0}^{Q-1} \text{expi } \Delta\omega(t_a + \Delta t_q) \tag{5-5}$$

This is a geometric series of Q terms, with ratio = $\text{expi}\Delta\omega\Delta t$ and sums to

$$y_d = \frac{\sin(\Delta\omega T/2)}{Q \sin(\frac{1}{Q}\Delta\omega T/2)} \text{expi } \Delta\omega(t_a + \frac{Q-1}{Q}\frac{T}{2}) \tag{5-6a}$$

$$y_d = \frac{\sin(\Delta fT\pi)}{Q \sin(\frac{1}{Q}\Delta fT\pi)} \text{expi } (\Delta f2\pi t_a + \frac{Q-1}{Q}\Delta fT\pi) \tag{5-6b}$$

When the number of sample points, Q, is large and when the time origin is chosen at the midpoint of the run, this reduces to

$$y_d = \frac{\sin(\Delta fT\pi)}{Q \sin(\frac{1}{Q}\Delta fT\pi)} \tag{5-6c}$$

This differs from the continuous case because of the periodicity of the denominator. When $\Delta fT/Q$ approaches unity, both denominator and numerator approach zero in such a way that the result approaches unity, as is also the case for zero Δf. This behavior is illustrated in Figure 5-2. The full response at $\Delta f = Q/T$, the sampling frequency, means that the signal to be analyzed must be analog prefiltered to prevent this false response, called aliasing. For large values of Q and for Δf less than half the sampling frequency, a good approximation to eq. (5-6c) is provided by the continuous form, eq. (5-3).

The minor lobes of the response function, either eq. (5-3) or eq. (5-6), are undesirable since they contaminate the transform of p(t) over a wide range of frequencies different from the target frequency. Side lobe suppression can be achieved through use of weighting functions, as described in Section 4.2. In this program only the Hamming weighting, eq. (4-4), has been used (in addition to rectangular or W(t) = 1 weighting).
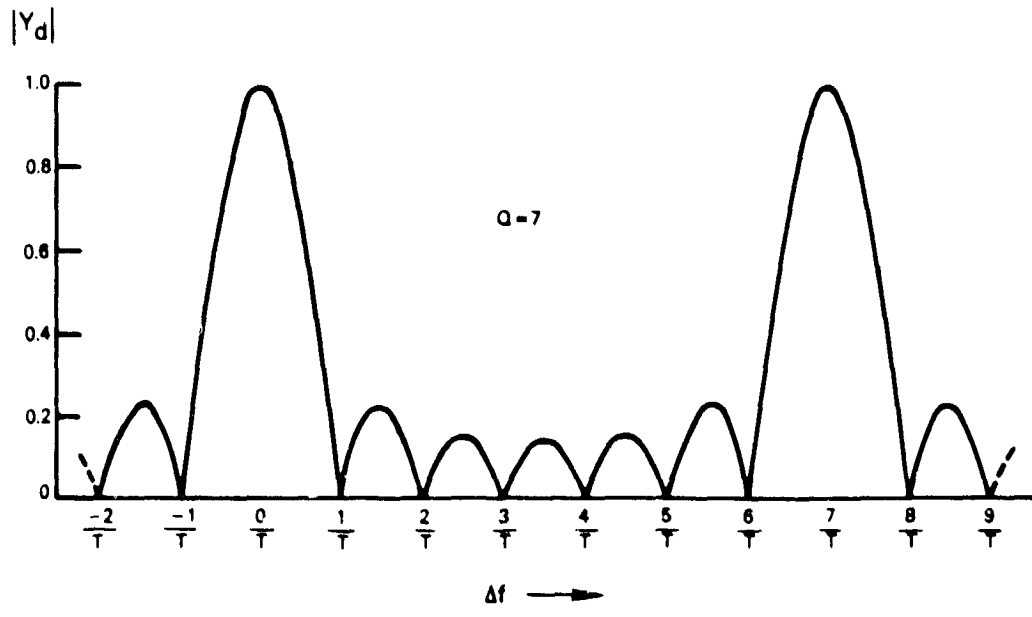
Figure 5-2   Discrete Analog of System Response Function

With a weighting function, $W(t)$, defined by eq. (4-4) the response function, taking $t_a = 0$ for simplicity, is

$$y = \frac{1}{T} \int_0^T W(t) \; \text{expi} \; \Delta\omega t \; dt \tag{5-7a}$$

or $\quad y_d = \frac{1}{Q} \sum_{q=0}^{Q-1} W(\Delta tq) \; \text{expi} \; (\Delta\omega tq) \tag{5-7b}$

With algebra similar to that used for the $W(t) \equiv 1$ cases, it can be shown, ref. 1, that the resulting frequency function amplitudes are

$$\left| y_H \right| = y(\beta) + 0.425926[y(\beta + 1) + y(\beta - 1)] \tag{5-8a}$$

where

$$\left| y(\beta) \right| = \frac{\sin(\beta\tau)}{\beta\tau} \tag{5-8b}$$

is used for the continuous case, eq. (5-7a)

and $\quad \left| y(\beta) \right| = \dfrac{\sin(\beta\pi)}{Q \sin(\frac{1}{Q}\beta\pi)}$ (5-8c)

applies to the discrete case, eq. (5-7b)

and also where $\beta = \Delta fT$ (5-8d)

It would be convenient for later use to employ a notation for the amplitude of the transform, $|y_H|$, which is the frequency response function for Hamming weighting, that parallels the functions dif( ) and diff( ) used for uniform weighting.

For $W(t)$ = Hamming weighting, eq. (4-4), the transform is

$$y = \frac{1}{T} \int_0^T W(t) \, \text{expi} \, \Delta\omega t \, dt \tag{5-9a}$$

with amplitude denoted by

$$\text{Hamm}(\Delta\omega T/2) = \frac{\sin \Delta\omega T/2}{\Delta\omega T/2} + 0.425926 \left[\frac{\sin(\Delta\omega T/2 + \pi)}{(\Delta\omega T/2 + \pi)} + \frac{\sin(\Delta\omega T/2 - \pi)}{(\Delta\omega T/2 - \pi)} \right] \tag{5-9b}$$

$$= \text{diff}(\Delta\omega T/2) + 0.425926[\text{diff}(\Delta\omega T/2 + \pi) + \text{diff}(\Delta\omega T/2 - \pi)] \tag{5-9c}$$

or by

$$\text{Ham}(\Delta fT) = \frac{\sin \Delta fT\pi}{\Delta fT\pi} + 0.425926 \left[\frac{\sin(\Delta fT + 1)\pi}{(\Delta fT + 1)\pi} + \frac{\sin(\Delta fT - 1)\pi}{(\Delta fT - 1)\pi} \right] \tag{5-9d}$$

$$= \text{dif}(\Delta fT) + 0.425926[\text{dif}(\Delta fT + 1) + \text{dif}(\Delta fT - 1)] \tag{5-9e}$$

In these expressions, the functions dif( ) and diff( ), defined in eq. (5-3) and eq. (5-4) are the frequency response function amplitudes for the uniformly weighted transform, with $W(t) = 1$.

The Hamming weighted system response function is represented in figure 5-3. Two important changes from the unweighted case, Figure 5-2, should be noted: The greatest side lobe is now about 44 dB below the main lobe, a reduction of about 30 dB. However, the main lobe is twice as wide as in the unweighted case.

28
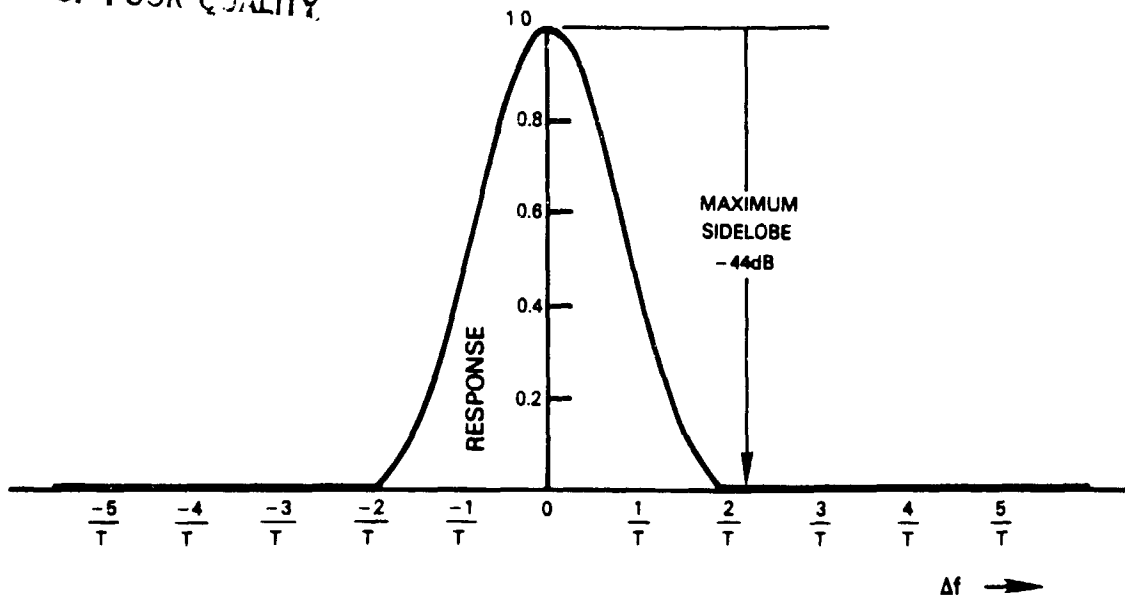
Figure 5-3   Hamming Weighted System Response Function

The extended main lobe or bandwidth can be compensated for by doubling the integration time, thus giving a frequency response that is as snarp as that of the unweighted transform but substantially without the side lobe contamination.

Under ideal operating conditions, as will be shown, the only components of $p(t)$ in the rotating microphone signal occur for $\Delta f = 0$ and at zeros of the basic response function of eq. (5-3) and eq. (5-6); therefore, there is no contamination and no need for weighting the transform. However, it will be shown that under real conditions signals are not restricted to these locations, and Hamming weighting is needed to reduce their contamination of the indicated target signal.

These frequency response functions will now be applied to the specific time signals generated in the traversing microphone system. Some simplifications are made for convenience:

1.   The time origin will be taken at the midpoint of the run so that the phase shift factors in eq. (5-2) will be unity (amplitude of the result remains the same).

2.   Since the number of points, Q, is large, the simpler continuous forms, eq. (5-2), can be used in place of the discrete expressions, eq. (5-6).

3.   Many properties of both Hamming-weighted transforms and the uniform weighting, $W(t)$ 1, are common. The simpler, uniform, case will be emphasized, and the pertinent distinctions between this case and the Hamming procedure will be pointed out.

29

Accordingly, eq. (5-2) and its representation, Figure 5-1 will be employed, with appropriate reference in the case of Hamming to eq. (5-8) and Figure 5-3. The procedure involves simply replacing Δf in the generic frequency response function with its specific values in terms of the traversing microphone system, m, M, n, N, T, Ω, and T.

Eq. (5-3), repeated here for convenience

$$y = dif(\Delta fT) = \frac{\sin(\Delta fT\pi)}{\Delta fT\pi}$$

is applied for the appropriate values of Δf arising in the transform of the pressure signal given by eq. (3-13), also repeated in slightly modified form, for the constant speed case.

$$Tr\left\{p(t)\right\} = \sum_{m}\sum_{n} \frac{C_m^n}{2}\frac{1}{T} \int_{-T/2}^{T/2} expi \left\{[(m - M)T - (n - N)\Omega]t\right\} dt \qquad (3-13)$$

$$+ \sum_{m}\sum_{n} \frac{C_m^{n\star}}{2}\frac{1}{T} \int_{-T/2}^{T/2} expi \left\{[-(m + M)T + (n + N)\Omega]t\right\} dt$$

(The conjugate terms involving $(C_m^{n\star})/2$ arise from the representation of p(t) as the real part of C_m^n expi $(m\theta - \omega t)$). It will now be shown that the contributions to the transform from conjugate terms and from off-target modes and orders can be made negligible, resulting in the correct target coefficient, C_M^N.

There are four combinations:

a. Target mode and order   m = M, n = N

b. Off-target mode, target order   m $\neq$ M, n = N

c. Target mode, off-target order   m = M, n $\neq$ N

d. Off-target mode, off-target order   m $\neq$ M, n $\neq$ N

30

For each case, the $\Delta\omega = 2\pi\Delta f$ (the arguments of the above expi functions) for the direct terms and for the conjugate terms $(C^*/2)$ must be evaluated. The results are:

Case	$\Delta\omega$ Direct Terms	$\Delta\omega$ Conjugate Terms
a. (Target m and n)	0	$-2M\Gamma +2N\Omega$
b. $m \neq M, n = N$	$(m-M)\Gamma$	$-(m + M)\Gamma + 2N\Omega$
c. $m = M, n \neq N$	$-(n - N)\Omega$	$-2M\Gamma + (n+N)\Omega$
d. $m \neq M, n \neq N$	$(m-M)\Gamma - (n - N)\Omega$	$-(m + M)\Gamma + (n + N)\Omega$

By estimating the above values of $\Delta\omega$ and evaluating the response function eq. (5-2), the properties of the system may be found.

Case a: Target m and n

The direct term $\Delta\omega = 0$ so it always contributes the correct result, $C_M^N/2$, independently of all system parameters.

However, there is an unwanted contribution from the conjugate term of amount $C_M^N/2$ diff$[(-2M\Gamma + 2N\Omega)T/2]$. The worst circumstance is when Δf is small, and the smallest Δf will be for N = 1 and M = 1 (M can not exceed N for propagation). The lowest frequency is then $\Delta\omega = 2(\Omega - \Gamma)$. In Section 5.2.1 it is shown that to prevent overlapping of adjacent line clusters from orders n and n+1, Γ must be restricted to sufficiently low speeds, in particular, $\Gamma/\Omega < 1/(2n+1)$ where n is the maximum order of interest. For 2BPF as the highest frequency of interest in the 32 blade P&WA fan rig, $\Gamma/\Omega < 1/65$, so Γ can be ignored in $(\Omega - \Gamma)$. The lowest frequency present in the conjugate term then is 2Ω. (This is for tracking shaft order, not BPF)

We thus have the worst possible case giving

$$\text{dif}(\Delta fT) = \frac{1}{\frac{2\Omega}{2\pi}T\pi} = \frac{1}{\Omega T}$$

As an extreme example, suppose T is as short as one second. Then dif$(\Delta ft) = 1/200\pi$ for a rig speed of 100 rps, and the conjugate term contribution is only 20 $\log_{10}$ diffΔf or -60 dB. This is an ignorable error. But even so, it is much larger than will occur in practice, for three reasons. First, an integration time of at least 10 seconds is more realistic, as will be discussed later. This duration would give another 20 dB reduction. Secondly, the frequency is unlikely to coincide with a minor peak in the response function. And, thirdly, the lowest order n of interest will most likely be blade order, rather than shaft order. For n = B = 32 in the P&WA 10-inch fan rig, still a further reduction of 30 dB results. Thus, a more realistic estimate is that the conjugate term contamination is less than -100 dB, truly ignorable.

31

It will be clear by this type of estimation that the effects of conjugate terms in the other cases b, c, and d are also ignorable since their associated $\Delta\omega$ are roughly the same order ($N\Omega$ or $2N\Omega$) as in the case "a" just considered. Continuing now with a discussion of the remaining direct terms, there results:

Cases c and d: (n ≠ N)

In these cases the direct term $\Delta\omega$ contains a term $(n-N)\Omega$ which will have a least value of Ω when $(n-N) = 1$. By the arguments presented above, the resulting $\Delta\omega$ will always be sufficiently high so that $dif(\Delta fT)$ is ignorable compared with unity.

Case b: m ≠ M, n = N

This case is the only situation where there is a possibility of contaminating the direct term with an off-target signal. This case involves a common n = N order but an off-target mode, m ≠ M. If $\Delta\omega = (m-M)\Gamma$ is substituted there results

$$dif(\Delta fT) = \frac{\sin(\Delta\omega T/2)}{\Delta\omega T/2} = \frac{\sin[(m - M)\Gamma T/2]}{(m - M)\Gamma T/2} \qquad (5\text{-}10)$$

Unlike the cases considered previously, the $\Delta\omega$ is not a function of shaft speed, Ω, but rather involves the much smaller traverse speed Γ. Consequently, the denominator in $dif(\Delta fT)$ will not make the result ignorable as it did previously.

Instead, $dif(\Delta fT)$ must be made small -- so that there is negligible contamination -- by arranging for the numerator to be small. This is easily done: Let $\Gamma T = L_\theta$, the total angular travel of the microphone during the traverse time, T. Then

$$dif(\Delta fT) = \frac{\sin[(m - M) L_\theta/2]}{(m - M) L_\theta/2} \qquad (5\text{-}11)$$

If L_θ is made an integral number, R, of full turns, then $L_\theta/2 = R\pi$ and the numerator vanishes for all m ≠ M. Thus, there will be no contamination of the target mode signal by any modes in the n = N tone cluster.

The basic operation of the traversing microphone system is represented in Figure 5-4. This shows the system targeted to mode M, and represents frequencies of neighboring modes located Γ' apart ($\Gamma' = [1/2\pi]\Gamma$) at the zeros of the response function. In Figure 5-4a one complete microphone turn (R = 1) is employed, and the use of 2 turns is shown in Figure 5-4b. The traverse speed, $\Gamma' = R/T$ rps is common in both cases, so in Figure 5-4b the time T doubles, narrowing the bandwidth of the frequency response. As will be shown later, a narrow bandwidth is desirable since it reduces the effect of broadband random noise upon the target mode coefficient measurement.

TARGET
m = M

(a)

1.0

1 TURN, R = 1

▼ MODAL FREQUENCIES ω_m^N

m = M + 3   m = M + 2   m = M + 1   m = M − 1   m = M − 2   m = M − 3

RESPONSE

$\frac{-3}{T}$ $\frac{-2}{T}$ $\frac{-1}{T}$ 0 $\frac{1}{T}$ $\frac{2}{T}$ $\frac{3}{T}$

FREQUENCY WITH RESPECT TO TARGET

(b)

2 TURNS, R = 2

1.0

▼ MODAL FREQUENCIES ω_m^N

RESPONSE

$\frac{-3}{T}$ $\frac{-2}{T}$ $\frac{-1}{T}$ 0 $\frac{1}{T}$ $\frac{2}{T}$ $\frac{3}{T}$

FREQUENCY WITH RESPECT TO TARGET
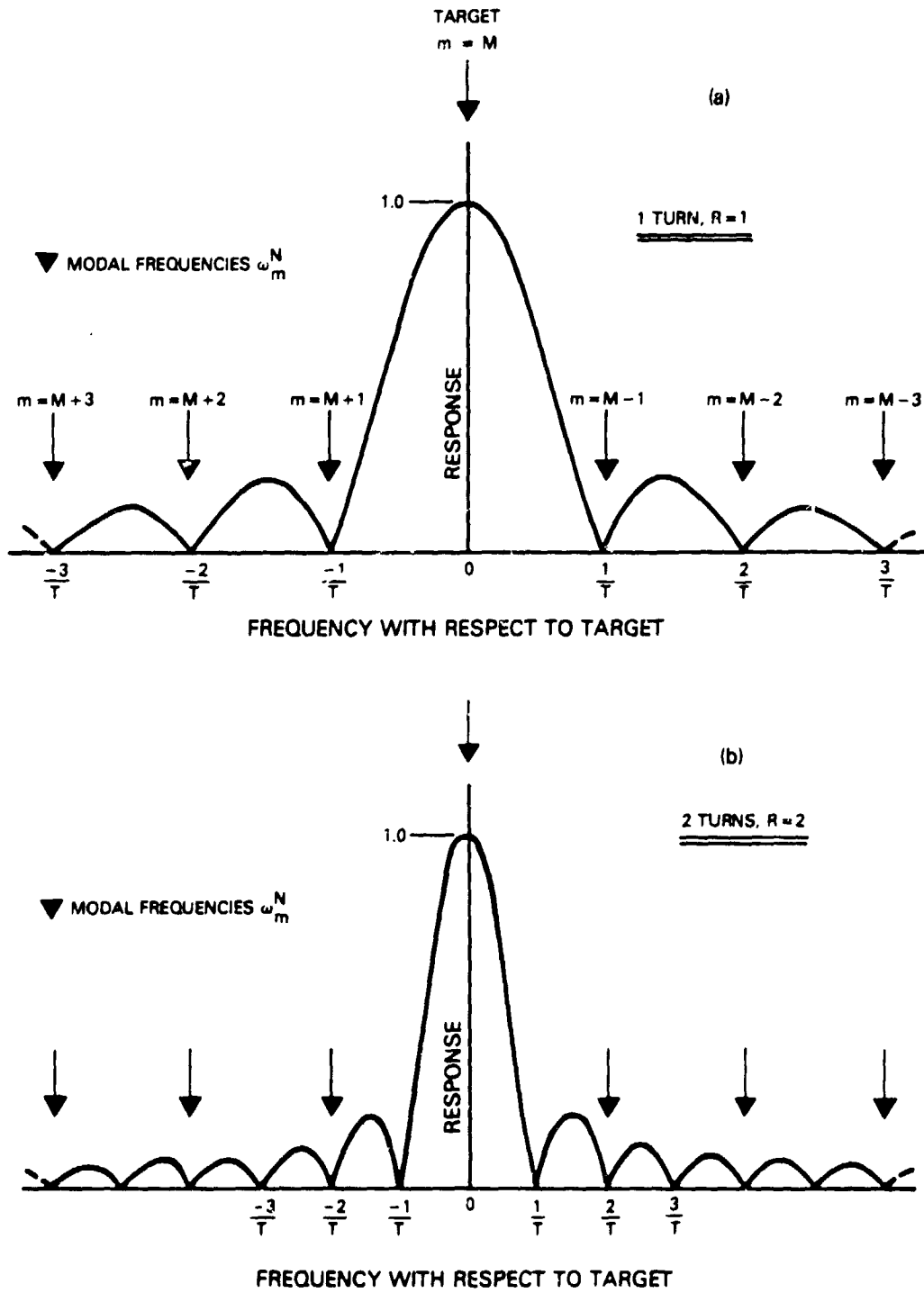
Figure 5-4   System Response to Target and Off-Target Modes
(Uniform Weighting)

33

If the traverse speed were reduced, the time required to execute R turns would increase and the bandwidth would be reduced. The frequencies of modes m $\neq$ M would also contract, maintaining zero contamination from nontarget modes.

The case of a Hamming weighted transform is shown in Figure 5-5. Because of the larger main beam width, use of a single turn, illustrated in Figure 5-5a results in an extremely large contamination, -7.4 dB, from modes immediately bordering the target. This contamination is removed by employing two complete traverse turns, as shown in Figure 5-5b.

Using these properties of the response function of the transform, it is now possible to select the design parameters of the system and to study the effects of departures from ideal operating conditions.

5.2 DESIGN PARAMETER SELECTION

5.2.1 Traverse Speed, Γ

An upper bound to the microphone traverse speed, Γ, may be determined from examination of eq. (3-10), which gives the frequency ω_m^n sensed by the microphone due to the mth circumferential mode of the nth rotor shaft order,

$$\omega_m^n = n\Omega - m\Gamma$$

It may be seen from this expression, and from Figures 3-2 and 3-3 that if Γ is made too large, the tone clusters associated with neighboring orders, n, will overlap, thus making identification difficult if not impossible.

It is necessary in order to prevent such overlap that the highest ω_m^n in the tone cluster associated with the largest order, n, of interest is less than the lowest ω_m^n generated by the (n+1)st harmonic. For subsonic fan tip speed operation, it is conservative to take the greatest $|m|$ that can propagate as equal to n.

Then the highest frequency at which C_m^n must be measured will be $\omega_m^n|_{max} = n\Omega + |m|\Gamma = n(\Omega + \Gamma)$. This corresponds to the reverse spin mode, m = -n.

The closest frequency to this will be generated by a forward spinning pattern of m = n + 1 in the tone cluster associated with the (n + 1) harmonic. This frequency is $\omega_m^{n+1}|_{min} = (n + 1)\Omega - (n + 1)\Gamma$.

TARGET
m = M

m = M + 1   m = M - 1   (a)

10

▼ MODAL FREQUENCIES ω_m^N 1 TURN, R = 1

RESPONSE

m = M + 2   m = M - 2

$\frac{-3}{T}$ $\frac{2}{T}$ $\frac{1}{T}$ 0 $\frac{1}{T}$ $\frac{2}{T}$ $\frac{3}{T}$

FREQUENCY WITH RESPECT TO TARGET

(b)

10

▼ MODAL FREQUENCIES ω_m^N 2 TURNS, R = 2

RESPONSE

$\frac{2}{T}$ $\frac{-1}{T}$ 0 $\frac{1}{T}$ $\frac{2}{T}$

FREQUENCY WITH RESPECT TO TARGET
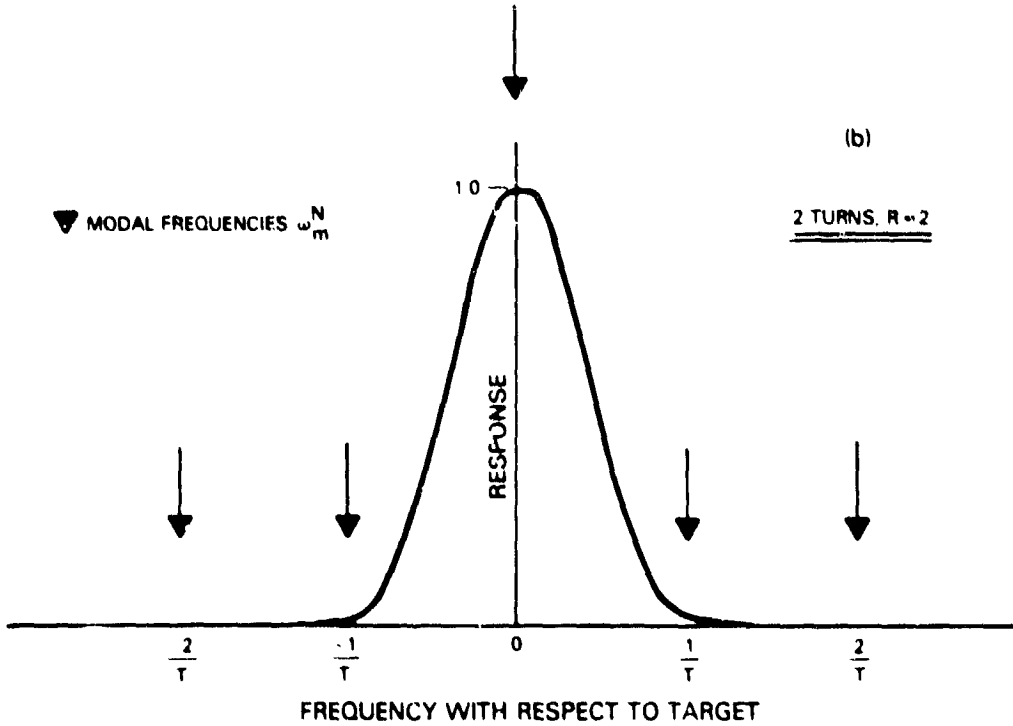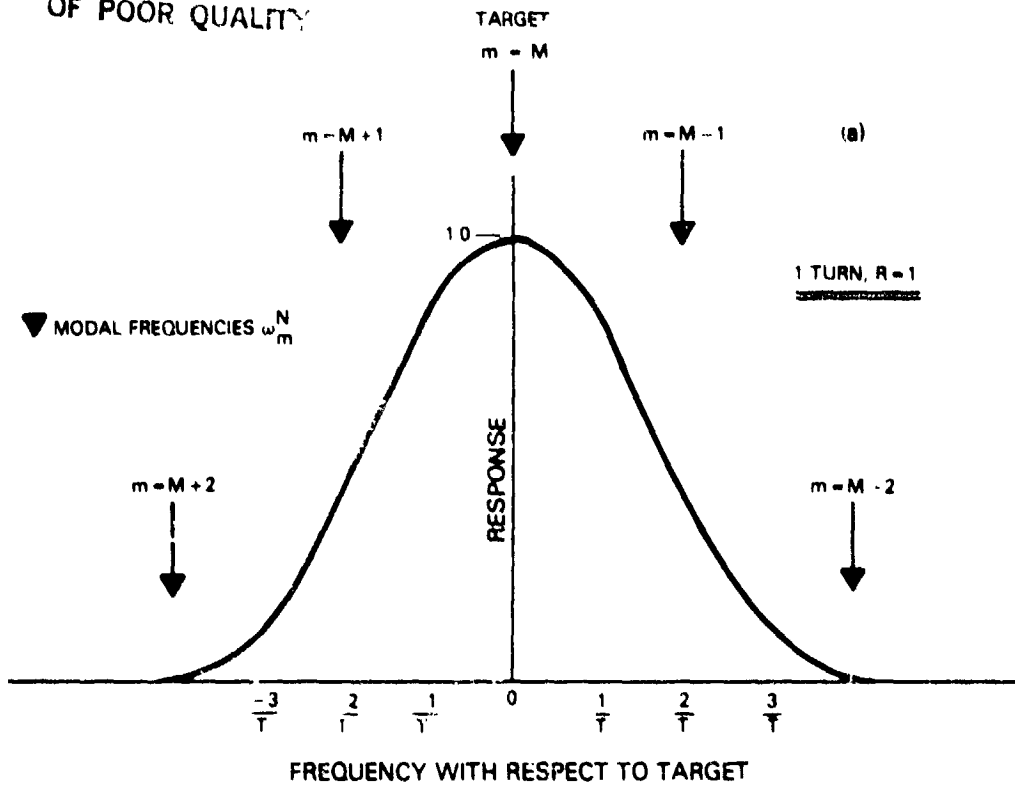
Figure 5-5   Hamming Weighted System Response to Target and Off-Target
                    Modes

35

Separation of the n and (n + 1) order tone clusters requires

$$\omega\,_m^n\bigg|_{max} < \omega\,_m^{n+1}\bigg|_{min}$$

or $\qquad n(\Omega + \Gamma) < (n + 1)(\Omega - \Gamma)$

This requires

$$\frac{\Gamma}{\Omega} < \frac{1}{2n + 1} \qquad\qquad (5\text{-}12)$$

Some illustrations will be of interest. Consider measurements on the 10-inch fan rig at 100 rps (6000 rpm) and in the JT9D engine at 40 rps (2400 rpm). And suppose mode measurements are required for harmonics up through n = 2B in one illustration and up to n = 3B as another illustrative case. With B = 32 and 46 in rig and engine, respectively, the greatest allowable traverse speeds are given in Table 5-1 below.

TABLE 5-1

MAXIMUM ALLOWABLE TRAVERSE SPEEDS

Highest Shaft Harmonic to Be Analyzed	10-Inch Fan Rig (100 rps rotor)	JT9D Engine (40 rps rotor)
n = 2B	0.775 rps	0.216 rps
n = 3B	0.518	0.144

These traverse rates seem reasonable from a test standpoint. They do not appear too fast for standard operation, and the lowest figure implies about seven seconds for one turn, which is not excessively long. Selection of a traverse speed would probably be based on as large a value as possible, under the above limitation, in order to reduce data acquisition time, and would also be governed by mechanical speed limitations of the specific drive system to be used.

5.2.2 Digitizing rate, Q/T

Because of the periodic nature of the discrete frequency response function, when the transform is targeted to a specific frequency, f, there will be additional full response to all signals at frequencies f $\pm$ Q/T, f $\pm$ 2 Q/T etc. These are called the aliases of f and will contaminate the target signal at f. To prevent this contamination it is necessary to select a sufficiently high digitizing rate or sampling frequency, Q/T, and also to remove from the signal to be digitized those frequency components that are much higher than the highest frequencies of interest. A simple guide for this procedure is to provide a low-pass analog filter that will attenuate the microphone signal by

36

about 45 dB--in this application--between the maximum frequency of interest, f_{max}, and twice this frequency, $2f_{max}$. Then the resulting signal to be digitized will have no significant components higher than $2f_{max}$. The digitizing rate is then selected as $2 \times 2 f_{max}$ or $4 f_{max}$. If, for example, interest is restricted to frequencies below 2BPF, a filter attenuating at least 45 dB at 4BPF must be provided. This filtered signal is then digitized at a rate of about 8BPF to ensure against aliasing. This is a conservative procedure: actually 6 BPF sampling rate is sufficient and with a sharper filter something slightly more than 4 BPF could be tolerated. Unless significantly higher frequencies need be analyzed, this procedure, which requires only simple filters on each microphone, is probably satisfactory.

The characteristics of the P&WA 10-inch fan rig were used for the majority of the computer-simulated tests of this program. Twice blade passage frequency, 2 BPF, was selected as the highest frequency of interest. With 32 blades and operating at 100 rps, twice blade passage frequency is 2 BPF = $2 \times 32 \times 100$ = 6400 Hz. The digitizing rate of $4 f_{max}$ is then $Q/T = 4 \times 6400 = 25,600$ Hz. (Note: Because the microphone signals were simulated in digital form by the synthesis computer program rather than obtained from a real test, analog filtering was not a part of the program.)

5.2.3 Traverse Time, T, and Turns, R

Traverse time, speed, and angular extent, L_θ are related by $L_\theta = \Gamma T$. In Section 5.1 it was shown that L_θ must be an integer number, R, of complete turns. Denoting traverse speed in rps by $\Gamma' = \Gamma/2\pi$, there follows

$$R = \Gamma'T$$

so that the traverse time follows from

$$T = R/\Gamma', \tag{5-13}$$

where R is an integer (1 or more for uniform weighting and 2 or more for Hamming).

It has now been shown (Section 5.2.1) that Γ must not exceed a calculable upper bound. Γ should be selected as large as can be conveniently produced, subject to this restriction. Then when R is selected, T follows from eq. (5-13). The design question comes down to: How many turns, R, are required? This question is not easily answered either in principle or in a specific test because it depends upon conditions that have not yet been considered in the discussion of the traversing microphone system, namely, the presence of broadband random noise in the microphone signal and the effects of variations in fan operating speed.

It will be shown later that both R and T will need to be larger than implied by eq. (5-13) for one or two turns. This implies selecting Γ as large as convenient (subject to the upper bound condition) and selecting R (and the associated time) in accordance with procedures to be described later on.

(At this point it may be appreciated that with broadband noise in the microphone signal, increasing T sharpens the frequency response of the transform and reduces broadband contamination. But it is not obvious that T should be increased by increasing R rather than by reducing Γ.)

Further discussion of these design parameters is given in Sections 5.3.5 and 6. A treatment of the number I and disposition, r_i, of the microphones across the duct annulus is found in Section 5.3.6.

5.3 EFFECTS OF DEVIATIONS FROM IDEAL OPERATING CONDITIONS

The results of computer-simulated tests and analysis, provided in Section 5.3, demonstrate the effects of reasonable deviations from ideal operating conditions. The algorithm for simulating the pressure-time history of a circumferentially traversing microphone and the algorithm for processing this data to retrieve the known input mode amplitudes, C_m^n, were programmed and checked out without deliberately simulating any errors. This checkout is described in Section 5.3.1.

The synthesized pressure values were rounded off prior to running the analysis program in order to simulate the effects of digitizing data and, to some degree, to simulate the effects of broadband random noise contamination. These results are presented in Section 5.3.2. Effects of microphone-angle and rotor-angle errors are discussed, respectively, in Sections 5.3.3 and 5.3.4, followed by a discussion in Section 5.3.5 of moderately large amplitude broadband random noise contamination. Section 5.3.6 discusses the errors in circumferential-radial mode coefficients, C_m ; a complete simulation-reduction case is presented, including radial modes.

The approach taken for the computer simulation was to input a set of modes at known complex amplitudes, usually (1+i0) or (0 + i0) and attempt to determine the amplitudes of a target set of modes, usually larger in number than the input set. Deviations from ideal operating conditions were accomplished by minor modifications to the computer code. Output from the simulation-reduction sequence was then compared with the known input value to evaluate the desired effect. The results were generally satisfactory in that the modes input with amplitudes different from zero were recovered practically unchanged while those input with zero amplitude were recovered with negligible amplitudes.

Since the quantities of interest were the differences between assumed and computed mode amplitudes and since these differences were usually small, the data are presented in table form rather than as plots. Where possible, the tables include output in both physical units and as decibels referenced to 1, i.e., 20 log (C/1). Double precision computation yielding approximately 16 decimal digits was used for the circumferential mode simulation-reduction program, but the result was rounded to eight significant digits for printing. A value of 5 in the 9th decimal place corresponds to 20 log (5×10^{-9}) = -166 dB, so that a mode amplitude, printed as zero to eight decimal places, is at least 166 dB below the usual input value of 1. This is considered sufficiently accurate relative to errors expected from deliberate changes.

38

5.3.1 Basic Computer System Checkout

Two separate but related computer programs were used to evaluate the circumferentially traversing microphone method of mode measurement. The first, or Radial Mode Program, computes a set of circumferential mode coefficients C_m^n (r_i) from an assumed set $C_{m\mu}^n$, which includes radial modes. Optionally, the deck can transform a set of C_m^n (r_i) to $C_{m\mu}^n$. As discussed in Appendix B, this program was formed from subroutines developed and documented elsewhere, its checkout consisting simply in running a case for which hand calculations were available in order to ensure the parts were assembled correctly.

The second, or Circumferential Mode Program, synthesizes the pressure field and rotor and traverse microphone angles as functions of time and allows for incorporation of deliberate errors of various sorts. It then performs the discrete Fourier transform required to recover the original mode amplitudes C_m^n. This second program incorporates all the novel features of the circumferentially traversing microphone method and, therefore, required a more thorough checkout. This was done by comparing output mode amplitudes with the known input values with no deliberate additional errors introduced. Agreement indicated proper functioning of the program.

A preliminary checkout of the results of the study of residual levels reported in Section 5.1 was made by evaluating various sums of exponentials for a large number of samples. The simulation produced levels much higher than had been expected, but investigation revealed this result to be associated with accumulated round-off error from the summing of a large number, typically 256,000, of single precision addends. Changing all operations from single to double precision eliminated this source of error, and the theoretical low residual levels of Section 5.1 were achieved. Since the cost of increasing precision was not very significant on the available computer, it was decided to do all programming for the Circumferential Mode Program in double precision.

Checkout cases were then run for this program. The first consisted of a single input mode, C_0^{32}, with a complex input level of $1 + i0 = 1\underline{/0^\circ}$. Targets included the input mode and several others covering a range thought to be typical and likely to uncover any problems. The rotor speed was selected as 100 rps, which is a convenient number near the range of the Pratt & Whitney Aircraft 10-inch rig. The traverse speed was 0.1 rps. The number of samples was selected as 256,000 and the time between samples was   t = 0.0000390625 seconds for a total run of 10 seconds. Contamination was not deliberately included.

The results are shown in Table 5-2. The input mode is seen to have been recovered correctly to eight decimal digits, corresponding to a loss of 0 dB relative to the input value 1. Contamination from the input mode generally did not affect the remaining modes, which have computed amplitudes of zero to eight decimals, corresponding to levels more than 166 dB below that of the input mode. The one exception to this statement is the M=0 N=288 target mode which is seen to be equal to the input mode. This frequency, $N\Omega$ = 28,800 Hz,

is one of the aliases of the input frequency 32 x 100 = 3,200 Hz, as discussed in Section 5.1 and in ref. 13, and, therefore, is as expected. If mode information were required at this higher frequency in an actual application, the sampling rate would be increased to eliminate the aliasing.

TABLE 5-2

RESULTS OF BASIC SYSTEM CHECKOUT WITH SINGLE INPUT MODE

Input

$m = 0$ $n = 32$ $C_0^{32} = 1 \underline{/0^0}$
Rotor Speed = 100 rev./sec
Traverse Speed = 0.1 rev./sec
Number of Time Increments = 256,000
Time Increment Between Samples = 0.0000390625 sec
Total Run Time = 10 sec

Output

	Target M	Target N	$|C_M^N|$ - Pressure Units	$|C_M^N|$ - dB re 1
Input Mode →	0	32	1.00000000	0
	1		.00000000	*
	32		.00000000	*
	0	33	.00000000	*
	32		.00000000	*
	0	256	.00000000	*
	1		.00000000	*
	2		.00000000	*
	0	288	1.00000000	0

* Greater than 166 dB below 1

Additional cases were run in which the number of input modes was increased to nine. The remaining input details were the same as in the previous case. Targets included some of the input modes as well as some assumed to be zero. A typical sample of the results is presented in Table 5-3. As can be seen, input modes were reproduced accurately and those not input produced zero output. It was,therefore, concluded that the program was operating correctly and ready to be used.

5.3.2 Effect of Pressure Rounding Error

In an actual application of the Traversing Microphone System, the pressure signal, p(t), is derived from a probe-mounted microphone and its associated electronics. Systematic errors such as harmonic distortion due to nonlinearities were assumed to have negligible effect on p(t). However, an attempt was made to quantify errors arising out of the digitizing process by rounding the simulated pressure values to various degrees and determining the resulting contamination for a large number of targets.

40

TABLE 5-3

RESULTS OF BASIC SYSTEM CHECKOUT WITH MULTIPLE MODE INPUT

Input

m	n	C
-16	32	$1\underline{/0^\circ}$
- 8		
- 4		
- 2		
0		
2		
4		
8		
16		

Output

	M	N	$\|C_M^N\|$ – Pressure Units	$\|C_M^N\|$ – dB re 1
Input Mode →	0	32	1.00000000	0
Input Mode →	16		1.00000000	0
	1		.00000000	*
	9		.00000000	*

*Greater than 166 dB below 1

For the first case run, the input traverse speed was 0.1 rev./sec, all values of n being set equal to 32. Total run time was 10 seconds. Time between successive samples was 0.0000390625, and the total number of samples was 256,000. To increase the number of distinct angular values used in the analysis transform $(M\theta - N\gamma)$ in eq. (4-2), rotor speeds were selected with values that were not small integer multiples of other parameters of the input. For this case, the value 100 + 200/9 was evaluated to the accuracy available in the double precision computer calculation, yielding a rotor speed of 122.222 . . . rev./sec. This procedure greatly increased the number of distinct angles used in the computer run.

Simulated pressures were computed at each instant of time for each input mode, m, and summed. The results were rounded to two decimal places, designated .xx, and then reduced. The effects of pressure rounding are shown in Table 5-4. Input modes were recovered quite well while noninput modes have levels approximately 85 dB below the reference input value of one pressure unit.

In order to determine the importance of the degree of rounding, a second series was run using only one input mode with the remaining simulation parameters as before. Results are presented in Table 5-5 for no rounding, rounding to two decimal places, .xx, and rounding to one decimal place, .x.

TABLE 5-4

EFFECT OF ROUNDING SIMULATED PRESSURES - SEVERAL INPUT MODES

Pressure Rounded to 2 Decimal Places (.XX)
Rotor Speed = 100 + 200/9 = 122.222... rev./sec
Traverse Speed = 0.1 rev./sec
Run Time = 10 sec
Input Amplitudes All = $1\underline{/0^0}$ Pressure Units
All n = N = 32

Input m	Target M	$|C_M^N|$ - Pressure Units	$|C_M^N|$ - dB re. 1
0	0	1.00006765	.00059
	1	.00006150	-84
2	2	1.00005894	.00051
	3	.00007121	-83
4	4	1.00005992	.00052
	5	.00004746	-86
6	6	1.00006335	.00055
	7	.00006109	-84
8	8	1.00005514	.00048
	9	.00006994	-83
10			
12			
14			
16			
18			
	27	.00006242	-84
	28	.00006561	-84
	29	.00005471	-85
	30	.00007549	-82
	31	.00004471	-87
	32	.00006487	-84
	33	.00005479	-85
	34	.00005446	-85
	35	.00006006	-84
	36	.00005776	-85
46			
48			
50			
52			
54			
	55	.00007029	-83
56	56	1.00006154	.00053
	57	.00006601	-84
58	58	1.00005765	.00050
	59	.00007357	-83
60	60	1.00005728	.00050
	61	.00006440	-84
62	62	1.00004586	.00040
	63	.00006396	-84
64	64	1.00006642	.00058

TABLE 5-5

EFFECT OF ROUNDING SIMULATED PRESSURE TO VARIOUS DEGREES - ONE INPUT MODE

Input

$m = 1$ $n = 32$ $C_1^{32} = 1\underline{/0^{\circ}}$ Pressure Units
Rotor Speed = $100 + 200/9 = 122.222...$ rev./sec
Traverse Speed = 0.1 rev./sec
Run Time 10 sec

Output

Rounding	M	N	$|C_M^N|$ - Pressure Units	$|C_M^N|$ - dB re 1
None	0	32	.00000307	-110
	1		1.00000296	.0000257
	2		.00000307	-110
	4		.00000307	-110
	16		.00000307	-110
	256		.00000307	-110
.XX	0	32	.00000218	-113
	1		1.00011299	.000981
	2		.00000365	-109
	4		.00000336	-109
	16		.00000355	-109
	256		.00000323	-110
	0	64	.00000795	-102
	1		.00000647	-104
	2		.00000671	-103
	4		.00000712	-103
	16		.00000643	-104
	256		.00000653	-104
.X	0	32	.00000533	-105
	1		1.00344668	.029000
	2		.00000646	-104
	4		.00000227	-113
	16		.00000532	-105
	256		.00000322	-110
	0	64	.00000878	-101
	1		.00000840	-102
	2		.00000783	-102
	4		.00000867	-101
	16		.00000780	-102
	256		.00000753	-102

For each amount of rounding. The input mode was recovered to approximately the same degree of accuracy. These simulations indicate that the effects of digitizing error are not significant contributors to errors in computed mode amplitudes.

5.3.3 Effect of Microphone Angle Error

A likely method for angle measurement with the Traversing Microphone System is as follows. A multitooth gear is attached to a shaft having a known mechanical speed ratio with respect to the traversing microphone axis. And a proximity transducer provides a series of electrical pulses as the gear teeth pass. The output of the transducer is digitized and the results processed to provide the required series of angle values. With this sort of device, two types of errors are probable and were studied by computer simulation for a variety of inputs. The first type is a systematic error; the second, a round-off error due to the digitizing process.

A systematic error could occur if, for example, the microphone accelerated as it traveled downward from top dead center and decelerated as it returned.

The equation selected to represent this type of behavior was

$$\theta = \theta_{True} + C_p \sin p \; \theta_{True}$$

where $p = 1$ for the example described.

The computer program was changed so as to modify the true value of θ, which was produced during the simulation portion of the program, by the above equation before being used in the analysis part of the program. Computer simulations were then made for a various numbers of error cycles, p, and error amplitudes, C_p. The remaining input values are shown in Table 5-6 together with the results of the computer simulation. Contamination of the noninput modes is in general low. The poorest results were for high M and for values of M near the input m, but even these would probably be acceptable for most applications. The figure of 0.1 degree (or six minutes) was judged to be attainable in practice, using state-of-the-art traverse angle measurement procedures.

Microphone traverse angles were then rounded to simulate digitizing error. Traverse speed was set to 0.1222... rev./sec to increase the number of distinct angular values used in the transform. Since the traverse speed was increased from 0.1 rev./sec, a compensating decrease in total run time was made to 8.181[+] sec, so that the total traverse would be comprised of only one complete revolution. Results of rounding are shown in Table 5-7 where the largest amplitude for a mode not included in the input is -88 dB, which is considered excellent.

44

TABLE 5-6

COMPUTED MODE AMPLITUDES WITH SYSTEMATIC ERRORS IN MICROPHONE ANGLE

Input

Input Mode Amplitude $1\angle 0°$ Pressure Units
Rotor Speed = 100 rev./sec
Avg. Traverse Speed = 0.1 rev./sec
Run Time = 10 sec

Output

No of Error Cycles	Error Amplitude (Degrees)	Input		Target		$\left\|C_M^N\right\|$ Pressure Units	$\left\|C_M^N\right\|$ - dB re 1
		m	n	M	N		
1	.1	1	32	1	32	.99999924	.000007
				2		.00174533	-55
				3		.00000343	-109
				5		★	★
				11		★	★
				1	33	★	★
				2		★	★
				3		★	★
				5		★	★
				11		★	★
				1	64	★	★
				2		★	★
				3		★	★
				5		★	★
				11		★	★
	.01			1	32	.99999999	0
				2		.00017453	-75
				3		.00000003	-150
				5		★	★
				11		★	★
	.1	128	32	128	32	.98756174	-0.1
				129		.11186193	-19
				130		.00640748	-44
				132		.00000732	-103
				138		★	★
4	.1	1	32	1	32	.99999924	.000007
				2		★	★
				3		★	★
				5		.00436328	-47
				11		★	★

★ Magnitude Less than 5 x 10^{-9} Physical Units and
Greater than 156 dB Below 1.

45

TABLE 5-7

COMPUTED MODE AMPLITUDES WITH ROUNDED MICROPHONE ANGLES

Input

    Angles Rounded to 0.1 Degree (.X)
    Rotor Speed = 100 rev./sec
    Traverse Speed = 0.1 + 2/90 = 0.1222... rev./sec
    Run Time = 8.181^{+} sec $\approx$ 1 Microphone Revolution
    m = 16   n = 32 C_{16}^{32} = 1$\angle 0^{o}$ Pressure Units

Output

M	N	$|C_M^N|$ - Pressure Units	$|C_M^N|$ - dB re 1
16	32	.99676576	-.028
17		.00003265	-90
18		.00000709	-103
20		.00000376	-108
24		.00000293	-110
16	64	.00003893	-88
17		.00001551	-96
18		.00000713	-103
20		.00000897	-101
24		.00001090	-99

5.3.4 Effect of Rotor Angle Error

Measurement of rotor angle is expected to be similar to traverse angle
measurement and result in the same sort of errors. A computer simulation
similar to that in the previous section was made to evaluate the systematic
and round off errors for this parameter. The computer program was modified to
adjust the rotor angle, γ, according to the following

$$\gamma = \gamma_{True} + D_q \sin q \, \gamma_{True}$$

which is the same form as for the traverse-angle study.

Input parameters and results of the systematic error study are shown in Table
5-8 and can be seen to be quite favorable. The effects of rounding to 0.1
degree are shown in Table 5-9 and are also excellent. Comparisons of these
results with those of the traverse angles study of Tables 5-6 and 5-7 show
that the systematic error with amplitude of 0.1 degree resulted in a larger
contamination when the error was in the rotor angle rather than the traverse
angle. For the rounding study, errors in the traverse angle resulted in larger
contaminations. It is expected that a more detailed analysis would show how
these results are related to the particular values of input variables
selected. The main conclusion from these two studies, however, is that since
results are acceptable for a large variety of inputs, a detailed analysis is
not needed.

TABLE 5-8

COMPUTED MODE AMPLITUDES WITH SYSTEMATIC ERRORS IN ROTOR ANGLE

Input

All Input $C_m^n = 1 \underline{/0^\circ}$ Pressure Units
Avg. Rotor Speed = 100 rev./sec
Traverse Speed = 0.1 rev./sec
Total Run Time 10 sec

No of Error Cycles	Error Amplitude (Degrees)	Input m	n	Target M	N	$\left\|C_M^N\right\|$ Pressure Units	$\left\|C_M^N\right\|$ - dB re 1
1	.1	1	32	1	32	.99922033	.006775
					33	.02878599	-31
					34	.00044004	-67
					48	★	★
					64	★	★
					65	★	★
	.01				32	.99999260	.000065
					33	.00287878	-51
					34	.00000440	-107
					48	★	★
					64	★	★
					65	★	★
	.1			16	32	★	★
					33	★	★
					34	★	★
					48	★	★
					64	★	★
					65	★	★
64	.1			1	32	.99922038	.006774
					33	★	★
					34	★	★
					48	★	★
					64	★	★
					65	★	★

★ Magnitude Less than 5×10^{-9} Physical Units and
Greater than 166 dB Below 1.

TABLE 5-9

COMPUTED MODE AMPLITUDES WITH ROUNDED ROTOR ANGLES

Input

    Angles Rounded to 0.1 Degree (.X)
    Rotor Speed = 100 + 200/9 = 122.22...rev./sec
    Traverse Speed = 0.1 rev./sec
    Run Time = 10 sec
    m = 16   n = 32 $C_{16}^{32} = 1\underline{/0^0}$ Pressure Units

Output

$\underline{M}$	$\underline{N}$	$\|C_M^N\|$ – Pressure Units	$\|C_M^N\|$ – dB re 1
16	32	.98706775	-0.113
17		.00000172	-115
18		.00000172	
20		.00000172	
24		.00000172	
16	64	.00001441	-97
17		.00001440	
18		.00001440	
20		.00001439	
24		.00001437	

5.3.5 Effects of Random Noise in Pressure Signal

The presence of broadband random noise has always been a source of difficulty
when measuring the coherent, discrete frequency components of fan noise.
Consider first a fixed microphone in the inlet duct, which may be either one
of an array of microphones, or a fixed position of a step-traverse. In the
absence of random noise, a very short time sample of the microphone signal,
corresponding to one rotor revolution, is sufficient to determine amplitude
and phase values of every harmonic of shaft frequency. The process can be
implemented by digital sampling of the signal, so that sampling is initially
triggered by a rotor position pulse. Subsequent samples of the wave are
obtained at intervals Δt apart, where Δt is small enough to prevent aliasing.
The resulting wave form (continuous or sampled as just described) can be
Four   analyzed by a computer to give amplitude and phase values of all
har.   s or orders of fan shaft frequency, BPF and its multiples being of
principal interest.

For determination of the circumferential mode structure associated with a
specific order, such as BPF, such measurements are replicated at a plurality
of circumferential locations. The number of such locations must at least equal

twice the highest order circumferential mode that can propagate at the specific order, which leads to a large number of microphones in large scale fans. In the absence of random noise, the large number of microphones can be replaced by a plurality of measurements taken by a single microphone that is step-traversed circumferentially. Consistent phase information is preserved among these readings, taken at different times during the run, by means of the rotor shaft trigger feature that initiates the time sweep. (There are problems here if the rotor speed varies during the total run and if also there are significant time delays involved in the propagation of modes from their source to the microphone plane) Since, ideally, the total recording time required at each microphone location is only a fraction of a second (one fan shaft revolution) the total running time for the test is not long, and is governed by how quickly the traverse can be stepped accurately from one circumferential location to the next.

The presence of random noise changes these features significantly. At a particular microphone location, the pressure signature recorded over one shaft revolution now differs from that obtained over another revolution. The extent of tne difference depends on the relative levels of the broadband noise and the coherent discrete frequency components. In practical fans the broadband signature contaminates the periodic component of the waveform.

Signal processing techniques have been available for some time to recover the periodic waveform (and/or its Fourier components) from the noise-dominated total signal. Such phrases as "signal enhancement," "waveform eduction," "synchronous detection," "periodic sampling," have been used for various processes that are basically similar, although possibly differing in some details. In essence, all methods for recovering the coherent signal from its noisy background employ time-averaging.

For the example used above to introduce the subject, suppose now that random noise is present in the signal. Values of the pressure, triggered at successive rotations of the fan, are no longer identical. The periodic component does repeat at each shaft impulse but the random contribution will generally differ with each sample. If digitization is initiated at a shaft impulse and proceeds at intervals Δt, the resulting waveform will be "hashy," like the continuous, pre-digitized wave. Now, to "enhance" the periodic component of the signal, let there be a set of data registers, each corresponding to some multiple of Δt, with the first register corresponding to the instant that the shaft impulse triggers the digitizing. Samples from several shaft rotations are accumulated in the registers, the first register receiving samples that all correspond to the shaft impulses, the next register storing samples taken Δt after the impulses, and so forth. After many such samples are stored, the accumulated readings are each divided by the sample number. The sum due to the periodic component, being the sum of identical readings will grow, and upon division, will give the value that would have been obtained during any single rotation in the absence of noise. On the other hand, the sum in each register due to the random noise will not grow in this manner. If the random signal has zero mean value the positive and negative contributions to each register tend to cancel out. It is clear that the time average of the random component in each register can be made as small as we please by taking a sufficiently large number of samples.

After a sufficiently large number of samples have been taken and averaged in this manner, the enhanced waveform will approach the pattern that would exist in the absence of random noise. The process is usually stopped when this waveform is considered to be "sufficiently smooth" in the judgment of the data-processing analyst. At that point, the enhanced waveform is Fourier analyzed for the harmonic coefficients that give amplitude and phase of the coherent, discrete frequency components of the sound field at that microphone location. This process is repeated at the number of microphone locations required for modal analysis. Since the time spent at each location to enhance the signal is comparatively long if the random component is large, the total running time for the test can easily become prohibitive.

Now it will be recognized that, since the operations of signal averaging and Fourier analysis, described above, are linear, their order of execution can be interchanged. This would serve no purpose in the foregoing mode analysis method, but it would be possible, if desired, to Fourier analyze the hashy signal over one revolution for the BPF component, to repeat this Fourier analysis for many successive revolutions, and to then average the resulting coefficients. This would give the BPF component amplitude and phase with the same accuracy as obtained originally.

This is essentially what is done in the Traversing Microphone System. During the entire run, consisting of perhaps several thousands of rotor revolutions, the traversing microphone signal is Fourier-analyzed (in parallel during the computation process) for one or two rotor harmonics (BPF and 2BPF usually) and for a plurality of corresponding modal frequencies, $\omega_M = N\Omega - M\Gamma$. During such a run, many thousands of samples are taken. For each target mode, in the absence of random noise, the product of the target mode component in the signal and the rotor generated signal, ω_M^N, will be identical and the average of the process will be the desired mode coefficient, C_M^N. (It has been shown that the components of off-target modes, $n \neq N$, $m \neq M$, will vanish). When random noise is added to the microphone signal, its contributions at the sampling instants will tend to zero average, as with the fixed microphone, since the Fourier and averaging operations are interchangeable.

It is thus seen that the traversing microphone method automatically provides "signal averaging" or "enhancement" of coherent versus broadband noise, and that no additional steps are needed specifically to obtain enhancement. While it is clear that any degree of enhancement or broadband noise reduction can be achieved with sufficiently long run time, a quantification of this enhancement is needed.

For this purpose it is helpful to examine the nature of the broadband noise present at the traversing microphone and displayed in its signal. The modal power spectral density function of fan broadband noise is useful here, and is represented in Figure (5-6). This function corresponds to the (amplitude) modal-frequency spectrum of coherent discrete frequency fan noise, described earlier and shown in Figure 3-3. Since the frequency distribution of random noise is continuous the delta functions or spikes, located at $(m, n\Omega)$, in the coherent modal spectrum, are now represented as "ridge lines" over which the

MODAL PSD S(m,ω), ALONG DASHED LINE

CONTRIBUTE TO MICROPHONE SIGNAL PSD, S(ω')

$S(\omega') = \Sigma_m S(m,\omega' + n\Gamma)$

$S(\omega')$

CIRCULAR FREQUENCY ω, ω'

POWER SPECTRAL DENSITY, S

CIRCUMFERENTIAL MODE NUMBER, m

-2   -1   0   1   2
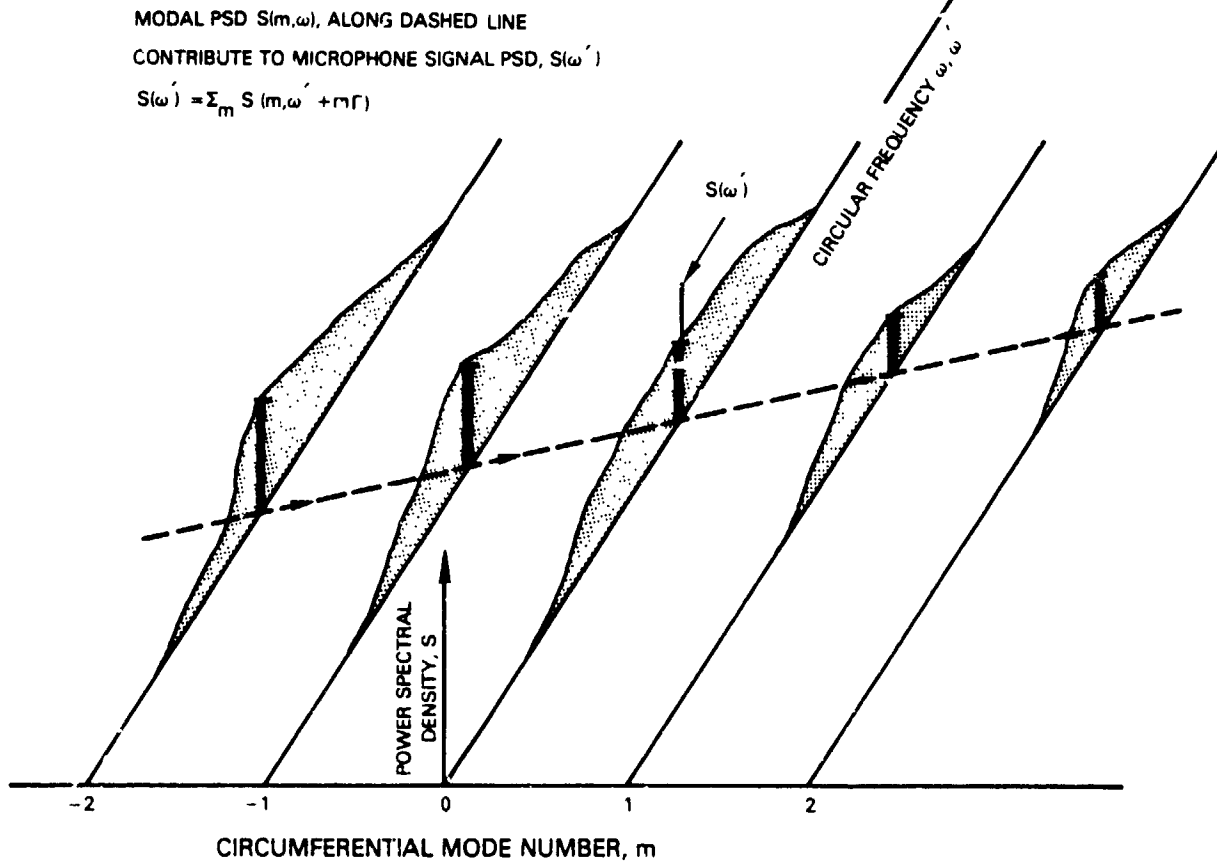
Figure 5-6   Modal Power Spectral Density Function for Random Noise
                  S(m,ω) and Resulting Microphone Signal S(ω')

power spectral density, $S(m,\omega)$ varies continuously with frequency. These
lines exist only for $\pm$ integer values of circumferential mode, m, as in the
coherent case.

It can be shown, (ref. 2), that in a so-called homogeneous fan duct field,
where the statistical properties of the random signal are independent of
θ-position, that the total power spectral density at any θ-location, $S(\omega)$ is
the sum over m of the modal psd: $S(\omega) = \sum_m S(m,\omega)$. This is just the sum of the
modal power spectral densities of all of the modal components.

Now it has been seen that, for the traversing microphone system to be able to
separate the modes corresponding to discrete harmonics, n, of fan speed, the
signals from neighboring harmonics, (n+1) must not have frequencies in
rotating coordinates, ω', that overlap those corresponding to harmonic n. This
requirement led to an upper bound for traverse speed Γ. Figure 5-3 showed how

51

modes at discrete frequencies in stationary coordinates transform to tone clusters in the rotating microphone coordinate system. A similar relation exists for the modal power spectral density function. However, due to the continuous frequency distribution, all propagating modes now contribute to the psd of the traversing microphone signal at any frequency, ω'. This relation is indicated in Figure 5-6 and makes it quite clear that the traversing microphone system is incapable of separating the random signal into its modal constituents. (For this purpose the methods described in ref. 2 and 8 may be used.)

The power spectral density of the traversing microphone signal can be expressed in terms of the modal psd, $S(m,\omega)$ and the traverse speed, Γ, as:

$$S(\omega') = \sum_{m} S(m, \omega' + m\Gamma) \tag{5-14}$$

If $\Gamma = 0$ the result is, of course, the psd of the signal from a stationary microphone at any θ-location in a homogeneous field. Since traverse speed is low (< 1 Hz) the broadband spectra of the traversing microphone is almost identical with that of a stationary microphone signal.

Although the traversing microphone system cannot be used to determine random modal psd, random noise seriously affects the results of applying the method to measure coherent, discrete frequency noise. To evaluate this effect we consider processing a random signal with the transforms previously employed, initially using the uniformly weighted transform.

In digital form the transform of the zero mean random signal, $r(t)$, is

$$y_i = \frac{1}{Q} \sum_{q=0}^{Q-1} r(t_i + t_q) \, \text{expi}(\omega_M^N t_q) \tag{5-15}$$

Here $\omega_M^N = N\Omega - M\Gamma$ is the target frequency. It is taken that the signal present is only $r(t)$, with no coherent modes present (or no mode corresponding to m=M, n=N). The initial time, t_i enters into the process, as it does in extracting coherent modes, where it will affect phase of the output, y, and this dependence is indicated by use of the i subscript.

Since r is a random variable, so also will be the result, y_i. Because y_i is a complex random variable, the most meaningful measure of its behavior concerns its amplitude, phase having little meaning, if any, in the random case. The easiest quantity to obtain is the square of its amplitude, $y_i y_i^*$, and since y_i is random, we require the mean or expected value of $y_i y_i^*$, $E(y_i y_i^*)$. It will be appreciated in advance that the actual value of the magnitude of y_i determined for a specific run will depend on the initial time, t_i, and the target frequency, ω_M^N, in any particular measurement, and will therefore deviate from the mean value. This mean value will now be found from:

52

$$E(y_i \ y_i^\star) = \frac{1}{Q^2} E\left\{\sum_{q=0}^{Q-1} r(t_i+t_q)\text{expi}\,\omega_M^N t_q \cdot \sum_{\ell=0}^{Q-1} r(t_i+t_\ell)\text{expi} -\omega_M^N t_\ell\right\} \qquad (5\text{-}16)$$

where the dummy index q is changed in the second sum to ℓ.

The expected value of a typical term in the expansion will be

$$E\left\{r(t_i+t_q)\cdot r(t_i+t_\ell)\text{expi}\,\omega_M^N(t_q-t_\ell)\right\} \qquad (5\text{-}17)$$

On substituting $\ell - q = k$ and $t_\ell - t_q = k\Delta\tau$, this becomes

$$E\left\{r(t_i+t_q)\cdot r(t_i+t_q+k\Delta\tau)\ \text{expi} -\omega_M^N k\Delta\tau\right\} \qquad (5\text{-}18)$$

The expected value of $r(t)\cdot r(t+\tau)$ is the autocorrelation function, $R(\tau)$, of the signal, $r(t)$, so that the typical term of eq. (5-18) can be written as

$$R(k\Delta\tau)\ \text{expi} -\omega_M^N k\Delta\tau \qquad (5\text{-}19)$$

In eq. (5-16) there are Q terms of the form of eq. (5-19) with k = 0, (Q-1) terms with k = ± 1, etc., and finally one term with k = $\pm$ (Q-1). Thus eq. (5-16) may be reduced to

$$E\ (y_i \ y_i^\star) = \frac{1}{Q} \sum_{k=-(Q-1)}^{Q-1} \left(1 - \frac{|k|}{Q}\right)\cdot R(k\Delta\tau)\ \text{expi}(-\omega_M^N k\Delta\tau) \qquad (5\text{-}20)$$

Now the autocorrelation function can be replaced by the following Fourier transform of the power spectral density

$$R(k\Delta\tau) = \int_{-\infty}^{\infty} S(\omega')\ \text{expi}\ (\omega' k\Delta\tau)d\omega' \qquad (5\text{-}21)$$

Substituting in eq. (5-21) and interchanging the order of integration and summation results in

$$E(y_i\ y_i^\star) = \int_{-\infty}^{\infty} S(\omega') \left\{ \frac{1}{Q} \sum_{k=-(Q-1)}^{Q-1} (1 - \frac{|k|}{Q})\ \text{expi}\ (\omega' - \omega_M^N)k\Delta\tau \right\} d\omega' \qquad (5\text{-}22)$$

It can be verified that with $\Delta\tau = \Delta t = T/Q$, the expression in $\{\ \}$ brackets equals the square of the magnitude of the sum

$$\left| \frac{1}{Q} \sum_{q=0}^{Q-1} \text{expi}\ (\omega' - \omega_M^N)q\Delta t \right|^2 \qquad (5\text{-}23)$$

Since this sum is the system frequency response function

$$\left| \frac{1}{Q} \sum_{q=0}^{Q-1} \text{expi}\ (\omega' - \omega_M^N)q\ \Delta t \right|^2 = \left[\frac{\sin(\omega' - \omega_M^N)T/2}{(\omega' - \omega_M^N)T/2} \right]^2 \qquad (5\text{-}24)$$

$$= \text{diff}^2(\omega' - \omega_M^N)T/2$$

The expected value of the square of the amplitude of the transform is simply

$$E(y_i\ y_i^\star) = \int_{-\infty}^{\infty} S(\omega')\ \text{diff}^2(\omega' - \omega_M^N)\ T/2\ d\omega' \qquad (5\text{-}25)$$

For a constant power spectral density in the neighborhood of the target frequency, ω_M^N, the expected value is just $S(\omega_M^N)$ times the area under the square of the transform frequency response function, diff $(\omega' - \omega_M^N)T/2$.

Since the widths of the main lobe and sidelobes of diff() are inversely proportional to T, the response to random noise, as measured by $E(y_i\ y_i^\star)$ can be reduced to any desired level by use of a sufficiently long averaging time, T. Hamming weighting combined with double averaging time will be additionally effective in essentially eliminating the side lobes of the diff function. The appropriate expression for $E(y_i\ y_i^\star)$ for this case is obtained by replacing diff() in eq. (5-25) by the Hamming response function, Hamm(), given by eq. (5-9).

Computer simulated tests were run to illustrate the performance of the traversing microphone system in measuring coherent blade passage frequency modes in the presence of broadband random noise. The random signal was simulated by a random sequence generated with a computer subroutine, whose

values were added at each instant, t_q, to the computer-simulated pressure due to selected coherent input modes. With input modes of unit peak amplitude, a root-mean-square random sequence of 12.8 units was used, giving a signal to (total) noise ratio of about -25 dB.

The first run employed 256,000 data points over a 10 second interval. In addition to the two unit input modes, C_0^{12} and C_{32}^{32}, other null input modes were targeted. Results are shown in Table 5-10.

TABLE 5-10

EFFECT OF BROADBAND NOISE ON COMPUTED MODE STRUCTURE

Input

$C_0^{32} = C_{32}^{32} = 1\underline{/0^0}$ Pressure Units
$\sigma_{noise} = 12.82$
Rotor Speed = 100 rev./sec.
Traverse Speed = 0.1 rev./sec
Number of Time Increments = 256000
Time Increment Between Samples = 0.0000390625 sec
Total Run Time = 10 sec

Output

M	N	$\left\|C_m^n\right\|$ - Pressure Units	$\left\|C_m^n\right\|$ - dB re 1
0	32	.977429	- .19
1	32	.017377	-35.
16	32	.054900	-25.
31	32	.043502	-27.
32	32	.913269	- .79

At targets corresponding to the null input modes the indicated results are relatively low, on the order of 30 dB below the unit coherent inputs. The input mode (0, 32) result is substantially unity (0.98 vs. 1). However, the (32, 32) mode reading at 0.913 has been seriously affected by the presence of random noise. If the random noise in this band had been at a level of about that measured in the other target bands, this C_{32}^{12} modal coefficient would have been obtained with accuracy comparable to the C_0^{12} mode. This specific result is not an anomaly, but rather reflects a property of applying a Fourier transform to a random function (ref. 13). This property is that repeated transforms of the random function, with a particular "target" frequency, display considerable scatter about their expected value, and also, that neighboring target values of the transform during any one run display significant variance. This scatter, which is on the order of the mean value itself, can account for some readings of coherent modes being satisfactory, while other modes are more seriously contaminated.

As eq. (5-25) shows, and consistent with other methods of enhancement, the contaminating effects of the random signal can be reduced by increasing run time. This corrective effect was next demonstrated by computer simulation.

For illustrative purposes, instead of increasing the run time beyond the previous 256,000 point run, a shorter run of 64,000 points was made to establish a new baseline, in order to save computation time.

The results of this new baseline are shown in Table 5-11, column 1. In this run the input unit coherent mode was (m=1, n=16). Next, Hamming weighting was applied, together with twice as long a run, to restore the original bandwidth and eliminate side lobes of the response function.

TABLE 5-11

EFFECT OF INCREASING RUN TIME ON RANDOM NOISE REJECTION
WITH HAMMING WEIGHTED SYSTEM

Input

C_1^{16} = 1$\underline{/0^0}$ Pressure Units
Rotor Speed = 100 rev./sec
Traverse Speed = 0.1 rev./sec
Time Increment Between Samples = 0.00015625 sec

Output

Time Increments		64000	128000	384000
Target		Baseline With No Hamming	Hamming 2 Turns	Hamming 6 Turns
M	N	$\left|C_M^N\right|$ - dB re 1	$\left|C_M^N\right|$ - dB re 1	$\left|C_M^N\right|$ - dB re 1
1	16	- .38	.08	- .02
2	16	-15	- 27	-24
3	16	-19	- 28	-22
4	16	-18	- 20	-25
8	16	-27	- 20	-29
16	16	-23	- 29	-27
32	16	-18	- 25	-27
1	17	-20	- 32	-40
1	18	-21	- 19	-28
1	32	-20	- 18	-27
Average Contamination		-20	-24	-28

Results of this case are given in column 2 and show a general reduction of 24 dB for null input targets. Column 3 corresponds to a 6-turn run, three times as long. An average reduction of about 4 more dB was achieved (vs 4.7 theoretically).

56

It is not possible to determine in advance, on the basis of such computer simulated tests, the specific run time required to conduct actual fan noise tests on a particular rig. For this purpose, the spectrum in the immediate neighborhood of the blade pasage frequency must be estimated. More elaborate computer simulation of the noise than that employed here would be necessary.

However, in an actual fan test it will be possible to determine when sufficient averaging time has been achieved. A conservatively long run of data should first be recorded, based on spectral estimates and further experience. Then, a reasonable segment of the total run should be processed. With a slight refinement of the basic traversing microphone method, it is possible to target frequencies where there will be no coherent modal signals. Several such null targets will yield an estimate of the very local power spectral density, and from this estimate, the probability that the neighboring mode coefficients have been affected by noise to an unacceptable degree can also be estimated. If this process indicates that a longer run should be made to further reduce the effects of broadband noise contamination, further data from the original recording can then be processed. By such a procedure, the accuracy required for a specific application can be achieved. This area of application of the traversing microphone method should be explored in more detail.

5.3.6 Errors in Circumferential-Radial Mode Coefficients, $C_{m\mu}^n$

The error investigation up to this point has focused on the circumferential mode coefficients C_m^n. When an actual measurement is made on a rig or engine, these C_m^n with their associated errors will be determined at a set of different radii resulting in a set of circumferential mode coefficents $C_m^n(r_i)$. The algorithm of Section 4.3 will then be used to determine a set of circumferential-radial coefficients, $C_{m\mu}^n$, for each m, n pair of interest. In this section, the impact of the errors in $C_m^n(r_i)$ on the final mode coefficients, $C_{m\mu}^n$, are studied with computer simulation and results of a complete test simulation are shown (i.e., one involving both simulation and both reduction algorithms).

The check of the effects of errors in the $C_m^n(r_i)$ was accomplished by a series of computer simulations using the Radial Mode Program discussed in Section 5.3.1 and Appendix B. After a set of $C_m^n(r_i)$ was formed by the simulation portion of the program from an assumed set of $C_{m\mu}^n$, the set was rounded and used as input to the reduction portion of the program, which recomputed the $C_{m\mu}^n$ with the included effects of the rounding errors.

Parameters for the first series of simulations were based on the Pratt & Whitney Aircraft 10-inch rig. For a hub-tip ratio of 0.437 and a normalized outer wall radius of one, the annulus was divided into five equal parts, and a microphone was assumed to be located at the center of each. From this, the normalized microphone radii used for this run were 0.4933, 0.6059, 0.7185, 0.8311, and 0.9437. A single input mode was given an amplitude $1\angle0^o$, and various larger sets that included the input were targeted. Results have meaning up to a target set size of 5 (the number of microphones), beyond which the matrices involved in the algorithm become singular. Inputs were selected

from various high and low m values for various cases, and it was found that the largest contamination occurred when the target set size equaled the number of microphones.

A typical example is shown in Table 5-12 for an input $m=1, \mu=0$ mode. The table includes the effects of no rounding, rounding inputs to 3 decimal places, and rounding to 2 decimal places. In all cases contamination of non-input modes by the round off noise is negligible. Based on previous work, ref. 1, this was not surprising since the condition number, CN, for this case was a low 9.07. As described in the reference, the condition number is the ratio of the extreme eigenvalues of a matrix and provides a measure of the magnification of relative errors in solving the matrix equation Ax=y. With one as a lowest possible value, values below 10 gave excellent solutions. Values in the hundreds gave good solutions. Values above 10,000, however, were unsatisfactory.

TABLE 5-12

CALCULATED MODE STRUCTURE
($\sigma = 0.437$, 5 Microphones, CN = 9.07)

Input

$m = 1 \quad \mu = 0 \quad C_{1,0} = 1\underline{/0^{\circ}}$ Pressure Units

Output

m	μ	No Rounding $\|C_{m\mu}\|$ - dB re 1	Input Rounded to .XXX (3 Decimal Places) $\|C_{m\mu}\|$ - dB re 1	Input Rounded to .XX (2 Decimal Places) $\|C_{m\mu}\|$ - dB re 1
1	0	- .00001	.00287	- .03568
1	1	- 110	- 72	- 52
1	2	- 109	- 70	- 55
1	3	- 119	- 96	- 80
1	4	- 113	- 85	- 49

A larger size input array was then selected, and a 10 microphone array was used. The annulus between $r' = r/b = 0.437$ (b is the outer wall radius) and $r' = 1$ was divided into ten equal parts, and the microphone was located in the center of each section, similar to the previous set of runs. Input $C_{m\mu}^{n}$ values and results of the computer simulation are shown in Table 5-13 for the cases of no rounding and rounding to 2 decimal places. For this case the condition number was 138 and, accordingly, the results were seen to be good. Modes input were recovered to within 0.1 dB and those not input were at least 40 dB below the input levels.

58

TABLE 5-13

CALCULATED MODE STRUCTURE
(σ = 0.437, 10 Microphones, 10 Modes Targeted, CN = 138)

m	μ	Input $C_{m\mu}$	No Input Rounding Output $\|C_{m\mu}\|$ - dB re 1	Input Rounded to 2 Decimal Places Output $\|C_{m\mu}\|$ - dB re 1
12	0	0	- 97.	- 43
	1	1 $\angle 0^0$	.00009	- .085
	2	1 $\angle 45^0$	- .00007	- .084
	3	-1	.00002	.036
	4	0	- 104	- 54
	5	1 $\angle 135^0$	.00001	.075
	6	0	- 122	- 56
	7	0	- 103	- 42
	8	0	- 110	- 56
	9	1 $\angle 270^0$	.00004	.052

To simulate measurement in a full-scale engine at moderate distances from the
fan face, a case was run with 10 microphones, for a hub-tip ratio of zero. The
normalized radius r' = 1 was divided into 10 equal parts and the microphone
was assumed to be located at the center of each segment. Five modes were
input with levels 1$\angle 0^0$, as shown in Table 5-14. Even without rounding, the
results were seen to be very poor, as might be expected when the condition
number of 5.1 x 10^5 is noted. In an attempt to overcome this problem, it was
recalled that the radial mode algorithm provides for least square curve
fitting, utilizing more microphones than the number of target modes. A
simulation case was therefore tried which targeted 7 modes using the same 10
microphone locations discussed in the preceeding paragraph. The results are
shown in Table 5-15. This procedure can be seen to have reduced the condition
number to 2.25 and the results became satisfactory (contamination at least 30
dB below input) even with rounding to 2 decimal places.

TABLE 5-14

CALCULATED MODE STRUCTURE
(σ = 0, 10 Microphones, 10 Modes Targeted, CN = 5.1 X 10^5)

m	μ	Input $C_{m\mu}$	No Rounding Output $\|C_{m\mu}\|$ - dB re 1
8	0	1$\angle 0°$	- .1
8	1	0	- 40.2
8	2	1$\angle 0°$	- .1
8	3	0	- 27.1
8	4	1$\angle 0°$	- 1.9
8	5	0	- 4.1
8	6	1$\angle 0°$	- 15.0
8	7	0	+ 2.1
8	8	1$\angle 0°$	- 10.9
8	9	0	- 15.7

TABLE 5-15

CALCULATED MODE STRUCTURE
(σ = 0, 10 Microphones, 7 Modes Targeted, CN = 2.25)

m	μ	Input $C_{m\mu}$	Output $|C_{m\mu}|$ - dB re 1 With input Rounded To 2 Decimal Places
8	0	0	- 39
8	1	0	- 47
8	2	0	-102
8	3	0	- 47
8	4	0	- 48
8	5	0	- 46
8	6	$1\underline{/0°}$	+ 0.1

Since the higher order modes tend to concentrate their energies away from the central axis of the duct, it might be expected that the determination of mode coefficients is very sensitive ᴠ minute measurement errors near r'=0. It might aiso be expected that a microphone distribution which concentrated the microphones toward the outer duct wall could be found which would make the calculation less sensitive to errors and allow fewer microphones to be used. Since work on the radial portion of the algorithm was not the primary task in this contract, no additional work was done to optimize microphone location. However, this topic should be pursued as considerable data reduction time and expense can be saved by reducing the required number of test radii.

The final case run with constant rotor and traverse speed was a checkout of the complete system to determine the combined effects of errors iᴠ the Traversing Microphone System and in the Radial Mode computation. A set of $C^n_{m\mu}$ was selected using as a partial guide results oᴠ mode measurements with flusn mounted microphones in the Pratt & Whitney Aircraft 10-inch rig, as reported in reference 2. The synthesis portion of the Radial Mode Program was then used to determine a set of circumferential mode amplitudes, $C^n_m(r_i)$. This set of amplitudes was used as input for the synthesis portion of the Circumferential Mode Program. Synthesized pressures were rounded and a new set of circumferential amplitudes was determined by the reduction portion of the Circumferential Program, using these rounded pressures. The output $C^n_m(r_i)$ containing the effect of the pressure rounding was then used with the reduction portion of the Radial Mode Program to produce a set of $C^n_{m\mu}$, containing the effects of the pressure rounding, whicn were compared with the original $C^n_{m\mu}$ set to evaluate the entire system.

A mode measurement test was described in Case 4 of reference 2, which utilizeu a 32 bladed rotor with a stator of 34 rods in a duct with hub-tip ratio = 0.437. At twice blade passage frequency (n=64) and a rotor speed of 5813 rpm, 53 modes were supported by the duct geometry; however, the rotor-stator interaction produced a strong m = -4 lobe patterr. With this information as

background, seven of the possible propagating modes were selected and given
assumed input values. Four were given values of $1+i0=1\underline{/0^0}$ for convenience.
Amplitudes for the m = -4 modes were obtained by using values from the
reference normalized so that the largest value had a magnitude of 1. This was
done to give some reasonable variation to the input values. The duct annulus
was divided into five equal radial segments, and four microphones were assumed
to be located where the segments touch. The input was then processed using the
procedure outlined in the previous paragraphs and the final results were
tabulated. The results can be compared with the input in Table 5-16. Modes
input were reproduced with accuracy to about 3 significant figures. Modes with
no input amplitudes suffered some contamination, but the worst mode amplitude
was about 54 dB below the typical input of 1.

TABLE 5-16

INPUT AND OUTPUT CIRCUMFERENTIAL-RADIAL MODE AMPLITUDES
FOR COMPLETE SYSTEM CHECKOUT

(Input Assumed Mode Amplitudes - $C_{m\mu}^{64}$ - Pressure Units)

	$\mu = 0$		$\mu = 1$		$\mu = 2$	
	Real	Imag	Real	Imag	Real	Imag
m = 3	1	0	1	0	-	-
m = -4	-.9259	.3778	.4244	-.2983	.1505	-.2231
m = 7	-	-	1	0	-	-
m = 12	1	0	-	-	-	-

(Output Computed Mode Amplitudes - $C_{m\mu}^{64}$ - Pressure Units)

	$\mu = 0$		$\mu = 1$		$\mu = 2$	
	Real	Imag	Real	Imag	Real	Imag
m = 3	1.0003	.0000	1.0007	.0000	.0007	-.0001
m = -4	-.9267	.3779	.4241	-.2991	.1508	-.2229
m = 7	.0005	-.0002	1.0005	.0000	-.0011	-.0004
m = 11	.0005	.0019	-.0001	-.0007	.0007	.0013
m = 12	.9997	-.0001	.0012	-.0007	-.0006	.0002

Table 5-17 shows the intermediate input and output to the circumferential
program portion of the test. Good agreement between input and output here
indicates pressure rounding does not produce serious errors, a result which
was seen previously in Section 5.7.2. Small errors here produced small errors
in the Radial Mode deck leading to overall excellent performance of the
system.

61

TABLE 5-17

INPUT AND OUTPUT CIRCUMFERENTIAL MODE AMPLITUDES FOR COMPLETE SYSTEM CHECKOUT

(Input Mode Amplitudes, $C_m^{64}(r_i)$, Computed From Assumed $C_{m\chi}$)
(Pressure Units)

	r_1 = 2.7666 in.		r_2 = 3.3333 in.		r_3 = 3.9002 in.		r_4 = 4.4670 in.	
	Real	Imag	Real	Imag	Real	Imag	Real	Imag
C_3^{64}	.73112	-	.60519	-	.39358	-	.19725	-
C_{-4}^{64}	.09723	-.13312	-.08466	.01846	-.28919	.14831	-.42652	.19259
C_7^{64}	.29568	-	.35275	-	.20836	-	-.08737	-
C_{12}^{64}	.00621	-	.03265	-	.10530	-	.21856	-

(Output $C_m^{64}(r_i)$ -- From Circumferential Mode Program - Pressure Units)

	Real	Imag	Real	Imag	Real	Imag	Real	Imag
C_3^{64}	.73165	.00015	.60539	-.00030	.34339	.00033	.19729	-.00011
C_{-4}^{64}	.09698	-.13324	-.08495	.01774	-.28958	.14858	-.42673	.19266
C_7^{64}	.29554	-.00043	.35292	.00048	.20891	-.00026	.08727	.00004
C_{11}^{64}	.00011	.00023	.00021	.0.024	-.00013	-.00020	.00006	.00033
C_{12}^{64}	.00631	.00027	.03266	-.00029	.10572	-.00014	.21857	-.00006

5.4 SUMMARY OF SYSTEM CHARACTERISTICS - CONSTANT SPEED

Analytical and computer-aided studies were conducted to determine the effects
of system parameters upon operation of the traversing microphone system.
Effects upon accuracy of deviations from ideal operating conditions, such as
input measurement errors and random noise were also evaluated. The principal
results are listed below.

• There are three input quantities to the system that are measured and,
consequently, subject to error: instantaneous microphone pressure, fan
shaft angle, and microphone traverse angle. Due to the digitized nature of
the input, these quantities are all subject to truncation or roundoff
error. Further, both angle readings are subject to systematic or
calibration error due to possible imperfections in laying out a digitized
angle scale. It is assumed that the microphones will be sufficiently free
from harmonic distortion so that systematic pressure errors may be ignored.

• A variety of forms of systematic angle error together with several
magnitudes were used in computer-simulated tests to determine the effects
of rotor and traverse angle input errors. With input errors that might
reasonably be expected from angle measurement devices, the errors in
circumferential mode coefficients were acceptable.

- Similarly, rounding errors due to digitizing fan and traverse angle readings to the nearest 0.1 degree were found to have acceptably small effect upon the accuracy of the circumferential mode coefficents.

- The system was extremely tolerant of large rounding errors introduced by the digitization of the microphone pressure signals. Rounding to the nearest 0.1 unit of pressure with maximum input mode strength of 1 pressure unit had negligible effect on the computed mode coefficients.

On the basis of these results it is concluded that the effects of errors in angle and pressure measurement that range from reasonable to large have acceptably small impact upon the accuracy of the computed circumferential mode coefficients.

In real fans broadband noise is present in addition to the coherent discrete frequency blade-passage harmonics. The traversing microphone system, like other, conventional methods for discrete mode measurement, must enhance the coherent signals with respect to the random noise. This enhancement is accomplished in the system by means of time-averaging, which is also the basis for other enhancement procedures.

- To evaluate the performance of the traversing microphone system in recovering coherent modes in the presence of broadband noise, computer-simulated tests were conducted using known input modes and a computer-generated random signal. The rms level of the random noise was about 25 dB above the levels of the modal signals. In this first run the results were mixed: some modal coefficients were recovered with acceptable accuracy, but others were excessively affected by the random noise. These results are typical for processing a random signal by a Fourier transform.

- Two steps were taken to demonstrate how these results can be improved. First, Hamming weighting was incorporated in the transform process to reduce the frequency response to random noise components that are more distant from the target mode. When the run time was doubled to compensate for increased main lobe width, the results were improved.

- Secondly, the run time was further increased in steps. With each doubling of time, the mean level of the system output due to broadband noise decreased by about 3 dB.

- These results show that the effects of broadband noise can be reduced to any desired level by use of sufficiently long averaging, a property common to other enhancement methods. The value of time required in practice will depend on the broadband noise characteristics of the specific fan.

- Since details of the broadband noise of a specific fan can only be estimated roughly prior to actual test, the traversing microphone method should employ a procedure that allows successively longer portions of the entire data acquisition run to be processed. By observing the effects of successively longer runs upon the results it should be possible to decide when sufficient enhancement has been completed.

- It is consi*ered advisable to develop in more detail the process for deciding when sufficient averaging time has been achieved, in order to avoid either excessive test and processing time on one hand, or insufficient data on the other.

The Traversing Microphone System computing procedure is organized to first compute the circumferential mode coefficients at each of the microphone radial locations. Corresponding to a specific circumferential mode, the set of these circumferential coefficients is then used as input to obtain the corresponding radial-circumferential mode coefficients, the final output of the entire process. The next phase of the error investigation concerned the accuracy of the final radial-circumferential mode coefficients, when errors were introduced into the input circumferential modes. Two fan geometries were used. One, the Pratt & Whitney Aircraft 10-inch fan rig (having a hub-tip ratio of 0.437) and the other, the JT9D engine, was taken as zero hub-tip ratio to represent the full cylindrical inlet section. The following results were obtained:

- A variety of combinations of input modes were simulated for the 0.437 hub-tip ratio fan, including a case where 10 radial modes could propagate. In all cases, using no more microphone locations than the number of propagating radial modes, excellent results were obtained for the output mode coefficients when inputs were rounded to 2 decimal places. Input target modes were in error by at most 0.1 dB and modes with null input strength were indicated as below -40dB. Much greater errors would still be acceptable in practice for the final radial-circumferential mode coefficients.

- When similar tests were simulated for the JT9D, zero hub-tip ratio geometry, the results differed drastically. With the number of microphones set equal to the number of propagating modes, the computed coefficients were seriously in error as a consequence of the poor condition number of the system of equations.

- The unsatisfactory state of the zero hub-tip ratio geometry was found to be correctable by employing 3 or 4 microphones more than the number of propagating radial r   . With this arrangement, comparable accuracy to that of the 0.437 hu .ip ratio cases was obtained. The system condition number returned to its previous low value, presumably due to the least squares fitting of the data that is implied by the computing algorithm.

- These results indicate that in cases where the traversing microphone method is to be used in actual tests on a low hub-tip ratio engine or rig, further studies should be made to determine the optimum radial placement of the microphones in order to minimize their number and the corresponding number of data channels. Because of the typical radial mode pattern, microphones will probably be concentrated near the outer wall.

Successful use of the Traversing Microphone System depends upon selecting its design and operating parameters to comply with certain requirements which are

64

summarized below. Generally, these requirements depend upon both the extent and accuracy of the modal information being sought, and also upon certain characteristics of the specific fan to be tested.

There are five principal parameters that must be selected in order to run a traverse test and process the data:

Traverse speed, Γ
Traverse turns, R
Run time, T
Digitizing rate, Q/T
Number of radial microphone positions, I

Rules that govern selection of these parameters are listed:

- **Traverse speed, Γ** . An upper bound to the allowable traverse speed depends upon the highest harmonic, n, of fan shaft speed for which modal coefficients are to be determined. This bound is given in terms of the fan speed, Ω, by

  $$\Gamma / \Omega < 1/(2n + 1)$$

  Unless this restriction is followed, modes of the nth fan shaft harmonic will be subject to contamination from noise associated with the (n+1)st harmonic. For measuring up to and including twice blade passage frequency, (n=2B) on the P&WA 10-inch fan at 6000 rpm, the highest allowable traverse speed is about 0.8 rps. On the JT9D engine at 2400 rpm the traverse speed should not exceed 0.2 rps.

  There is no comparable, clear-cut lower bound for the traverse speed. However, to minimize the undesirable effects of fan speed variations, and also to expedite signal enhancement in the presence of broadband noise, the traverse speed should be selected as high as is convenient, consistent with the above upper bound.

- **Traverse turns, R.** Data for processing must correspond to an integer number of complete traverse revolutions. Under ideal, constant fan speed, zero random noise conditions, one turn is sufficient. With Hamming weighting, 2 turns are the required minimum. However, due to fan speed variations and to random noise, several complete turns may be needed. The specific number cannot be established in advance. For a particular fan test, speed variation effects must be analyzed and broadband noise estimates must be made. These will provide a basis for estimating the R requirement.

- **Traverse time, T.** Time, speed, and traverse turns are, naturally, related. It will be most convenient to select speed as high as is conveniently possible, as described previously. Then, provided only that R is integer greater than 2, R will follow from the approximate run time, T, required. This run time, T, will be determined by the level of fan broadband noise

in the neighborhood of the fan harmonics; more specifically the signal-to-noise ratio. As run time increases, the broadband noise effect is reduced as a result of signal enhancement. The extent of enhancement required to produce modal coefficients with a prescribed accuracy cannot be determined accurately in advance of the test. Consequently, a conservatively long run time must be allowed for in the data acquisition. How much of the data need to be processed for prescribed accuracy can be established during the data-processing phase. Details of the procedure will be clarified with further study and will lead to sharper specification of the required run time.

- <u>Digitizing rate, Q/T, for microphone signal</u>. For the information recorded during a test run to be processed, it must be supplied to the computer in digital form. It will be most accurate, and probably most convenient, to employ digital transducers directly for measurement of fan shaft angle and microphone traverse angle. Since pressure measuring microphones deliver an analog signal, these signals must be digitized for subsequent processing. The digitizing rate, or sampling frequency, is set by the well-known (Nyquist) criterion: Digitizing rate must exceed twice the highest frequency contained (at a significant level) in the analog signal to be digitized. This requirement dictates that the microphone signals be low-pass filtered by analogue filters prior to digitizing. If for example, a top frequency of twice blade passage (2BPF) will be analyzed for mode structure, an analog filter that is essentially flat to 2BPF and then falls to -40 dB at 4BPF could be used for pre-filtering. The resulting filtered signal would then be sampled at a rate of 2 x 4BPF or a frequency of 8BPF.

- <u>Number of radial microphones, I</u>. The number of microphones must at least equal the highest number of propagating radial modes present at the highest fan frequency of interest. This number will be associated with the m=0 circumferential mode and should be determined before test. For fans with hub-tip ratios greater than about 0.5, a number of microphones equal to the number of propagating modes was found to be sufficient. For lower hub-tip ratio fans, 3 or 4 more microphones were found to be essential for acceptable accuracy. For twice blade passage frequency, the 10-inch P&WA fan rig at 6000 rpm required 5 microphones for determining 5 radial modes. The zero hub-tip ratio JT9D fan inlet at 2400 rpm needed 10 radial microphone locations to evaluate 7 radial modes. These requirements, including possible variation of microphone placement from equi-spaced locations, may be modified to optimize the procedure as a result of further study.

66

6.0 SYSTEM CHARACTERISTICS - VARIABLE SPEED

6.1 BACKGROUND

Rotor speed variations during mode measurement tests on engines and fan rigs have long been recognized as a source of inaccuracy. As fan speed changes slightly, the phase of each mode, as measured at a microphone distance x from the source, will shift according to the change in $k_{xm\mu} x$. If two or more modes contribute to the microphone pressure, the resulting signal will change in amplitude as well as phase. Even if only a single mode is present, the standard use of a time-averaging procedure to enhance the coherent signal with respect to broadband noise will lead to a false value for the modal amplitude.

In order to understand how this problem affects the traversing microphone system (and all mode measurement methods as well) an analysis of the propagation of modes under conditions of small variations in frequency or speed has been made. Before describing this unsteady analysis, a simple, quasi steady-state interpretation is given first.

6.2 SIMPLE INTERPRETATION OF EFFECT OF SPEED VARIATIONS

The essential results of the effects of speed variation on mode measurement are most easily determined by considering the pressure at a fixed microphone location due to but a single (m, μ) mode. If the rotor plane is considered to be the source location, then at a distance x forward in the duct, at some fixed angle and radius, the pressure can be written as

$$p(x,t) = Re\left\{C_{m\mu} \, expi \, (k_{xm\mu} x - \omega t)\right\} \qquad (6\text{-}1)$$

where $\quad \omega = n\Omega$

and $\quad k_{xm\mu} = \sqrt{k^2 - k_{m\mu}^2} \quad$ for ignorable axial Mach number

$\qquad k = \omega / c$

$\qquad k_{m\mu} = $ eigenvalue for (m, μ) mode.

Under constant speed conditions, if the circular frequency is designated by ω_0, the modal pressure can be represented in the complex plane in the conventional manner shown in Figure 6.1a. The phase angle of the modal signal, $\phi = k_{xo}x$, is measured with respect to a rotor-generated reference signal of frequency $\omega_0 = n\Omega_0$.

Now let the speed change slightly by $\Delta\Omega$. There will eventually be a change in phase at the microphone given by $\Delta\phi = \Delta(k_x x)$, as shown in Figure 6.1b.

The magnitude of the phase shift can be obtained in terms of the frequency change, $\Delta\omega$ (corresponding to the speed change $\Delta\Omega$), from
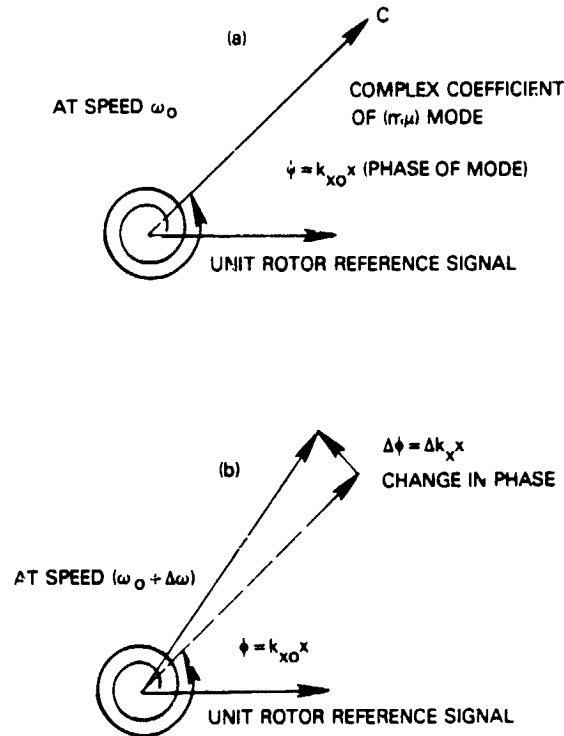
Figure 6-1   Effects of Speed Change on Modal Phase

$$\Delta\phi = \Delta(k_x x) \approx \frac{dk_x}{d\omega}\Big|_{\omega_0} \Delta\omega\, x \qquad (6-2)$$

The quantity $d\omega/dk_x$ is called the group velocity, V_g, for the (m,μ) mode at $\omega = \omega_0$. Then

$$\Delta\phi = \Delta\omega \frac{x}{V_g} \text{ , and if } \frac{x}{V_g} \text{ is called the delay time, } \tau \text{ , the phase shift}$$

can be expressed as   (6-3)

$$\Delta\phi = \Delta\omega\, \tau$$

Suppose that a measurement run is made in which the frequency is $\omega_0 + \Delta\omega$ for half the time, and drops to $\omega_0 - \Delta\omega$ for the remainder. Figure 6-2a shows this speed variation and the corresponding two values of the complex pressure, phase shifted $+ \Delta\phi = + \Delta\omega\tau$ from the orientation that would correspond to the mean frequency, ω_0. Because time averaging is used to suppress random noise, the measured signal is the average of the two extreme complex pressures shown. This average signal has an amplitude which is reduced by the factor $\cos(\Delta\omega\tau)$. It is clear that if the speed variations take the form of a "square wave" of any frequency, the same result obtains. This attenuation of modal signal amplitude is here called "Loss of Signal."

68

TIME AVERAGED SIGNAL = $\overline{C(\omega)}^t$

SPEED VARIATION	MODAL COEFFICIENT VARIATION	RESULTING SIGNAL

(a)

$\omega_0 + \Delta\omega$

ω_0

$\omega_0 - \Delta\omega$

$C(\omega_0 + \Delta\omega)$

$+\Delta\omega\tau$

$-\Delta\omega\tau$

$C(\omega_0 - \Delta\omega)$

SIGNAL $= \underbrace{C \cdot \cos(\Delta\omega\tau)}_{\text{LOS}}$

COMPLETE LOS
FOR $\Delta\omega\tau = \pi/2$

(b)

$\omega_0 + \Delta\omega$

ω_0

$\omega_0 - \Delta\omega$

SIGNAL $= \underbrace{C \cdot J_0(\Delta\omega\tau)}_{\text{LOS}}$

COMPLETE LOS
FOR $\Delta\omega\tau = 765\pi$

(c)

$\omega_0 + \Delta\omega$

ω_0

$\omega_0 - \Delta\omega$

SIGNAL $= C \cdot \underbrace{\dfrac{\sin(\Delta\omega\tau)}{\Delta\omega\tau}}_{\text{LOS}}$

COMPLETE LOS
FOR $\Delta\omega\tau = \pi$

Figure 6-2   Effects of Three Types of Speed Variation on Resultant Mode
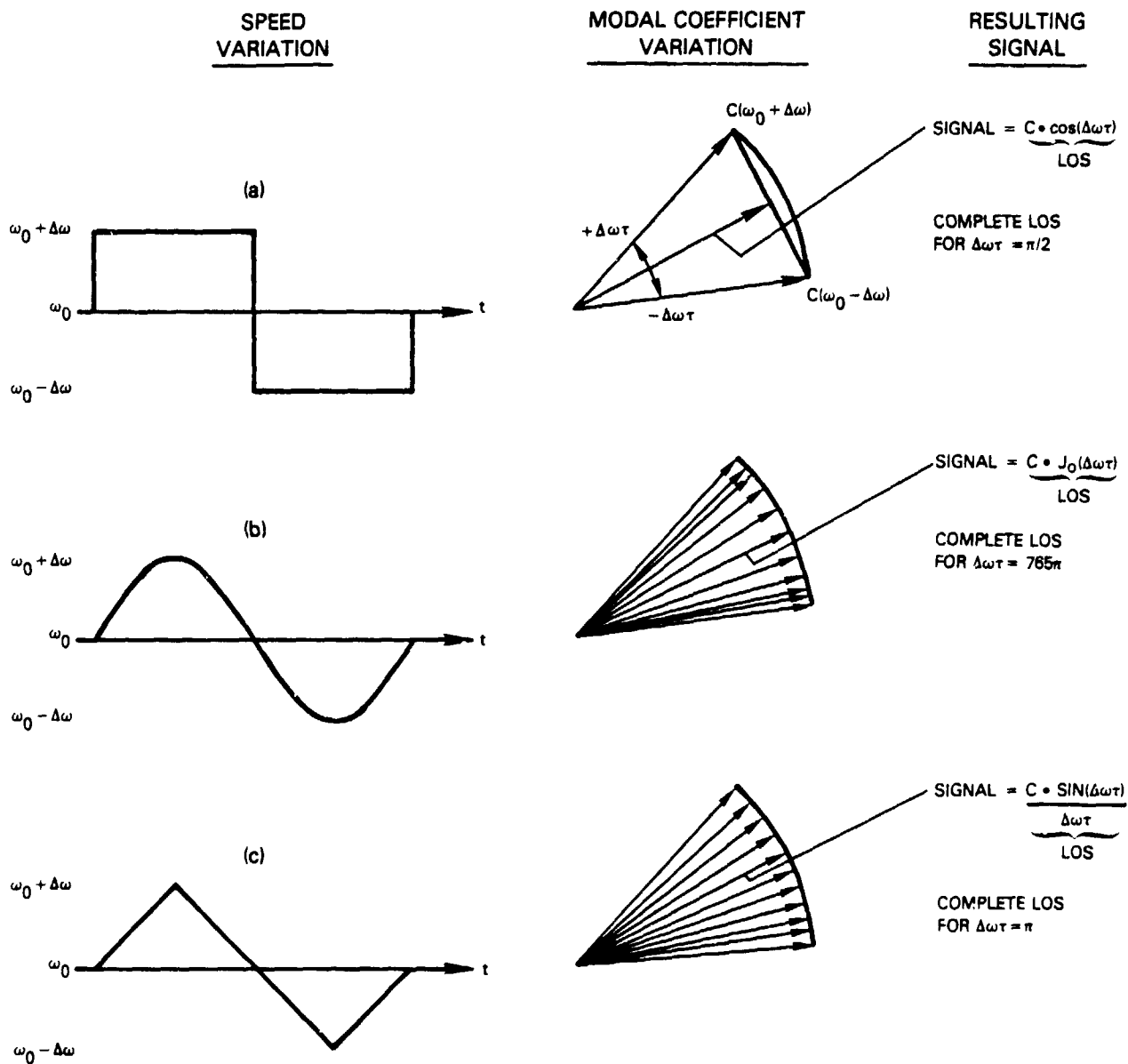   Coefficient

Figures 6-2b and 6-2c illustrate the effect of two other types of speed variation - sinusoidal and sawtooth. The expressions for the corresponding loss of signal (LOS) will be developed presently. The foregoing analysis for a one cycle square wave is obviously applicable, except possibly for transient effects in the neighborhood of the $2\Delta\omega$ frequency jump. It is not obvious, however, that the other forms of speed variation shown in Figures 6-2b and 6-2c, can also be analyzed on the same quasi steady-state basis. For this reason, and because the microphone pressure must be related to the rotor reference signal in the traversing microphone method, it is necessary to develop a more fundamental approach to the speed variation process.

6.3 PROPAGATION OF MODES DURING SPEED VARIATIONS

Corresponding to a single (m, μ) mode, the pressure distribution in a reference plane, $x = 0$, which may be considered the source location, under constant frequency $(\omega = \omega_0)$, operation may be expressed as

$$p(0, t, r, \theta) = Re\{P(0, t, r, \theta)\}$$

where $P(0, t, r, \theta) = C_{m\mu} \, \psi_{m\mu}(r, \theta) \, expi - \omega_0 t$

If the eigenfunction, $\psi_{m\mu}(r, 0)$ is suppressed for simplicity this becomes

$$P(0, t) = C_{m\mu} \, expi - \omega_0 t, \tag{6-4}$$

which gives the temporal behavior of the mode at $x = 0$ for constant frequency.

If this mode is "switched on" at $t = 0$, the pressure at location x will be

$$p(x, t) = Re\{C_{m\mu} \, expi \, [k_{xm\mu}(\omega_0) x - \omega_0 t]\}$$

$$+ \text{transient}$$

For times sufficiently long for the transient to decay, the solution is simply

$$p(x, t) = Re\{P(x, t)\}, \tag{6-5}$$

where $P(x, t) - C_{m\mu} \, expi \, [k_{xm\mu}(\omega_0) x - \omega_0 t]$

Consider now the behavior when the frequency varies (see ref. 14). Specification of the time dependence at $x = 0$ requires the replacement of the angle $\omega_0 t$, for constant frequency, by the integral

$$\int_0^t \omega(t)dt, \text{ giving}$$

$$P(0, t) = C_{m\mu} \, expi \, [- \int_0^t \omega(t) \, dt] \tag{6-6}$$

70

Suppose that the frequency varies by a small amount, $+\Delta\omega$, about a mean value, ω_0, and let this variation be harmonic, with frequency, ν, that is small compared to ω_0

$$\omega(t) = \omega_0 + \Delta\omega \cos(\nu t + \phi) \tag{6-7}$$

Then, $$\int_0^t \omega(t)dt = \omega_0 t + \frac{\Delta\omega}{\nu} \sin(\nu t + \phi) + b \tag{6-8}$$

where b is the constant of integration, $-\frac{\Delta\omega}{\nu} \sin\phi$.

The source pressure is then

$$P(0, t) = C_{m\mu} \text{ expi } [-\omega_0 t - \frac{\Delta\omega}{\nu} \sin(\nu t + \phi) - b] \tag{6-9}$$

$$= C_{m\mu} \text{ expi } - (\omega_0 t + b) \text{ expi } [\frac{-\Delta\omega}{\nu} \sin(\nu t + \phi)]$$

The second exponential is a familiar expression in the analysis of frequency-modulated signals and can be expanded (ref. 14) according to the generic form

$$\text{expi}(x \sin\alpha) = \sum_{q=-\infty}^{\infty} J_q(x) \text{ expi } q\alpha \tag{6-10}$$

There results

$$P(0,t) = C_{m\mu} \sum_{q=-\infty}^{\infty} J_q\left(\frac{\Delta\omega}{\nu}\right) \text{ expi } - [(\omega_0 + q\nu) t + q\phi + b] \tag{6-11}$$

The source pressure is thus expressed as a linear combination of harmonic motions involving the mean frequency, ω_0, and the sidebands, $\omega_0 \pm \nu$, $\omega_0 \pm 2\nu$, etc.

Consequently, the pressure at x may be found as the superposition of the $P(x,t)$ appropriate to each of the modulated frequencies, implied by eq. (6-11). If the source is "switched on" at t=0, with a behavior given by eq. (6-11), then after the transients have decayed, the pressure at x will accordingly be given by

$$P(x,t) = C_{m\mu} \sum_{q=-\infty}^{\infty} J_q\left(\frac{\Delta\omega}{\nu}\right) \text{ expi } \left\{[k_{xm\mu}(\omega_0+q\nu)]x-(\omega_0+q\nu)t-q\phi-b\right\} \tag{6-12}$$

where $k_{xm\mu}$ $(\omega_0 + q\nu)$ is the axial wavenumber evaluated at frequencies $(\omega_0 + q\nu)$.

For small frequency variations about a mean, ω_0, that are not too close to cutoff, the wavenumber can be approximated by

$$k_{xm\mu}(\omega_0 + q\nu) = k_{xm\mu}(\omega_0) + d\, k_{xm\mu} \qquad (6\text{-}13)$$

$$= k_{xm\mu}(\omega_0) + \left.\frac{dk_{xm\mu}}{d\omega}\right|_{\omega_0} q\nu$$

The expression $\left.\dfrac{dk_{xm\mu}}{d\omega}\right|_{\omega_0}$ is the reciprocal of the group velocity, $V_{gm\mu}$, for

the mode.

Then the quantity $[k_{xm\mu}(\omega_0 + q\nu)]$ x in eq. (6-12) can be written as

$$k_{xm\mu}(\omega_0 + q\nu)x = k_{xm\mu}(\omega_0)x + q\nu \frac{x}{V_{gm\mu}}$$

The factor $x/V_{gm\mu}$ is the time delay for the changes in frequency in the wave to arrive at station x, and will be called $\tau_{m\mu}$

$$\tau_{m\mu} = \frac{x}{V_{gm\mu}} = \left.\frac{dk_{xm\mu}}{d\omega}\right|_{\omega_0} \cdot x \qquad (6\text{-}14)$$

So

$$k_{xm\mu}(\omega_0 + q\nu)x = k_{xm\mu}(\omega_0)x + q\nu\,\tau_{m\mu}$$

and eq. (6-12) becomes

$$P(x,t) = C_{m\mu}[\text{expi } k_{xm\mu}(\omega_0)x] \sum_{q=-\infty}^{\infty} J_q\left(\frac{\Delta\omega}{\nu}\right)\text{expi-}[(\omega_0+q\nu)t - q\nu\,\tau_{m\mu} + q\phi + b]$$

$$= C_{m\mu}[\text{expi } k_{xm\mu}(\omega_0)x][\text{expi-}\omega_0\tau] \sum_{q=-\infty}^{\infty} J_q\left(\frac{\Delta\omega}{\nu}\right)\text{expi-}[(\omega_0+q\nu)(t-\tau_{m\mu}) + q\phi + b] \qquad (6\text{-}15)$$

Comparing eq. (6-15) and (6-11) it is seen that the q-sum in (6-15) can be obtained from that in (6-11) by replacing t with $(t-\tau_{m\mu})$. Accordingly, the pressure at x can be obtained from the pressure at 0 by

$$P(x,t) = P[0,(t - \tau_{m\mu})] \text{ expi } [k_{xm\mu}(\omega_0) x - \omega_0 \tau_{m\mu}] \tag{6-16}$$

This result shows that a variable frequency wave at one location is replicated at a more distant location after a characteristic time delay, $\tau_{m\mu}$. While eq. (6-16) was derived on the basis of a single frequency harmonic modulation it is clear that the same result holds for more general frequency variations, provided that the total excursion about the mean frequency is sufficiently small to allow the approximation for the change in wavenumber used in eq. (6-13).

The exponential factor in eq. (6-16) is of interest. It is a phase shift of the signal that may be interpreted readily by applying eq. (6-16) to the special case of constant frequency, $\omega = \omega_0$. In this case the result is

$$P(x,t)=[C_{m\mu} \text{ expi- } \omega_0(t - \tau_{m\mu})]\left\{\text{expi}[k_{xm\mu}(\omega_0)x- \omega_0 \tau_{m\mu}]\right\}$$

Here the quantity in square brackets is $P[0,(t - \tau_{m\mu})]$, the pressure at $x=0$ for $\omega = \omega_0$, time delayed by $\tau_{m\mu}$. Combining exponentials

$$P(x,t) = C_{m\mu} \text{ expi}[k_{xm\mu}(\omega_0) x- \omega_0 t]$$

which is the obvious constant frequency result, exhibiting the phase shift $k_{xm\mu}(\omega_0)x$ with respect to the wave at $x=0$.

Another form of the phase shift factor in eq. (6-16) may be obtained. Replace: $\tau_{m\mu}$ by $x/V_{gm\mu}$, and $k_{xm\mu}$ by $(k_{xm\mu}/\omega_0)\omega_0 = \omega_0/V_p$, where $\omega_0/k_{xm\mu}$ is the phase velocity, $V_{pm\mu}$. Then

$$k_{xm\mu}(\omega_0) \ x - \omega_0 \tau_{m\mu} = \omega_0 x \cdot \left(\frac{1}{V_{pm\mu}} - \frac{1}{V_{gm\mu}}\right)$$

For highly propagating modes the phase and group velocities are approximately equal, so this phase shift vanishes and the relation becomes

$$P(x,t) \underset{\omega_0 \to \infty}{\longrightarrow} P(0,(t-\tau_{m\mu}))$$

The phase shift between $x = 0$ and $x = x$ in this case is given entirely by $P(x,[t - \tau_{m\mu}]) - P(0,[t - \tau_{m\mu}])$, which amounts to $\omega_0 \tau_{m\mu} = \omega_0 x/c$ = kx in the case of negligible flow velocity.

Another case of interest is the one discussed in Section 6.2 to introduce the subject: Let the frequency be constant at ω_0 for a time, and then let it suddenly change to $\omega_0 + \Delta\omega$ and remain there. By inserting these two steady state values in eq. (6-16) it is verified that the phase of $P(x,t)$ and also the phase of $P[0,(t - \tau_{m\mu})]$ changes by $\Delta\omega \tau_{m\mu}$, as was obtained by the quasi steady-state analysis of Section 6.2.

These results, which govern the propagation of variable frequency waves in general, will now be applied specifically to determine the behavior of the traversing microphone system under variable speed operating conditions.

6.4 EFFECTS OF SPEED VARIATIONS ON TRAVERSING MICROPHONE SYSTEM

6.4.1 Effect of Traverse Speed Variation

Before considering the effects of rotor speed, Ω, variation, described above, upon the traversing microphone system, the results of deviations from constant traverse speed, T, will be examined, in order to clear the way for discussion of the more significant topic of variable rotor speed.

Under constant rotor speed, Ω, and allowing for traverse speed variations by writing $\theta = \theta(t)$ in place of Tt, the transform of the pressure for the mth circumferential mode of target order $n = N$ is, neglecting previously discussed conjugate terms:

$$Tr\left\{p_m^N(t)\right\} = \frac{1}{T} \int_{t_1}^{t_1+T} p_m^N(t)\, V_M^N(t)\, dt$$

$$= \frac{1}{2} C_m^N \; \frac{1}{T} \int_{t_1}^{t_1+T} \exp i\,[m\theta(t)-N\Omega t]\cdot\exp i\,-[M\theta(t)-N\Omega t]\,dt$$

$$= \frac{1}{2} C_m^N \; \frac{1}{T} \int_{t_1}^{t_1+T} \exp i[(m-M)\theta(t)]\,dt \tag{6-17}$$

In the important case of the target $m = M$ mode, the integrand is unity so the result is perfect:

$$Tr\left\{p_M^N(t)\right\} = \frac{1}{2} C_M^N \tag{6-18}$$

For the off-target, $m = M$, modes, it has been seen in Section 5.1 that when θ is a linear function of time (T = constant), the integral vanishes if the length of run, T, corresponds to one or more complete revolutions of θ .

If traverse speed $T(t)$ departs from constant value, T_0, by a small variation, $g(t)$, we can write

$$T(t) = T_0 + g(t) \tag{6-19}$$

so $\qquad \theta(t) = \int_0^t T(t)\,dt = T_0 t + G(t) \tag{6-20}$

where $\qquad G(t) = \int_0^t g(t)dt$ will be small compared with $\Gamma_0\, t$ and, of course, is

nonlinear.

Then, eq. (6-17) becomes

$$Tr\left\{C_m^N\right\} = \frac{1}{2} C_m^N \; \frac{1}{T} \int_{t_1}^{t_1+T} expi\; [(m-M)\; \Gamma_0 t + (m-M)\; G(t)]\; dt$$

$$= \frac{1}{2} C_m^N \; \frac{1}{T} \int_{t_1}^{t_1+T} expi\; [(m-M)\; \Gamma_0 t]\cdot expi\; [(m-M)G(t)]dt \tag{6-21}$$

If $G(t)$ is small in $t_1 < t < (t_1 + T)$ the second factor will be approximately constant over the integration, so that the result will be approximately zero instead of vanishing exactly.

To estimate this effect of traverse speed variation, computer simulated runs were made for both linear and sinusoidal types of speed variations. For the example of linear speed variation, $g(t)$ was chosen as 0.001t. With Γ_0 equal to 0.1 and a run time of 10 sec, this corresponded to a 10% speed change at the end of the run. This unrealistically large speed variation was selected in order to demonstrate the departures from constant speed more clearly.

Results of the simulation are shown in Table 6-1. Contamination of modes not input is seen to fall off as the difference between input and target m number becomes large. Even with this rather unrealistic speed variation results are acceptable.

Sinusoidal speed variation was simulated by the relation

$$g(t) = \Delta\Gamma \sin 2\frac{\pi \mathcal{L}}{T}t$$

where $\Delta\Gamma$ is the amplitude of the variation and $\mathcal{L}$ is the number of complete cycles of variation in the run time, T. Results of this simulation are shown in Table 6-2 for a $\Delta\Gamma = 0.001$ and both one and four cycles of speed variation. Contamination in this case is clearly insignificant.

6.4.2 General Formulation for Rotor Speed Variation

For analytical investigation of the effect of speed variations, the integral form of the order transforms of Sections 3 and 4 will be used

$$Tr\left\{p(t)\right\} = \frac{1}{T} \int_{t_1}^{t_1+T} p(t)\; W(t)\; V_M^N(t)\; dt \tag{6-22}$$

where $\qquad V_M^N(t) = expi\; -\; [M\theta(t)-N\gamma(t)]$ \qquad\qquad\qquad (6-23)

75

TABLE 6-1

EFFECT OF LINEAR ACCELERATION OF TRAVERSE MICROPHONE ON COMPUTED MODE AMPLITUDES

Input

C_0^{32} = 1$\angle 0°$ Pressure Units
Rotor Speed = 100 rev./sec
Traverse Speed = 0.1 + 0.001 t rev./sec
Number of Time Increments = 244349
Time Increment Between Samples = 0.0000390625 sec

Total Run Time = 9.54+ sec

Output

m	$\left|c_m^{32}\right|$ Pressure Units	$\left|c_m^{32}\right|$ - dB re 1
0	1.00000409	0.000036
1	.01449415	- 37
2	.00725714	- 43
4	.00362829	- 49
8	.00181279	- 55
16	.00090537	- 61
32	.00045265	- 67

TABLE 6-2

EFFECT OF SINUSOIDAL SPEED VARIATION OF TRAVERSE MICROPHONE ON COMPUTED MODE AMPLITUDES

Input

C_0^{32} = 1$\angle 0°$ Pressure Units

Rotor Speed = 100 rev./sec
Traverse Speed = .1 + .001 sin $(2\pi\ell t/T)$ rev./sec
Number of Time Increments = 256000
Time Increment Between Samples = .0000390625 sec
Total Run Time = 10 sec

Output

m	ℓ = 1 $\left|c_m^{32}\right|$ - Pressure Units	$\left|c_m^{32}\right|$ - dB re 1	ℓ = 4 $\left|c_m^{32}\right|$ - Pressure Units	$\left|c_m^{32}\right|$ - dB re 1
0	1.00000000	0	1.00000000	0
1	.00050000	- 66	.00000024	- 132
16	.00000024	- 132	.00000024	- 132
31	.00000024	- 132	.00000024	- 132
32	.00000024	- 132	.00000024	- 132

is the target signal for the Mth circumferential mode of order N. $\theta(t)$ is microphone angle, $\gamma(t)$ is rotor shaft angle, $W(t)$ is identically one for uniform weighting and, for Hamming weighting, is given by eq. (4-4).

Based on the preceeding analysis of the propagation of variable frequency waves, the expression for the pressure of the (m,μ) mode will be taken as

$$p_{m\mu}^n(t) = Re\left\{C_{m\mu}^n \text{ expi } [m\theta(t)-n\gamma(t-\tau_{m\mu}^n)]\right\} \qquad (6-24)$$

This expression is used in place of the full expression for p, which involves m and μ summation, to simplify the resulting forms so that the effects of nonlinear shaft angle variations and delay time will stand out more clearly. Further, the phase shift factor of eq. (6-16) is suppressed for similar reasons; it may be considered to be lumped with the mode coefficient, $C_{m\mu}^n$. The delay time, $\tau_{m\mu}$, is the time for a speed change in the fan rotor to be sensed by the microphone responding to the (m,μ) mode. It is generally different for all modes and also includes any $\sim$ namic delay for modes excited by the interaction of the rotor wakes with downstream stators.

With eq. (6-24) for pressure, the transform of eq. (6-22), using uniform weighting becomes

$$Tr\left\{p_{m\mu}^n(t)\right\} = \frac{1}{2} C_{m\mu}^n \frac{1}{T} \int_{t_1}^{t_1+T} \text{expi } [m\theta(t) - n\gamma(t - \tau_{m\mu}^n)] \text{ expi } -[M\theta(t) - N\gamma(t)]dt$$

The conjugate terms are omitted since they are small, as has been described in Section 3. This expression becomes

$$Tr\left\{p_{m\mu}^n(t)\right\} = \frac{1}{2} C_{m\mu}^n \frac{1}{T} \int_{t_1}^{t_1+T} \text{expi}[(m-M)\theta(t)-n\gamma(t-\tau_{m\mu}^n) + N\gamma(t)] dt \qquad (6-25)$$

We can make the approximation

$$\gamma(t-\tau_{m\mu}^n) = \gamma(t)-\tau_{m\mu}^n \frac{d\gamma(t)}{dt} \qquad (6-26)$$

$$= \gamma(t)-\tau_{m\mu}^n \Omega(t)$$

So that

$$Tr\left\{p_{m\mu}^n(t)\right\} = \frac{1}{2} C_{m\mu}^n \frac{1}{T} \int_{t_1}^{t_1+T} \text{expi } [(m-M)\theta(t)+(N-n)\gamma(t)+n\tau_{m\mu}^n \Omega(t)] dt \qquad (6-27)$$

Now, unless $n = N$, the factor expi $(N-n) \gamma(t)$ ensures that the integrand will oscillate rapidly so that the time average can be made sufficiently small to be ignored. The important cases, therefore, are for the target $n=N$ order, for which the transform becomes

$$Tr\left\{p_{m\mu}^N (t)\right\} = \frac{1}{2} C_{m\mu}^N \frac{1}{T} \int_{t_1}^{t_1+T} \text{expi } [(m-M)\theta(t) + N \tau_{m\mu}^N \Omega(t)] \, dt \tag{6-28}$$

It will be observed that if the time delay is zero, the variable speed $\Omega(t)$ presents no complication: for an integral number of microphone turns the integral vanishes unless $m = M$, in which case the transform equals $1/2 \ C_{M\mu}^N$, as in the constant speed case.

The speed variation can now be written in terms of its mean value, Ω_0 and a small time variation, $f(t)$

$$\Omega(t) = \Omega_0 + f(t) \tag{6-29}$$

This gives

$$Tr\left\{p_{m\mu}^N (t)\right\} = \frac{1}{2} C_{m\mu}^N \text{expi } N\Omega_0 \tau_{m\mu}^N \cdot \frac{1}{T} \int_{t_1}^{t_1+T} \text{expi}[(m-M)\theta(t)+N f(t)\tau_{m\mu}^N] dt \tag{6-30}$$

When the microphone angle $\theta(t)$ is replaced by $\theta(t) = \Gamma t$, we get

$$Tr\left\{p_{m\mu}^N (t)\right\} = \frac{1}{2} C_{m\mu}^N \text{expi } N\Omega_0 \tau_{m\mu}^N \cdot \frac{1}{T} \int_{t_1}^{t_1+T} \text{expi}[(m-M) \Gamma t + Nf(t) \tau_{m\mu}^N] dt \tag{6-31}$$

If the integrand in eq. (6-31) is compared with the constant speed case for the target $n = N$ frequency, eq. (3-13), it is seen that the term $(m-M)\Gamma t$ for constant speed is now supplemented by the term $Nf(t) \tau_{m\mu}^N$ which depends on the speed variation, $f(t)$, and the delay time, $\tau_{m\mu}^N$. This modification will alter the previously obtained constant speed results.

6.4.3 Linear Speed Variations

In order to interpret eq. (6-31) and to obtain illustrative numerical results, specific forms for the speed variation, $f(t)$, will be taken. The simplest case is a linear speed variation, for which $f(t) = at$, so that

$$\Omega(t) = \Omega_0 + at \tag{6-32}$$

For clarity of illustration, the limits of integration in eq. (6-31) will be taken from $-T/2$ to $T/2$ so that the mean speed, Ω_0, is attained at $t = 0$. In addition, the constant phase shift factor, $\exp i\ N\Omega_0\ \tau^N_{m\mu}$, will be suppressed. (Note: if the phase shift factor of eq. (6-16) had been retained in eq. (6-24) it would have combined with $\exp i\ N\Omega_0\ \tau^N_{m\mu}$ above to give $k^N_{xm\mu}x$, which simply transfers the phase of $C^N_{m\mu}$ from $x = 0$ to $x = x$ under constant speed conditions.)

Under these conditions we have

$$Tr\left\{ p^N_{m\mu}(t) \right\} = \frac{1}{2}\ C^N_{m\mu}\ \frac{1}{T}\ \int_{-T/2}^{T/2} \exp i\ [(m-M)T + Na\,\tau^N_{m\mu}\,]t\ dt \tag{6-33}$$

It can be seen that the frequency differences between the target mode, MT, and other modes, mT, which under constant speed are integer multiples of microphone speed are now shifted by $Na \cdot \tau^N_{m\mu}$.

The process is easily understood intuitively on the basis of an analog tracking filter. As speed changes, the frequency of the rotor reference signal or tracking signal changes in a precise match. But, due to the time delays for the modes to propagate to the microphone, the microphone pressure signal lags behind the tracking signal, creating a frequency mismatch.

The integral in eq. (6-33) can be readily evaluated to give

$$Tr\left\{ p^N_{m\mu}(t) \right\} = \frac{1}{2}\ C^N_{m\mu}\ \frac{\sin\ [(m-M)T + Na\,\tau^N_{m\mu}\,]\ T/2}{[(m-M)T + Na\,\tau^N_{m\mu}\,]\ T/2} \tag{6-34a}$$

or, more briefly,

$$Tr\left\{ p^N_{m\mu}(t) \right\} = \frac{1}{2}\ C^N_{m\mu}\ \text{dif}\ [(m-M)T + Na\,\tau^N_{m\mu}\,]\ T/2 \tag{6-34b}$$

For interpretive purposes it will be a little more convenient to switch signs in the argument of the diff function, which is allowable since it is an even function, giving

$$Tr\left\{ p^N_{m\mu}(t) \right\} = \frac{1}{2}\ C^N_{m\mu}\ \text{diff}\ [(M-m)T + Na\,\tau^N_{m\mu}\,]\ T/2 \tag{6-34c}$$

In the constant speed case, where $a = 0$, for the $m = M$ target mode the function diff [ ] is unity, and for all other modes it vanishes. The effect of linear speed variation is seen to introduce a shift in frequency from these values, producing two types of error: 1) The response for the target mode is

reduced by the factor diff $[Na \, \tau^N_{m\mu}]T/2$; this is called here "loss of signal," LOS. And 2) the non zero response for neighboring off-target (m = M) modes due to shifting from the zeros of the function is called contamination. Both effects can be readily calculated from eq. (6-34). These effects are illustrated in Figure 6-3.

As a check of these results, and to bring out some important design features, a six-part computer simulated test series was run, the results of which are plotted in Figure 6-4.

A set of computer simulated tests was run, using the following parameters for the 10-inch P&WA fan rig.

Mean rotor speed	100 rps
Rotor acceleration	1 rps/sec
Run time	10 secs
Order n = N	32 (blade order)

A delay time, $\tau^N_{m\mu}$ of 9.375 x 10^{-4} seconds was selected for illustrative purposes to give a frequency shift of 0.3/T, and was used for modes m = 0, + 1, + 2. The extent to which this delay corresponds to actual operating conditions is treated extensively in Section 6.5.

The results of Run 1, a 1-turn traverse in 10 seconds, using uniform weighting ($W(t)$≡1) are shown in Figure 6-4. The target signal has fallen 1.4dB and there is contamination from the bordering mode of -8.7dB. (Under constant speed conditions this contamination would be zero or "−∞"dB). These LOS and contamination figures are certainly not ignorable.

With these Run 1 results as reference, a sequence of modified data acquisition and processing procedures was applied to the same rig operating conditions, in order to show how these results can be improved.

In Run 2, Figure 6-4 the microphone traverse speed is doubled to produce 2 turns in the 10 second run. This spreads the modal frequencies farther apart and prevents the immediate bordering frequency from encroaching into the main lobe of the response function. The contamination from this bordering mode has now dropped from -8.7dB to -16.4dB. (The LOS is unchanged.)

Further reduction of contamination may be had by additional microphone speed increases, but this would only shift the bordering mode frequency to successive minor lobes, which fall slowly. A more effective procedure is to introduce Hamming weighting in the transform. These results are given in Run 3, Figure 6-4. The nearest mode contamination has dropped to -26.7dB, and the LOS is now -0.6dB instead of -1.4.

The greatest contamination is now resulting from intrusion of the neighboring mode into the main lobe of the response function, which has been broadened as a result of Hamming. This can be corrected by further moderate microphone speed increases to move the bordering mode frequency farther away from the target.
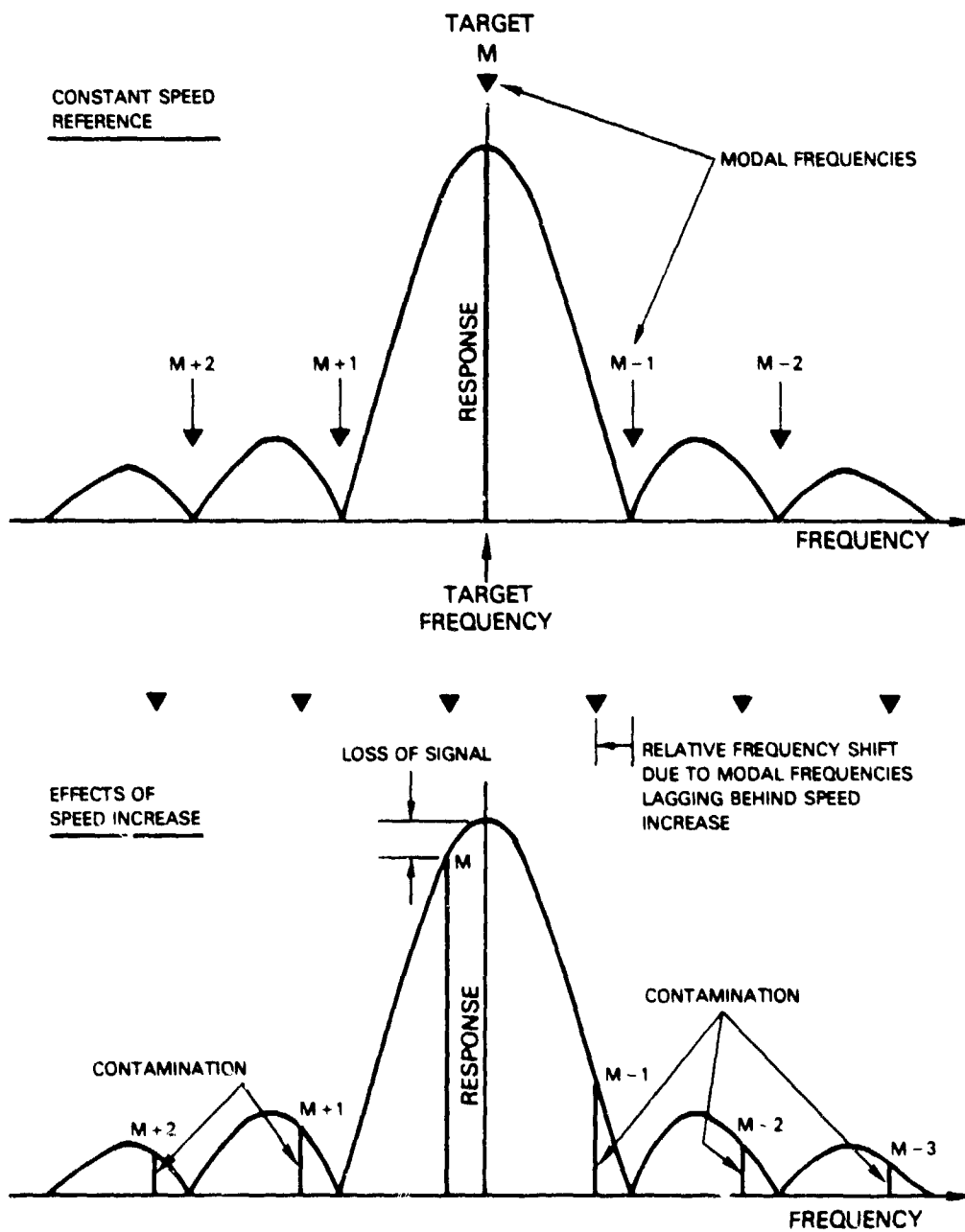
Figure 6-3   Loss of Signal and Contamination Resulting From Linear Speed
                  Increase

81

TARGET FREQUENCY

MODAL FREQUENCIES

RUN 1

M
−1.4dB

M-1
−8.7dB

M+3   M+2   M+1   M−2   M−3   M−4

REFERENCE SHOWS LOSS OF
SIGNAL AND CONTAMINATION
RECTANGULAR WINDOW
R = 1 TURN
Γ = 0.1 rps

RUN 2

M
−1.4dB

M-1
−16.4dB

M+1   M−2

DOUBLE MICROPHONE SPEED
RECTANGULAR WINDOW
R = 2 TURNS
Γ = 0.2 rps

RUN 3

M
−0.6dB

M+1   M-1
−26.7dB

M-2
−45dB

ADD HAMMING WINDOW
HAMMING WINDOW
R = 2 TURNS
Γ = 0.2 rps

RUN 4

M
−0.6dB

m+1   M-1
−58dB

INCREASE MICROPHONE SPEED
HAMMING WINDOW
R = 3 TURNS
Γ = 0.3 rps

RUN 5

M
−0.6dB

M-1
−45dB

INCREASE MICROPHONE SPEED
HAMMING WINDOW
R = 4 TURNS
Γ = 0.4 rps

RUN 6

FULL RESPONSE
M

ZERO CONTAMINATION
ALL MODES

INCORPORATE TIME DELAY
IN TARGET SIGNAL
HAMMING WINDOW
R = 4 TURNS
Γ = 0.4 rps

Figure 6-4   Effect of Linear Speed Variations

82

Figure 6-4, Runs 4 and 5 represent speed increases giving 3 traverse turns and 4 turns. The contamination is now less than -40dB in both cases.

It is clear from these results that Hamming is extremely beneficial when used with a moderate number of traverse turns.

There is still another procedural modification that will improve not only the contamination (which has now been reduced to levels that are probably acceptable), but will also improve the loss of target mode signal, which now stands at -0.6dB. The reasoning that leads to this modification is quite simple: Both LOS and contamination problems arise because the modal frequencies are shifted with respect to rotor-generated target signal frequency. This frequency shift is, in turn, a consequence of the time delay, $\tau_{m\mu}$ for the mode to arrive at the microphone during a speed change. If the transform equation were modified by introducing a matching time delay, $\tau = \tau_{m\mu}^{N}$, i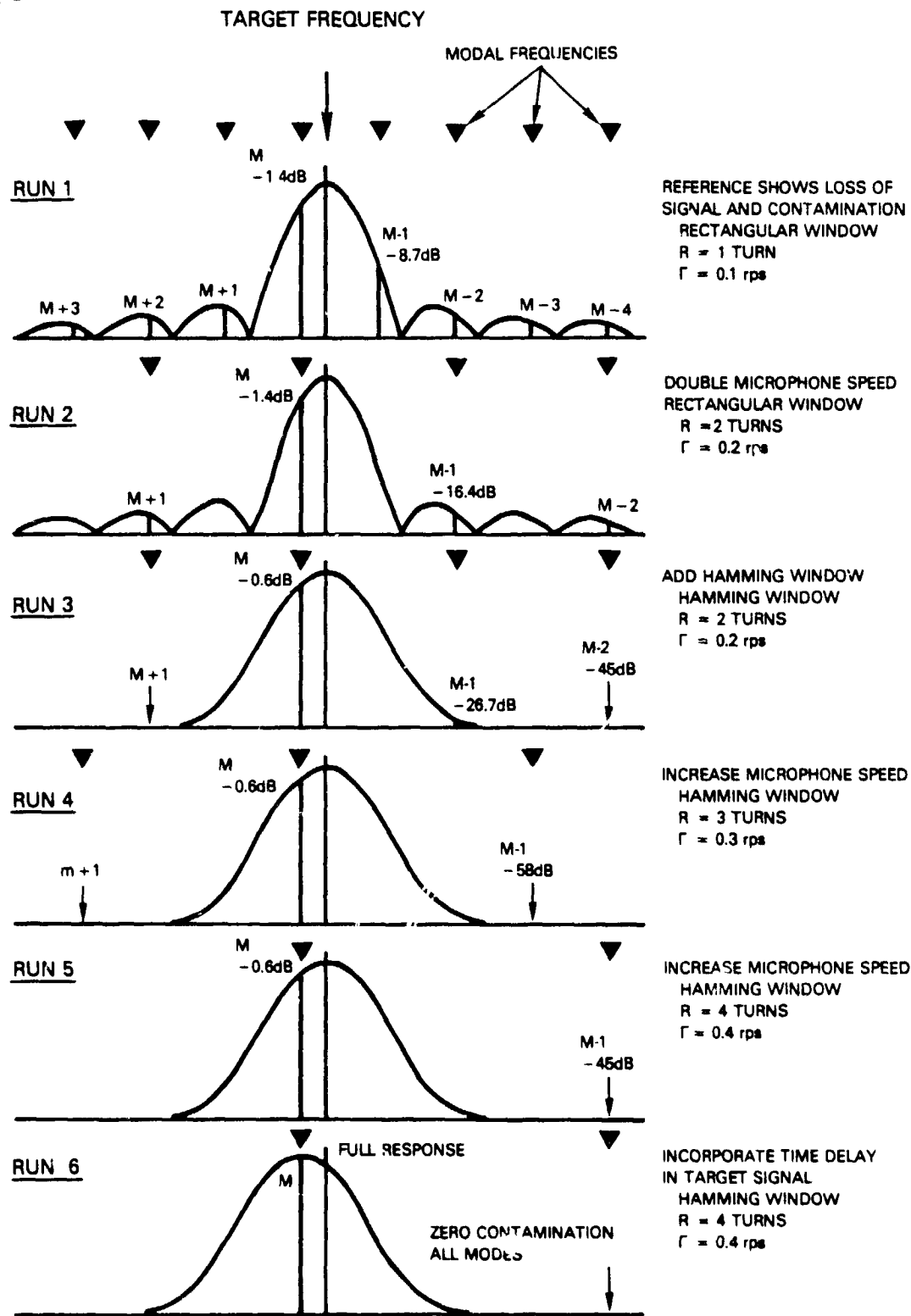n the rotor signal, V_M, both the modal signal and the delayed rotor target signal would be frequency-locked as rig speed varied.

This delayed reference signal is computed from eq. (6-23) simply by replacing $\gamma(t)$ by $\gamma(t-\tau)$ to give

$$V_M^N(t-\tau) = \exp i - [M\theta(t) - N \ \gamma(t-\tau)] \tag{6-35}$$

(Note that $t-\tau$ replaces t only in the rotor angle function, γ, and not in the microphone angle, θ.)

The transform of the modal pressure, eq. (6-25), now becomes

$$Tr\left\{p_{m\mu}^{n}(t)\right\} = \frac{1}{2} C_{m\mu}^{n} \ \frac{1}{T} \ \int_{t_1}^{t_1+T} \exp i \ [(m-M)\theta(t)-n \ \gamma(t-\tau_{m\mu}^{n})+N \ \gamma(t-\tau)]dt$$

For the important $n = N$ order case, this is

$$Tr\left\{p_{m\mu}^{N}(t)\right\} = \frac{1}{2} C_{m\mu}^{N} \ \frac{1}{T} \int_{t_1}^{t_1+T} \exp i \left\{(m-M)\theta(t)+N[\ \gamma(t-\tau)- \gamma(t-\tau_{m\mu}^{N})]\right\} dt \tag{6-36}$$

If the computer-applied delay, τ, in the rotor signal is made equal to the modal delay, $\tau_{m\mu}^{N}$, the factor of N vanishes giving

$$Tr\left\{p_{m\mu}^{N}(t)\right\} = \frac{1}{2} C_{m\mu}^{N} \ \frac{1}{T} \ \int_{t_1}^{t_1+T} \exp i \ [(m-M)\Gamma t]dt$$

for traverse speed Γ.

All time delays and speed variations have disappeared and the result is the same as in the constant speed case; there is neither loss of signal nor contamination if an integer number of turns is used.

This result is shown as Run 6 in Figure 6-4, where a delay time equal to the modal delay has been incorporated in the rotor reference signal of a computer simulation. The common frequency shift of the modal signals and the delayed target signal may be noted, together with full target signal recovery and the complete absence of contamination.

It will be equally clear that the use of this simple procedure in an actual engine or rig test will not produce such dramatic improvement. For one thing, all modes do not have common delay times, $\tau_{m\mu}^{N}$, because they generally have different wavenumbers, $k_{xm\mu}$, and different sources in the engine or rig. Another consideration is that the source locations are either unknown or are known with limited accuracy. The aerodynamic delay time for rotor wake impingement on downstream sources contributes a further uncertainty to selecting the rotor signal delay, τ. Extension of this procedure to handle these complications is considered feasible but was beyond the scope of the current investigation.

6.4.4 Sawtooth Speed Variations

The foregoing analysis for linear speed variation has been presented in considerable detail since this form of variation gives a constant frequency shift that is easy to visualize and produces effects that are readily interpretable in terms of the frequency response function.

However, examination of recorded time histories of rotor speed variation in several engines and rigs shows that the typical variation present is a somewhat irregular hunting about a mean speed, rather than a linear, long time speed drift. This is fortunate, both for the operation of the machine, and also for use of the traversing microphone system. In the previous 6-part illustrative sequence all simulated runs were of 10 second duration for illustration. Now, it has been shown in Section 5.3.5 that the run time, T, may have to be extended to reduce contamination due to broadband noise. In the examples of Figure 6-4, if T is increased beyond 10 seconds the main lobe bandwidth of the response will be narrowed. This narrowing will attenuate the target mode signal, even with Hamming, and even with a rotor signal time delay that differs somewhat from the modal delay $\tau_{m\mu}^{N}$.

It is therefore important to examine more realistic, hunting type speed variations. This subsection treats sawtooth variations and in the next section sinusoidal variations are examined.

Consider an irregular sawtooth speed fluctuation, shown in Figure 6-5.

For the qth segment of constant acceleration, a_q, beginning at time, t_q, of duration T_q, the basic transform for the target mode, m = M and n = N will be, from eq. (6-28)

84
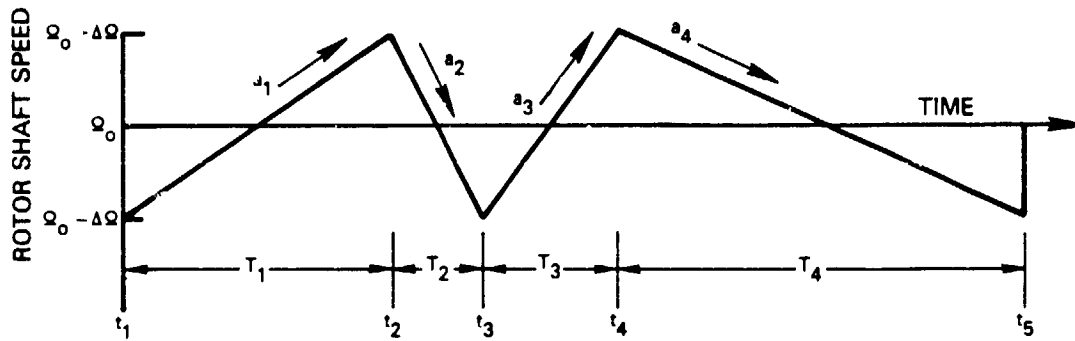
Figure 6-5   Sample Irregular Sawtooth Speed Fluctuation

$$Tr\left\{ p_{M\mu}^{N}(t)\right\} = \frac{1}{2} C_{M\mu}^{N} \frac{1}{T_q} \int_{t_q}^{t_q+T_q} expi(N \tau_{M\mu}^{N} \Omega_q(t))dt \tag{6-37}$$

Since $\Omega(t) = \Omega_0$ at the midpoint, t_{oq}, of the interval T_q, we have

$$\Omega_q(t) = \Omega_0 + a_q(t-t_{oq}), \tag{6-38}$$

Where $\qquad t_{oq} = t_q + \frac{1}{2} T_q \tag{6-39}$

Then

$$Tr\left\{ p_{M\mu}^{N}(t)\right\} = \frac{1}{2} C_{M\mu}^{N} \; expi \; [N\tau_{M\mu}^{N}(\Omega_0 - a_q t_{oq})] \tag{6-40}$$

$$X \frac{1}{T_q} \int_{t_q}^{t_q+T_q} expi \; (N\tau_{M\mu}^{N} a_q t)dt$$

Using the generic form

$$\frac{1}{L} \int_{\alpha}^{\alpha+L} expi(\beta \theta)d\theta = \frac{sin\beta L/2}{\beta L/2} expi \; \beta(\alpha+L/2) \tag{6-41}$$

$$= diff(\beta L/2) \; expi \; \beta(\alpha+L/2),$$

the transform becomes

$$\text{Tr}\left\{p_{M\mu}^{N}(t)\right\} = \frac{1}{2} C_{M\mu}^{N} \quad \text{expi} \ [N\tau_{M\mu}^{N}(\Omega_0 - a_q t_{oq})]\text{diff}[N\tau_{M\mu}^{N} a_q T_q/2] \qquad (6\text{-}42)$$

$$\text{X expi} \ [N\tau_{M\mu}^{N} a_q t_{oq}]$$

$$= \frac{1}{2} C_{M\mu}^{N} \quad \text{diff} \ [N\tau_{M\mu}^{N} a_q T_q/2] \ \text{expi} \ (N\tau_{M\mu}^{N}\Omega_0)$$

But the product $a_q T_q/2$ is simply the speed excursion, $\Delta\Omega$, which is common to all segments of the time history. Hence

$$\text{Tr}\left\{p_{M\mu}^{N}(t)\right\} = \frac{1}{2} C_{M\mu}^{N} \quad \text{diff} \ (N\Delta\Omega \ \tau_{M\mu}^{N}) \ \text{expi} \ (N\Omega_0 \tau_{M\mu}^{N}) \qquad (6\text{-}43)$$

It is seen that this result does not depend on the individual acceleration, a_q, of the qth segment, nor upon its duration, T_q, nor upon the time, t_q, that the acceleration began.

The transform for the general sawtooth speed variation, Figure 6-5 follows readily: We write for the pressure transform, following eq. (6-37)

$$\text{Tr}\left\{p_{M\mu}^{N}(t)\right\} = \frac{1}{2} C_{M\mu}^{N} \frac{1}{T} \int_{t_1}^{t_1+T} g(t)dt, \qquad (6\text{-}44)$$

where t_1 is the beginning of the complete run, T is the total time, $T = T_1 + T_2 + \ldots + T_Q$, and $g(t) = g_q(t) = \text{expi} \ [N\tau_{M\mu}^{N}\Omega_q(t)]$ for appropriate subintervals.

Then

$$\text{Tr}\left\{p_{M\mu}^{N}(t)\right\} = \frac{1}{2} C_{M\mu}^{N} \frac{1}{T}\left\{\int_{t_1}^{t_1+T_1} g_1(t)dt + \int_{t_2}^{t_2+T_2} g_2(t)dt + \ldots \int_{t_Q}^{t_Q+T_Q} g_Q(t)dt\right\} (6\text{-}45)$$

Now the qth integral in the above, I_q, can be written as

$$I_q = T_q \cdot \frac{1}{T_q} \int_{t_q}^{t_q+T_q} g_q(t)dt \qquad (6\text{-}46)$$

$$= T_q \ \text{diff} \ (N\Delta\Omega \ \tau_{M\mu}^{N}) \ \text{expi} \ (N\Omega_0 \tau_{M\mu}^{N}),$$

where, as has been noted, the diff and expi functions are common to all segments. So

$$\mathrm{Tr}\left\{ P_{M\mu}^{N}(t) \right\} = \frac{1}{2} C_{M\mu}^{N} \, \mathrm{diff}(N\Delta\Omega \, \tau_{M\mu}^{N}) \mathrm{expi}(N\Omega_{0} \, \tau_{M\mu}^{N}) \frac{1}{T} \left\{ T_{1} + T_{2} + \ldots + T_{Q} \right\}$$

The T-sums add to T, clearing the expression of run time. Also the factor expi $(N\Omega_{0}\tilde{\tau}_{M\mu})$ is just a phase shift, constant over the run and will be discarded here as it was for the linear variation. The result is then, simply

$$\mathrm{Tr}\left\{ D_{M\mu}^{N}(t) \right\} = \frac{1}{2} C_{M\mu}^{N} \, \mathrm{diff} \, (N\Delta\Omega \, \tau_{M\mu}^{N}) \tag{6-47}$$

$$\text{or} \quad = \frac{1}{2} C_{M\mu}^{N} \, \frac{\sin (N\Delta\Omega \, \tau_{M\mu}^{N})}{(N\Delta\Omega \, \tau_{M\mu}^{N})}$$

This result corresponds to that obtained by the quasi steady state approach in Section 6.2.

This result should be compared with eq. (6-34b) for the case of unlimited linear speed drift, which becomes for the target mode case m = M

$$\mathrm{Tr}\left\{ P_{M\mu}^{N}(t) \right\} = \frac{1}{2} C_{M\mu}^{N} \, \mathrm{diff} \, (\mathrm{Na} \, \tau_{M\mu}^{N} \, T/2) \tag{6-48}$$

In this case, under constant acceleration, as T increases, the loss of signal increases. In the sawtooth case, eq. (6-47), which can be obtained by replacing a·T/2 by $\Delta\Omega$ in eq. (6-48), it is the combination $N\Delta\Omega \, \tilde{\tau}_{M\mu}$ which governs loss of signal. To minimize LOS the magnitude of speed fluctuations, $\Delta\Omega$, and the delay times, should be low. No variation of operating parameters such as run time, T, and traverse speed, Γ, will affect the LOS. The delay times, $\tau_{m\mu}^{n}$ are beyond control; however, as was seen in the set of runs in the previous section, introduction of a compensating time delay in the rotor reference signal is an effective countermeasure for speed variation.

6.4.5 Sinusoidal Speed Variations

A still more realistic form of fan speed variation is a sinusoid fluctuation or a combination of such fluctuations. The sinusoidal speed variation of amplitude $\pm \Delta\Omega$, circular frequency, ν, about a mean speed Ω_{0} is given by

$$\Omega(t) = \Omega_{0} + \Delta\Omega \sin (\nu t + \phi), \tag{6-49}$$

where ϕ is an arbitrary phase angle.

From eq. (6-28) for the basic transform under general small speed variation, for the target order n = N, use of eq. (6-49) gives

$$\text{Tr}\left\{p^N_{m\mu}(t)\right\} = \frac{1}{2}C^N_{m\mu}\frac{1}{T}\int_{t_1}^{t_1+T}\text{expi }[(m-M)T\,t+N\,\tau^N_m\;(\Omega_0+\Delta\Omega\sin(\nu t+\phi))]dt \quad (6\text{-}50)$$

$$= \frac{1}{2}C^N_{m\mu}\frac{1}{T}\int_{t_1}^{t_1+T}\text{expi }(\Delta M T t)\text{ expi }[N\,\tau^N_{m\mu}\Delta\Omega\sin(\nu t+\phi)]dt$$

Here, $\Delta M = (m-M)$, and the constant phase shift factor, expi $N\tau^N_{m\mu}\Omega_0$, has been dropped, as before, for simplicity.

The exponential with sinusoidal argument in the integrand is replaced by its Bessel function expansion, eq. (6-10), to give

$$\text{Tr}\left\{p^N_{m\mu}(t)\right\} = \frac{1}{2}C^N_{m\mu}\frac{1}{T}\int_{t_1}^{t+T}\text{expi}(\Delta M T t)\sum_{q=-\infty}^{\infty}J_q(N\Delta\Omega\tau^N_{m\mu})\text{ expi }q(\nu t+\phi)dt \quad (6\text{-}51)$$

$$= \frac{1}{2}C^N_{m\mu}\sum_{q=-\infty}^{\infty}J_q(N\Delta\Omega\tau^N_{m\mu})\text{ expi }(q\phi)\frac{1}{T}\int_{t_1}^{t_1+T}\text{expi }(\Delta M T+q\nu)t\;dt \quad (6\text{-}52)$$

This result can be used to evaluate loss of signal and contamination. These are best handled separately. For loss of signal of the target mode $\Delta M = 0$ and

$$\text{Tr}\left\{p^N_{M\mu}(t)\right\} = \frac{1}{2}C^N_{M\mu}\sum_{q=-\infty}^{\infty}J_q(N\Delta\Omega\;\tau^N_{M\mu})\text{ expi }(q\phi)\frac{1}{T}\int_{t_1}^{t_1+T}\text{expi }(q\nu t)dt \quad (6\text{-}53)$$

$$= \frac{1}{2}C^N_{M\mu}J_0(N\Delta\Omega\;\tau^N_{M\mu}) \quad (6\text{-}54)$$

$$+\frac{1}{2}C^N_{M\mu}\sum_{q\neq 0}J_q(N\Delta\Omega\;\tau^N_{M\mu})\text{ expi}(q\phi)\text{diff}(q\nu T/2)\text{expi }q\nu(t_1+T/2)$$

This general result simplifies drastically if there are an integral number of cycles of speed variation in T. In this case the time integral in eq. (6-53), (and the diff function in eq. (6-54)) vanishes, giving as the sole surviving term:

$$\text{Tr}\left\{\rho_{M\mu}^{N}(t)\right\} = \frac{1}{2} C_{M\mu}^{N} \; J_0 \; (N\Delta\Omega \; \tau_{M\mu}^{N}) \tag{6-55}$$

The argument of J_0 is the same quantity, $N\Delta\Omega\,\tau_{M\mu}^{N}$, that governed the attenuation of the target signal in the case of sawtooth speed variation, eq. (6-47), i.e.:

$$(\text{sawtooth}) \; \text{Tr}\left\{\rho_{M\mu}^{N}(t)\right\} = \frac{1}{2} C_{M\mu}^{N} \text{ diff } (N\Delta\Omega \; \tau_{M\mu}^{N})$$

Since the first zero of $J_0(x)$ is at $x = 0.76\pi$ and the first zero of diff(x) is at $x = \pi$, there will be a complete loss of signal in the sinusoidal speed variation case when $N\Delta\Omega\tau = 0.76\pi$, compared with $N\Delta\Omega\tau = \pi$ for the square wave variation. This result may be appreciated from examination of Figure 6-2, which represents the time-varying phase shift of a mode at a fixed microphone location, analyzed on a quasi steady-state basis. The time average of the vector is least (most LOS) for a square wave variation, where the vector jumps between extreme positions. In the sawtooth or drift case the vector position is uniformly distributed between extremes. The sinusoidal case is intermediate; proportionally more time is spent near the extremes of the excursion than in the linear case, but obviously not as much as for the square wave.

The result eq. (6-55) is independent of the frequency of the speed variation, ν, just as the sawtooth wave case result eq. (6-47) did not depend on details of the wave shape. However, both results were based on an integer number of $\pm\Delta\Omega$ speed excursions during the run. This will not generally occur in practice, (neither will pure sinusoidal or sawtooth waves). However it is possible to verify that eq. (6-55) is a good approximation to eq. (6-54): Since $J_q(x)$ for small x decreases rapidly with q, and since $J_1(x) \leqslant J_0(x)$, even ignoring the attenuation provided by diff $(q\nu T/2)$ in eq. (6-55), the contribution of the q-sum will be small compared with the J_0 term. If a more conservative estimate should be desired for the loss of signal, the square wave case, $\cos (N\Delta\Omega\,\tau_{M\mu}^{N})$ may be used.

Realistic estimates of the loss of signal that may be encountered in practice are given in Section 6.5.

Contamination of the signal by neighboring off-target modes will next be examined with the use of eq. (6-52) which applies to the $\Delta M \neq 0$, or $m \neq M$ case. The time average may be given immediately in terms of the diff ( ) function, where $(\Delta M\Gamma + q\nu)$ is the frequency difference. Discarding unessential phase shift factors, the result is

$$\text{Tr}\left\{\rho_{m\mu}^{N}(t)\right\} = \frac{1}{2} C_{m\mu}^{N} \sum_{q=-\infty}^{\infty} J_q(N\Delta\Omega \; \tau_{m\mu}^{N}) \text{ diff } (\Delta M\Gamma + q\nu)T/2 \tag{6-56}$$

The contribution of J_0 will be zero since, with $q = 0$, the diff function will be diff $\Delta M\Gamma T/2$ which vanishes for an integral number of turns, ΓT.

Of the remaining $q \neq 0$ terms, J_1 for $q = +1$ dominates for small argument. Unless diff $(\Delta M\Gamma +)T/2$ can be made small, the transform may be significantly contaminated. If $\Delta M\Gamma = + \nu$, diff $( ) = 1$ and the worst contamination results. We cannot depend on being at a zero of diff $( )$, since ν is an arbitrary frequency. The bordering modes, $\Delta M = +1$, are the most critical since they give diff $(\Gamma - \nu)$ as the most dangerous case in the sense of making a small argument of the function and a large value of diff $(\Gamma - \nu)$. Neither will it do to require that Γ be made very much larger than ν, for this could result in an impractically high traverse speed or a speed that would violate the constraint for time cluster separation, eq. (5-12).

The solution to this contamination problem is to employ Hamming weighting in the transform of the pressure signal. It can easily be seen that if this $W(t)$ is inserted in the integrand of eq. (6-50) it will carry through and appear in the time integral of eq. (6-52) to give

$$Tr\left\{p^N_{m\mu}(t)\right\} = \frac{1}{2}C^N_{m\mu}\sum_{q=-\infty}^{\infty} J_q(N\Delta a \tau^N_{m\mu})\exp i(q\phi)\frac{1}{T}\int_{t_1}^{t_1+T} W(t)\exp i(\Delta M\Gamma+q\nu)t \, dt \quad (6-57)$$

Now, the time average can be obtained simply as the function

$$\frac{1}{T}\int_{t}^{t+T} W(t)\exp i(\Delta M\Gamma+q\nu)t \, dt = \text{Hamm}[(\Delta M\Gamma+q\nu)T/2] \quad (6-58)$$

where Hamm $( )$ is defined by eq. (5-9) and is illustrated in Figure (5-3).

Consequently, the solution of eq. (6-57) that corresponds to the solution eq. (6-56) for uniform weighting is

$$Tr\left\{p^N_{m\mu}(t)\right\} = \frac{1}{2}C^N_{m\mu}\sum_{q=-\infty}^{\infty} J_q(N\Delta\Omega \, \tau^N_{m\mu})\text{Hamm}(\Delta M\Gamma+q\nu)T/2 \quad (6-59)$$

As for uniform weighting, the worst contamination will be from J_1 for $q=+1$ and for bordering modes, $\Delta M = + 1$. Here, the argument of the Hamm function is, again, $(\Gamma-\nu)T/2$, for the most serious situation.

Now if we put $\Gamma = 2\pi\Gamma'$, $\nu = 2\pi\nu'$, where Γ' and ν' are in Hz, the argument of Hamm $( )$ is

$$(\Gamma'-\nu')T\pi. \quad (6-60)$$

Since the major lobe of the Hamming response ends at $\Delta f = 2/T$, contamination can be reduced to trivial levels (-40dB) by selecting the traverse speed, τ', such that $(\tau' - \nu') > 2/T$. (Without Hamming a comparable reduction would require, approximately that $(\tau' - \nu') > 100/T$.)

This requirement may be conveniently expressed in terms of number of microphone turns, $R = \tau'T$, and number of cycles of speed variation cycles = $\nu'T$ during the run of length T

$$R - (\text{no. of speed cycles}) > 2. \tag{6-61}$$

$$\text{or} \quad R > (\text{no of speed cycles}) + 2$$

Since the number of speed variation cycles generally increases with time it may be more instructive to express T as R/τ' in the requirement

$$(\tau' - \nu') > \frac{2}{T}$$

$$\text{obtaining} \quad (\tau' - \nu') > 2\frac{\tau'}{R}$$

$$\text{or} \quad \tau' > \frac{R}{R-2}\nu' \tag{6-62}$$

With R = 3 turns, τ' must be $> 3\nu'$, for R=4, $\tau' > 2\nu$, R = 5 gives $\tau' > 1.67\nu'$, R = 10 gives $\tau' > 1.25\nu$.

This shows that to avoid contamination the traverse speed must exceed the frequency of speed variation, and also to prevent having to use a traverse speed that is inconveniently high or violates the top speed constraint, the use of a moderately large number of turns is required.

In the application of the traversing microphone method to engine or fan rig tests, it is clear that the specific speed characteristics of the fan must be examined in order to select the best traverse speed and number of turns.

Some computer simulated runs were conducted in this program to illustrate sample loss of signal and contamination resulting from sinusoidal speed variations. The first case consisted of a sinusoidal variation of rotor speed

$$C - 2$$

with no time delay to verify that it is the time delay that is the important source of error. The form of the speed variation was the same as used for the sinusoidal speed variation in traverse angle, namely

$$g(t) = \Delta\Omega \sin\frac{2\pi\ell}{T}t$$

Results are shown in Table 6-3 for $\Delta\Omega = 10$ and ℓ equal to one and four. Recovery of the input mode was seen to be perfect to the accuracy displayed, verifying that for a microphone traverse near the source of a mode, i.e., $\tau_m^n = 0$, rotor speed variation is unimportant.

TABLE 6-3

EFFECT OF SINUSOIDAL SPEED VARIATION OF ROTOR ON COMPUTED MODE AMPLITUDES
NO TIME DELAY
(Measurement at Source)

Input

$C_0^{32} = 1\angle 0^0$ Pressure Units
Rotor Speed = $100 + 10 \sin (2\pi\ell t/T)$ rev./sec
Traverse Speed = .1 rev./sec
Number of Time Increments = 256000
Time Increment Between Samples = .0000390625 sec
Total Run Time = 10 sec

Output

| | $\ell = 1$ | | $\ell = 4$ | |
m	$\|C_m^{32}\|$-Pressure Units	$\|C_m^{32}\|$-dB re 1	$\|C_m^{32}\|$-Pressure Units	$\|C_m^{32}\|$-dB re 1
0	1.00000000	0	1.00000000	0
1	.00000000	<-166	.0000000C	<-166
16	.00000000	<-166	.00000000	<-166
31	.00000000	<-166	.00000000	<-166
32	.00000000	<-166	.00000000	<-166

Time delay was then introduced for a series of runs where changes in $\Delta\Omega/\Omega$, τ_m^n and the number of cycles of speed variation, ℓ, were studied. Results are shown in Table 6-4. Output mode amplitudes were rounded to 4 significant decimal places in this table to make comparisons easier.

Comparison of cases 1, 2 and 3 shows rather large loss of signal for the input C_0^{32} mode and large contamination for the adjacent C_1^{32} mode. It also shows that it is the product $\tau_m^n \Delta\Omega/\Omega$ which controls the magnitudes of the loss of signal and contamination. Cases 2, 12 and 13 show the effect of changing τ_m^n, and it can be seen that increasing τ_m^n increases both loss of signal and contamination. Similarly, increasing $\Delta\Omega/\Omega$ increases both loss of signal and contamination as seen in cases 2, 9, 10 and 11.

92

ORIGINAL PAGE IS
OF POOR QUALITY

TABLE 6-4

EFFECT OF SINUSOIDAL SPEED VARIATION OF ROTOR ON COMPUTED MODE AMPLITUDES
WITH TIME DELAY

Input

$C_0^{32} = 1 \angle 0^\circ$ Pressure Units
Avg. Rotor Speed = 100 rev./sec

Rotor Angle $= 100 (t - \tau_m^n) + 100 \frac{\Delta\Omega}{\Omega} \frac{1}{2\pi\ell/T} \left\{ 1 - \cos [2\pi\ell (t - \tau_m^n)/T] \right\}$

Traverse Speed = .1 rev./sec
Number of Time Increments = 256000
Time Increment Between Samples = .0000390625 sec
Total Run Time = 10 sec

Output

Case No.	$\frac{\Delta\Omega}{\Omega}$	τ_m^n sec	No. of Cycles-ℓ	$\left|C_0^{32}\right|$	$\left|C_1^{32}\right|$	$\left|C_{16}^{32}\right|$	$\left|C_{31}^{32}\right|$	$\left|C_{32}^{32}\right|$
				Output Mode Amplitudes-Pressure Units				
1	.05	.00062500	1	.9037	.2989	*	*	*
2	.1	.00031250		.9037	.2989	*	*	*
3	.2	.00015625		.9037	.2989	*	*	*
4	.1	.00031250	.5	.9814	.1319	.0004	.0001	.0001
5			1.5	.9127	.2291	.0012	.0003	.0003
6			2	.9037	*	*	*	*
7			4	.9037	*	.0004	*	*
8			8	.9037	*	.0477	*	.0004
9	.05		1	.9755	.1551	*	*	*
10	.2			.6425	.5122	*	*	*
11	.4			.0550	.4938	*	*	*
12	.1	.00062500		.6425	.5122	*	*	*
13	.1	.00015625		.9755	.1551	*	*	*

* Less than 5×10^{-9}
NOTE: See text Section 6.4.5 for discussion of this table.

Changes discussed to this point affected only the input mode amplitude and
that of the adjacent mode. Changing the number of cycles of variation,
however, results in contamination being spread to different modes. This can be
seen by comparing cases 2, 4, 5, 6, 7 and 8. A noninteger number of cycles,
as would be the usual result of an actual test, introduces contamination into
all modes (cases 4 and 5). This contamination appears to increase with
increasing proximity to the input mode.

6.5 PRACTICAL SIGNIFICANCE OF SPEED VARIATIONS

It has been seen that the dominant factor in producing loss of target signal
and contamination from off-target modes is the total phase shift excursion in
the microphone plane, $\Delta\phi = (N\Delta\Omega\tau_m^N)$. In preparing for an engine or fan rig

93

test, there will presumably be available sufficient fan speed data to determine the probable fluctuations, $\Delta\Omega$, and some information about the frequency of these fluctuations, (which, together with $\Delta\phi$, affects contamination). It then remains to estimate representative values of the delay time, $\tau_{m\mu}^N$. With $\tau_{m\mu}^N$ estimated, $\Delta\phi$ can be found, and then the LOS can be estimated using diff $\Delta\phi$, $J_0 (\Delta\phi)$, or $\cos(\Delta\phi)$, as is summarized in Figure 6-2. The potential user of the traversing microphone method can then decide whether these estimated losses are acceptable for the accuracy required. If the estimated losses turn out to be excessive, then a modified procedure, outlined in Section 6.6, must be developed and employed. It cannot be overemphasized that excessive loss of signal is not in any way a consequence of using the traversing microphone system; it occurs in any conventional fixed microphone method that uses time-averaging to enhance the coherent fan harmonic signals with respect to broadband noise.

In this section estimates of LOS will be given for three configurations: the 10-inch P&WA rig, the JT9D engine, and the NASA LeRC 21-inch fan rig. Contamination estimates were not made since it was shown in Section 6.4 that use of Hamming with multiple traverse turns can reduce contamination to acceptable levels. (Loss of signal is not improved by this procedure.)

The modal delay time, $\tau_{m\mu}^N$, generally involves an aerodynamic delay and a propagation delay. The propagation delay is the time for changes in frequency at the source to propagate to the microphone plane, and was given by eq. (6-14). For stator sources downstream of the rotor, an aerodynamic delay between rotor speed changes and their corresponding wake interaction effects at the stator is involved. For illustrative purposes here, it was assumed that the rotor was the source of interaction modes, so that aerodynamic delays were not involved.

In the following work, the N or n superscripts on $k_{xm\mu}$, $\tau_{m\mu}$, etc., are dropped for simplicity. The frequency at which such quantities are evaluated is taken to be, $N\Omega_0 = \omega_0$, the mean frequency of the target order modes in stationary coordinates.

It has been shown that the modal delay time, by eq. (6-14), is

$$\tau_{m\mu} = \frac{x}{V_{gm\mu}} = \frac{dk_{xm\mu}}{d\omega}\bigg|_{\omega_0} x$$

Since axial wavenumber, $k_{xm\mu}$, depends on cutoff ratio, $\tau_{m\mu}$ will vary widely at any given frequency, ω_0. To describe this situation requires that we determine how the propagating modes are distributed with respect to delay time. With such information we can find what fraction of the modes exceed a specified delay time, and consequently, what fraction of the propagating modes will suffer a loss of signal greater than a preselected amount. In short, we will determine for a sequence of acceptable LOS of 0.5dB, 1dB, 2dB, 3dB and 6dB, what percent of the propagating modes have loss of signal greater than

these values. It will be seen that this procedure provides a convenient, easily understood way of deciding whether the basic traversing microphone system can provide sufficient accuracy or whether modified procedures are necessary.

Starting with eq. (6-14) we can write

$$\tau_{m\mu} = \frac{dk_{xm\mu}}{d\omega} \, x = \frac{dk_{xm\mu}}{dk} \frac{dk}{d\omega} \, x$$ (6-63)

$$= \frac{dk_{xm\mu}}{dk} \frac{x}{c}$$

This can be expressed as

$$\tau_{m\mu} = \frac{\tau_{m\mu}}{\tau_c} \, \tau_c ,$$ (6-64)

where $\tau_c = x/c$ (6-65)

is the time for a free-space wave (no flow) to travel distance x

and $\tau_{m\mu} / \tau_c = \frac{dk_{xm\mu}}{dk}$ (6-66)

is the delay time magnification, relative to free space, for changes in frequency to arrive at x.

Now the wavenumber, $k_{xm\mu}$, is taken in the form

$$k_{xm\mu} = \frac{k}{1-M_x^2} [M_x + \sqrt{1-(1-M_x^2) \, \zeta_{m\mu}^2}] ,$$ (6-67)

where $\zeta_m = k_{m\mu}/k$ (6-68)

is called "cut-on ratio."

(This is the reciprocal of the more commonly used "cutoff ratio," $\xi = k/k_{m\mu}$).

Eq. (6-67) applies for waves traveling forward from rotor toward inlet, and M_x, the axial flow Mach number, is a positive quantity.

As fan speed changes ω, k, ζ, and M_x all change. The derivative required for obtaining $\tau_{m\mu} / \tau_c$ can then be expressed as

$$\frac{\tau_{m\mu}}{\tau_c} = \frac{dk_{xm\mu}}{dk} = \frac{\partial k_{xm\mu}}{\partial k} + \frac{\partial k_{xm\mu}}{\partial \zeta_{m\mu}} \frac{d\zeta_{m\mu}}{dk} + \frac{\partial k_{xm\mu}}{\partial M_x} \frac{dM_x}{dk} \qquad (6\text{-}69)$$

The rate of change of Mach number can be obtained from engine data given in the form:

$$M_x = aN_1 + b, \qquad (6\text{-}70)$$

where N_1 is shaft speed, rps, and the constants a and b apply to the specific fan rig or engine.

N_1 and k are related by

$$k = \frac{\omega}{c} = \frac{2 \pi N_1 N}{c} \qquad (6\text{-}71)$$

A numerical procedure was used to obtain from eq. (6-67) through eq. (6-71) a tabulation of $\tau_{m\mu}/\tau_c$ versus $\zeta_{m\mu}$. Figure 6-6 shows this relation for the second harmonic of blade passage frequency in the JT9D engine at 3400 rpm. The large magnification of delay for high ζ (near cutoff) is noteworthy. Even highly propagating modes (ζ near zero) have delay times of about 7 times their $\tau_c = x/c$ values. These magnifications are significantly larger than the $M_x = 0$ case due not only to flow but also due to the rate of change of flow with respect to fan speed.

With τ/τ_c determined as a function of ζ, the phase shift, $\Delta\phi = \Delta\omega \cdot \tau_c \cdot \tau_{m\mu} / \tau_c$, can be found, and the loss of signal can be calculated using $J_0 (\Delta\phi)$.

With loss of signal obtained as a function of cuton ratio, ζ, it remains only to determine the percentage of propagating modes that exceed ζ and that, consequently, exceed that loss of signal. For this purpose, the cumulative distribution of propagating modes is required as a function of ζ. This will be obtained by means of modal density functions.

Rice has shown (ref. 15) that the modal density function with respect to cutoff ratio, ζ, in the case of $M_x = 0$ is given by

$$D_\zeta N = 2/\zeta^3 \qquad (6\text{-}72)$$
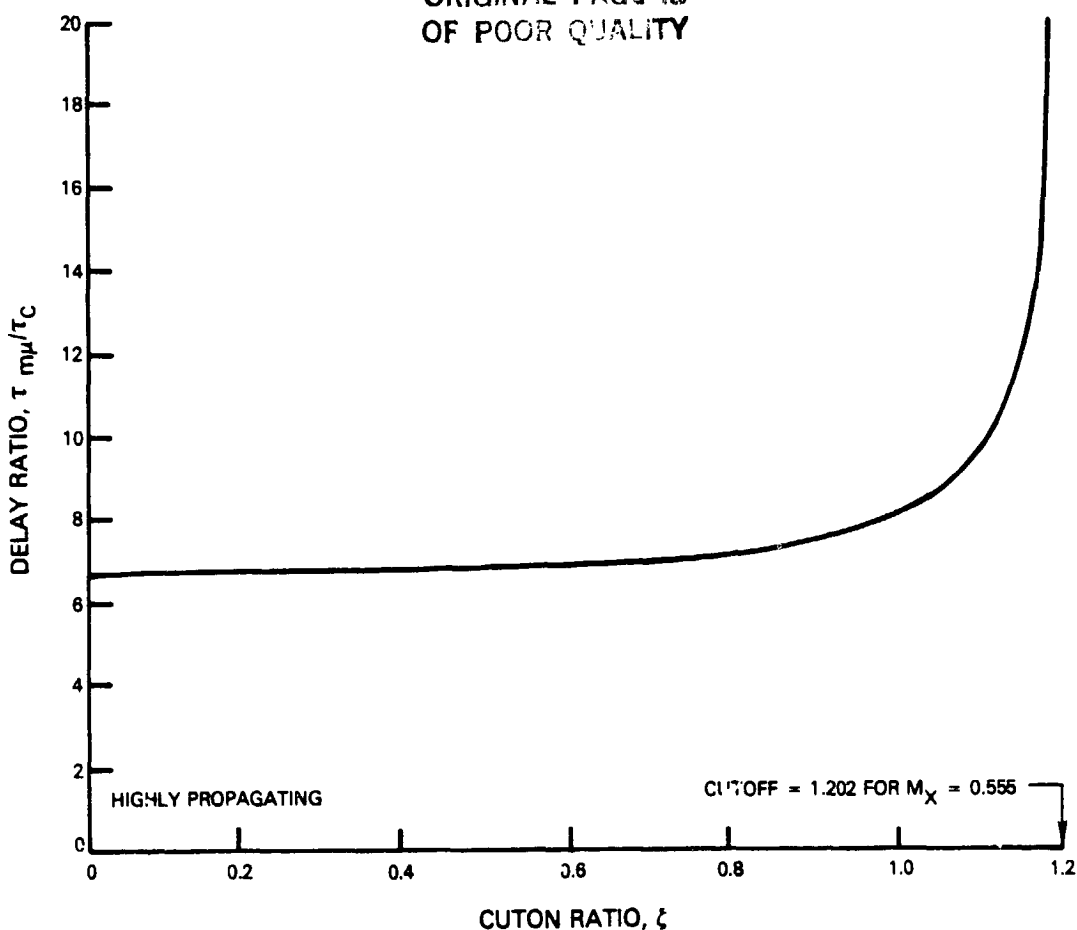
Figure 6-6   Variation of Delay Time With Cuton Ratio
                ($M_X = 0.555$)

The density function, $D_\xi N$ is the derivative, $dN/d\xi$, and can be interpreted readily from the relation

$$\text{Fraction of propagating modes between } \xi = \xi_1, \text{ and } \xi = \xi_2 = \int_{\xi_1}^{\xi_2} (D_\xi N) d\xi \qquad (6\text{-}73)$$

The cumulative distribution function N_ξ is the fraction of modes having cutoff ratios less than ξ, or

$$N_\xi = \int_1^\xi (D_\cdot N) d\xi \qquad (6\text{-}74)$$

These density and distribution functions are shown in Figure 6-7.

97

MODAL DENSITY WITH RESPECT TO CUTOFF RATIO

$$D_\xi N = \frac{2}{\xi^3}$$

MODAL DENSITY WITH RESPECT TO CUTOFF RATIO, $D_\xi N$

N_ξ

CUTOFF

CUTOFF RATIO, $\xi = \frac{k}{k_{m\mu}}$

HIGHLY PROPAGATING MODES

MODAL DISTRIBUTION FUNCTION

$$N_\xi = 1 - \frac{1}{\xi^2}$$

MODAL DISTRIBUTION FUNCTION, N_ξ

CUTOFF RATIO, $\xi = \frac{k}{k_{m\mu}}$

Figure 6-7   Rice's Modal Density and Distribution Functions

For the purposes of this section the density and distribution functions are required with respect to the variable ζ, the reciprocal of ξ used above. The conversion is made by the change of variable rule for density functions:
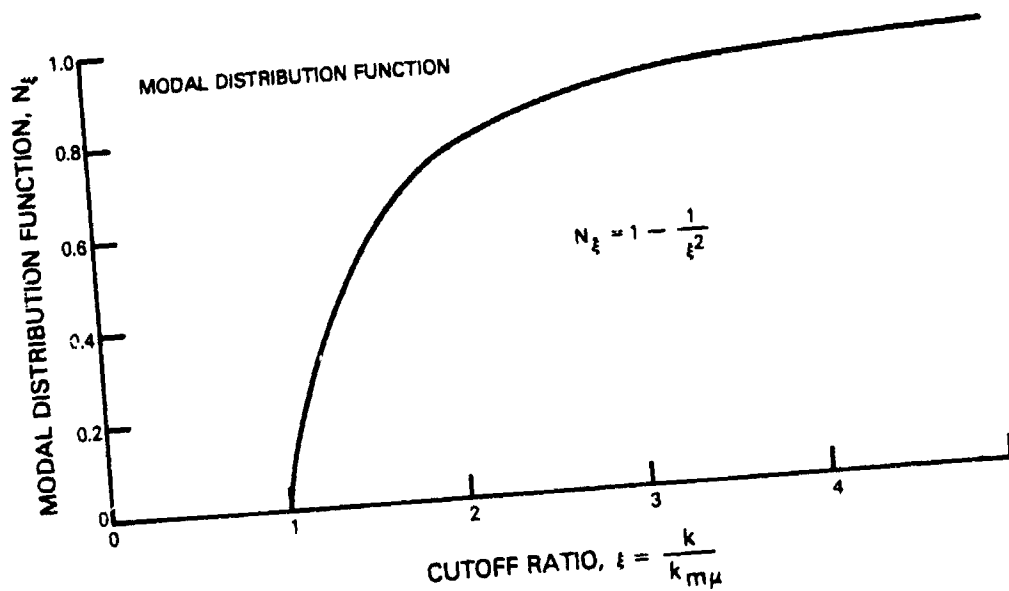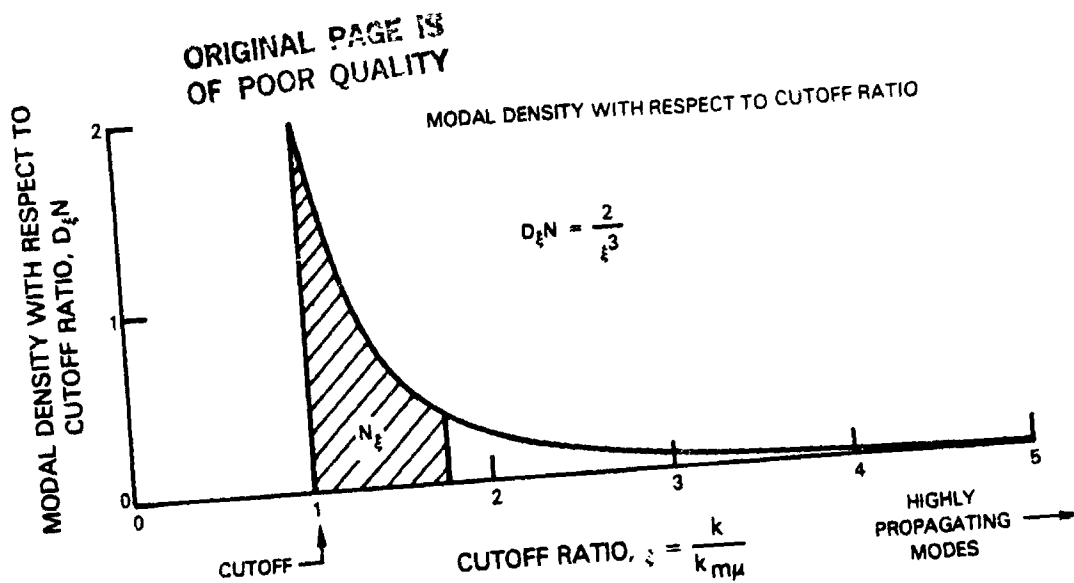
$$D_\zeta N = \frac{dN}{d\zeta} = \frac{dN}{d\xi} \left| \frac{d\xi}{d\zeta} \right| = D_\xi N \left| \frac{d\xi}{d\zeta} \right| \tag{6-75}$$

This results in

$$D_\zeta N = \frac{2}{\xi^3} \left| \frac{-1}{\zeta^2} \right| = \frac{2}{\xi^3} \cdot \xi^2 = \frac{2}{\xi} = 2\zeta \tag{6-76}$$

This density function, which is simpler than the one for cutoff ratio, is shown in Figure 6-8a, for the zero Mach number case.

Because of its linearity the density function, $D_\zeta N$, is easily modified to account for flow at axial Mach number M_x. From the wavenumber function, eq. (6-67) the cutoff point, when the radical becomes imaginary, occurs when $(1-M_x^2)\, \zeta_{m\mu}^2 = 1$. The range of ζ for propagation thus extends from zero to $\sqrt{1/(1-M_x^2)}$. This extension is shown in Figure 6-8b, together with the reduced slope of the density function, required to maintain unit area under the curve.

The cumulative distribution function, or fraction of modes with cuton ratio less than ζ is
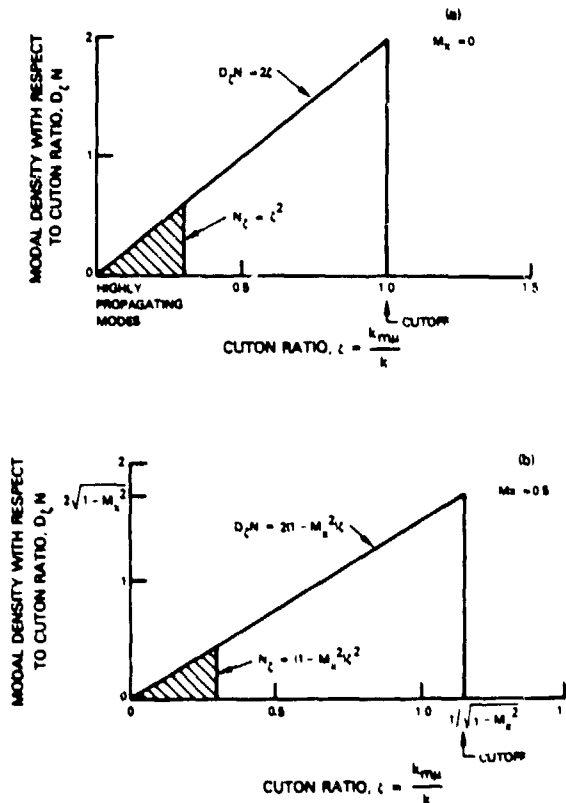

Figure 6-8   Modal Density as a Function of Cuton Ratio

$$N_\zeta = \int_0^\zeta (D_\zeta N)d\zeta = (1-M_x^2)\,\zeta^2 \qquad\qquad (6\text{-}77)$$

Now from the above relation, (N_ζ vs ζ), and from ($\tau_{m\mu}/\tau_c$ vs ζ) of Figure 6-6, the relation ($\Delta\phi$ vs ζ) is found, using $\Delta\phi = \Delta\omega\,\tau_c$ · τ/τ_c. Finally, the relations (N_ζ vs ζ) and ($\Delta\phi$ vs ζ) give the relation ($\Delta\phi$ vs N_ζ).

This relation, ($\Delta\phi$ vs N_ζ) is shown in Figure 6-9. It shows the fraction of modes having phase shifts less than or greater than selected values of $\Delta\phi$. The left hand entry is the minimum possible phase shift - all modes will exceed this value. Moving to the right side of the figure indicates the fraction of modes that will exceed successively larger phase shifts. The associated loss of signal, corresponding to LOS = 20 $\log_{10} J_0$ ($\Delta\phi$) is shown on the vertical scale to the right of the figure. Values plotted in Figure 6-9 are for the JT9D engine, and correspond to the distribution of modal delay time ratio, $\tau_{m\mu}/\tau_c$, which has been presented in Figure 6-6.

Using this distribution a table can be constructed to show what fraction of modes will undergo a loss of signal greater than a sequence of pre-selected values.

It is found, for example, that all modes have LOS greater than 0.6dB, 22% have LOS > 1dB, 7.5% have LOS > 2dB, etc. As an indication of the serious implication of such figures, suppose that a LOS of 6dB could be tolerated in a very crude test. It turns out that 2.8% of the propagating modes would have even greater loss of signal. This amounts to about 80 possible modes of twice blade passage order in the JT9D.

These distributions were determined for three fan configurations, the 10-inch P&WA fan rig, the JT9D engine, and the 21-inch NASA LeRC fan rig. (Actually, expanded logarithmic graphs were used to obtain better accuracy than the linear scales of Figure 6-9 can provide.) The following tabulation gives percent modes exceeding selected LOS for these fans (see Table 6-5). Relevant data used in the calculations is also tabulated.

A glance at the table shows two things quickly: The 10-inch rig figures seem quite satisfactory, and the 21-inch rig figures are obviously unacceptable since all modes have at least 9.6dB loss of signal. The results for the JT9D are not as black or white, but they are certainly cause for concern - if results are required within 1dB LOS, 22% of the modes will fail to meet this standard.

Some explanation of the large differences among the three rigs is helpful. From the tabulation of data it is noted that the observed speed variations of both the 10 inch rig and JT9D engine are less than + 2 rpm, whereas the 21-inch rig has a figure of + 60 rpm. The cause of this comparatively large speed variation is a result of the speed control system. Despite closely equal speed variations in the 10-inch rig and JT9D engine, the LOS results are clearly worse for the full-scale engine. This turns out to result from larger

100
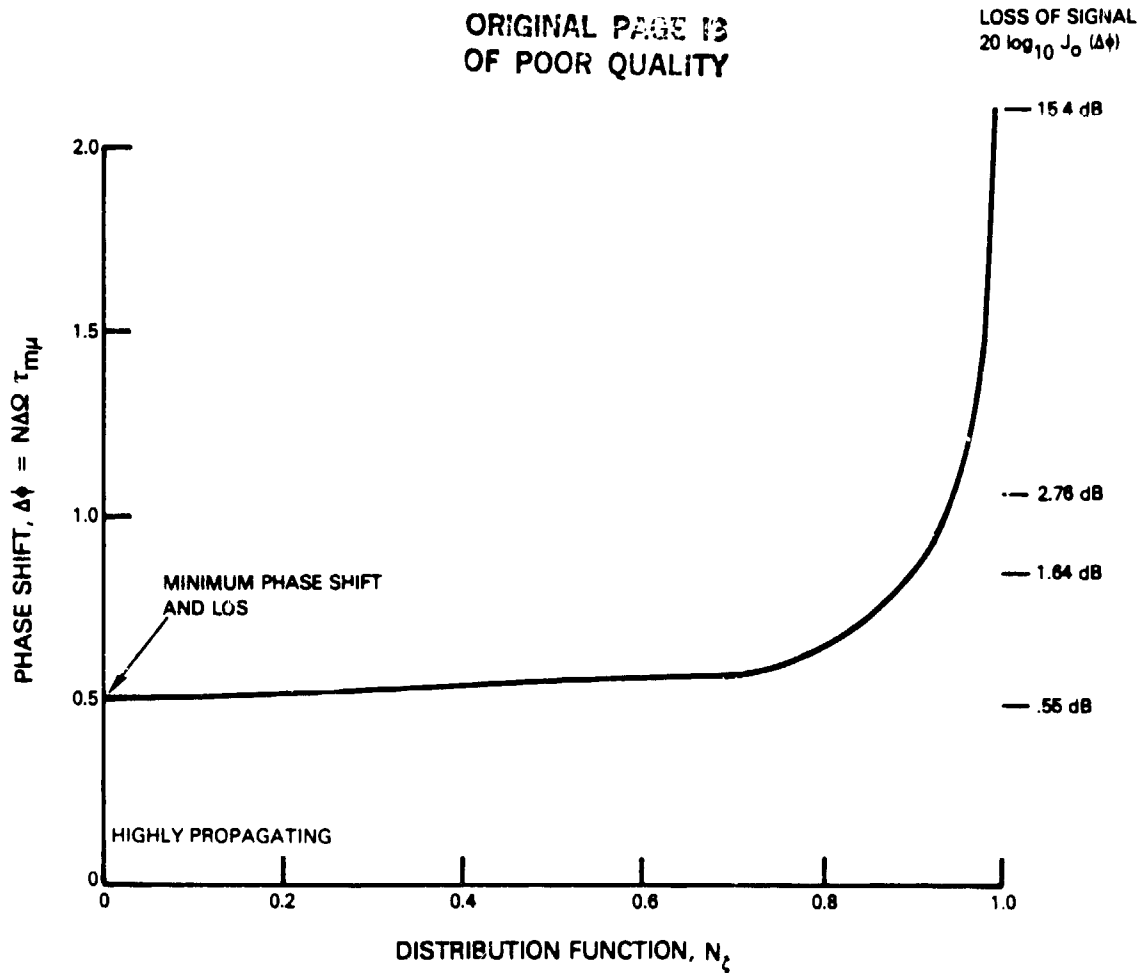
Figure 6-9   Distribution of Phase Shift and Loss of Signal

full-scale distances between fan and assumed microphone locations, but more importantly, it is due also to the difference in delay time ratio, $\tau_{m\mu}/\tau_c$, in the two fans. In the JT9D, $\tau_{m\mu}/\tau_c$ is much higher than in the 10-inch rig because both the axial Mach number and the rate of change of M_x with speed are higher.

It is concluded from this exercise that the basic traversing microphone system is likely to be satisfactory for use on the 10-inch rig, but on other rigs and engines may produce marginal or poor results, due to the effects of speed variations. (In some applications, where the dominant modes are known, and are known to have small delay times, the effects of speed variations will not be as severe.)

There is, however, a modification that can be easily incorporated in the data processing part of the traversing microphone system that will improve the results significantly. This modification is described next in Section 6.6.

TABLE 6-5

EFFECT OF SPEED VARIATIONS ON LOSS OF SIGNAL - (LOS)
CHARACTERISTICS OF THREE RIGS

BASIC TRAVERSE SYSTEM

	Percent of Modes Exceeding LOS		
LOS	10-inch rig	JT9D (T.O.)	NASA Fan
0.5 dB	0.4%	100%	100%
1	0.2	22	100
2	< 0.1	7.5	100
3	< 0.1	4.5	100
5	< 0.1	2.8	100
(Minimum LOS)	0.002 dB	0.6 dB	9.6 dB

DATA

Speed Variation Observed	$\pm$ 1.5 rpm	$\pm$ 1.25 rpm	+60 rpm
Speed Variation Used	1.5x1.5	1.25x1.5	60x1
Distance	0.61m (2 ft)	1.52m (5 ft)	0.79m (2.6 ft)
M_x	0.1	0.56	0.31
rpm	6000	3400	12,000
order (2BPF)	64E	92E	56E

6.6 COMPENSATION FOR SPEED VARIATIONS

A simple modified procedure for reducing the effects of speed variation will now be described.

Unuer a general type of speed variation, from eq. (6-22), eq. (6-23), and eq. (6-24), and using uniform weighting, the modal pressure of target n = N order has the transform:

$$Tr\left\{p_{m\mu}^{N}(t)\right\} = \frac{1}{2} C_{m\mu}^{N} \frac{1}{T} \int_{t_1}^{t_1+T} expi\left[m\theta(t)-N\gamma(t-\tau_{m\mu}^{N})\right] V_M^N(t)\ dt \qquad (6-78)$$

where the target reference signal is

$$V_M^N(t) = expi - \left[M\theta(t)-N\gamma(t)\right]$$

For the target, m = M mode, this becomes simply

$$Tr\left\{p_{M\mu}^{N}(t)\right\} = \frac{1}{2} C_{M\mu}^{N} \frac{1}{T} \int_{t_1}^{t_1+T} \text{expi-N } \gamma(t-\mathcal{T}_{M\mu}^{N}) \cdot \text{expi N } \gamma(t) \, dt \qquad (6\text{-}79)$$

or

$$Tr\left\{p_{M\mu}^{N}(t)\right\} = \frac{1}{2} C_{M\mu}^{N} \frac{1}{T} \int_{t_1}^{t_1+T} \text{expi N}[\gamma(t)-\gamma(t-\mathcal{T}_{M\mu}^{N})] \, dt \qquad (6\text{-}80)$$

If, hypothetically, the modal delay, $\mathcal{T}_{M\mu}^{N}$, were ignorably small, (as for a highly propagating mode measured very close to its source), then the factor $[\gamma(t) - \gamma(t - \mathcal{T}_{M\mu}^{N}]$ would be essentially zero, the integrand would be constant = 1, and the transform would give $1/2\ C_{M\mu}^{N}$ with no loss of signal. This would apply to completely arbitrary histories of small speed variations. (It was confirmed by computer simulation, as reported in Section 6.4, that with zero time delay the result was unaffected by speed variations.)

It has been shown, however, that $\mathcal{T}_{M\mu}^{N}$ is not always sufficiently small in practice and that serious loss of signal is obtained. But there is another way of making the quantity $[\gamma(t)- \gamma(t-\mathcal{T}_{M\mu}^{N})]$ essentially zero: If the rotor reference signal $\gamma(t)$ were to be delayed by a time. $\mathcal{T}$, closely equal to the modal delay, the quantity in brackets would become

$$[\gamma(t-\mathcal{T})- \gamma(t-\mathcal{T}_{m\mu}^{N})]$$

and for $\mathcal{T} \approx \mathcal{T}_{M\mu}$ this would also become essentially zero, resulting in the full transform, $1/2\ C_{M\mu}^{N}$.

Accordingly, let a new target reference signal be formed to replace $V_{M}^{N}(t)$. The required signal to produce the effect described above may be denoted by $V_{M}^{N}(t,\mathcal{T})$ and is defined by

$$V_{M}^{N}(t,\mathcal{T}) = \text{expi} - [M\theta(t)-N\ \gamma(t-\mathcal{T})] \qquad (6\text{-}81)$$

Note that t is replaced by $(t - \mathcal{T})$ only in the rotor angle signal $\gamma(t)$, and not in the microphone angle signal, $O(t)$. The delayed rotor angle signal $\gamma(t-\mathcal{T})$ is obtained from the digitized, direct rotor signal by time-shifting in the computer program that executes the transform.

With the modified target signal, eq. (6-81), the transform becomes

$$\mathrm{Tr}\left\{ p_{M\mu}^{N}(t)\right\} = \frac{1}{T} \int_{t_1}^{t_1+T} p_{M\mu}^{N}(t) \cdot V_M^N(t,\tau)\, dt$$

$$= \frac{1}{2} C_{M\mu}^{N} \frac{1}{T}\int_{t_1}^{t_1+T} \mathrm{expi}\; N\;[\,\gamma(t-\tau)-\gamma(t-\tau_{M\mu}^{N})\,]dt \qquad (6\text{-}82)$$

If it were possible to know the value of $\tau_{M\mu}^{N}$ then τ could be assigned an equal value and the result of performing the transfo m eq. (6-82) would be exactly the desired quantity, $1/2\; C_{M\mu}^{N}$. In practice, the $\tau_{M\mu}^{N}$ can at best be estimated approximately due to uncertainty of source location, unknown aerodynamic delays, and other factors. It is therefore necessary to evaluate eq. (6-82) when τ and $\tau_{M\mu}^{N}$ differ by some amount, $\Delta\tau_{M\mu}^{N}$.

Replacing $\gamma(t-\tau)$ and $\gamma(t-\tau_{M\mu}^{N})$ in eq. (6-82) by their expansions in terms of speed, eq. (6-26), gives

$$\mathrm{Tr}\left\{p_{M\mu}^{N}(t)\right\} = \frac{1}{2}C_{M\mu}^{N} \frac{1}{T}\int_{t_1}^{t_1+T} \mathrm{expi}\; N\left\{[\gamma(t)-\tau\Omega(t)]-[\gamma(t)-\tau_{M\mu}^{N}\Omega(t)]\right\}dt$$

$$= \frac{1}{2} C_{M\mu}^{N} \frac{1}{T}\int_{t_1}^{t_1+T} \mathrm{expi}\; [N\Omega(t)(\tau_{M\mu}^{N}-\tau)]dt$$

or

$$\mathrm{Tr}\left\{p_{M\mu}^{N}(t)\right\} = \frac{1}{2} C_{M\mu}^{N} \frac{1}{T}\int_{t_1}^{t_1+T} \mathrm{expi}\;[N\Omega(t)\,\Delta\tau_{M\mu}^{N}]\, dt \qquad (6\text{-}83)$$

where $\qquad \Delta\tau_{M\mu}^{N} = \tau_{M\mu}^{N} - \tau \qquad\qquad\qquad (6\text{-}84)$

Then, if eq. (6-29), i.e., $\Omega(t) = \Omega_0 + f(t)$

$$\mathrm{Tr}\left\{p_{M\mu}^{N}(t)\right\} = \frac{1}{2} C_{M\mu}^{N}\,\mathrm{expi}\;(N\Omega_0\,\Delta\tau_{M\mu}^{N})\,\frac{1}{T}\int_{t_1}^{t_1+T} \mathrm{expi}\;(N\,f(t)\,\Delta\tau_{M\mu}^{N})dt \qquad (6\text{-}85)$$

This is the same result as given by eq. (6-31) except that $\tau_{M\mu}^{N}$ has now been replaced by the (presumably) smaller quantity $\Delta\tau_{M\mu}^{N} = \tau_{M\mu}^{N} - \tau$.

Consequently, the results of the previous section, 6.5, apply directly to the modified transform, except that smaller $\Delta\tau_{M\mu}^{N}$ replace the original $\tau_{M\mu}^{N}$ delays, and result in less severe loss of signal.

For all types of speed variations treated analytically (drift, sawtooth wave, sinusoidal) the appropriate expression from which LOS can be obtained, (the transform for m=M, n=N) is now evaluated with $\Delta\tau^N_{M\mu}$ replacing the original $\tau^N_{M\mu}$. Specifically, for sinusoidal speed variations which were used to estimate performance of 3 fan configurations, the loss of signal is given by

$$J_0(\Delta\phi) = J_0(N\Delta\Omega\,\Delta\tau^N_{M\mu}) \qquad (6-86)$$

To determine the improvement that incorporation of a compensating time delay makes in the LOS for the 3 fan configurations of Table 6-5, it is unnecessary to repeat the detailed calculations that were involved. A simple procedure will give the result, as is now illustrated for the case of the JT9D.

Referring to Figure 6-9, giving the phase shift and LOS distribution function for the JT9D, it is seen that at the left hand side there is a minimum phase shift of 0.50 radians. Highly propagating modes sustain this shift, and for modes nearer cutoff the shift and LOS are larger, as shown. If now a compensating time delay were inserted in the rotor reference signal that would produce this same 0.50 shift, then the resulting minimum shift would be reduced to zero. Highly propagating modes would sustain essentially no loss of signal. However, modes nearer cutoff would still be attenuated at reduced amounts.

This procedure can be improved to benefit a larger number of modes if a desired limit of LOS is established by overcompensating the time delay. For example, suppose it is required that the loss of signal not exceed 1dB. (Table 6-5 shows that without compensation 22% of the modes fail this requirement). One decibel corresponds to $J_0(\Delta\phi) = 0.890$, which corresponds to $\Delta\phi = +0.67$. If a delay of τ is selected such that $\Delta\phi = N\Delta\Omega(\tau^N_{M\mu} - \tau) = -0.57$ for the highest propagating modes, then these modes are shifted -0.67 radians, giving LOS = 1dB. Now, however, for modes approaching cutoff, the phase shift increases toward zero, reducing LOS. At some fraction of propagating modes the LOS becomes zero. For modes still closer to cutoff the phase shift turns positive, until, when $\Delta\phi = +0.67$ the 1dB limit is reached. This point determines the new, much larger range of modes satisfying the 1dB LOS requirement.

Figure 6-10 illustrates this modification and shows that now only 1.4% of the modes will have LOS greater than 1dB, versus 22% with no compensation. This procedure can be repeated to determine the fraction of modes exceeding other values of loss of signal.

Table 6-6 shows the result of incorporating such time delays in the reference rotor signal for the three fan rigs. The uncompensated figures, taken from Table 6-5 are included to make comparison more convenient. (Compensation for the 10-inch rig was considered unnecessary.)
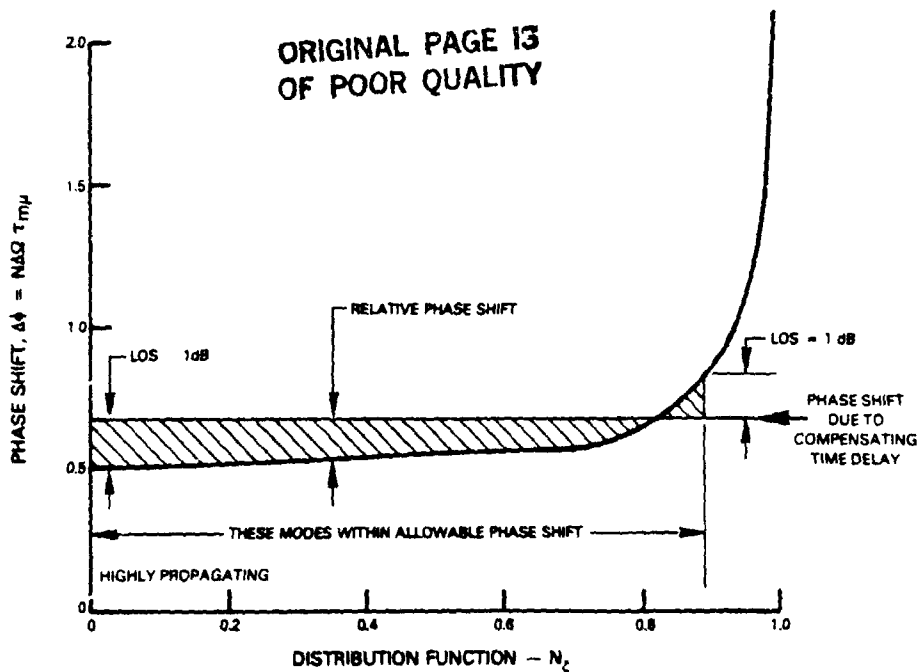
Figure 6-10   Effect of Compensating Time Delay in Reference Signal on Phase
Shift and LOS

TABLE 6-6

EFFECT OF SPEED VARIATIONS ON LOSS OF SIGNAL (LOS)
WITH AND WITHOUT TIME DELAY

BASIC TRAVERSE SYSTEM

	Percent of modes exceeding LOS		
LOS	10-inch rig.	JT9D (T.O.)	NASA Fan
0.5 dB	0.4%	100%	100%
1	0.2	22	100
2	0.1	7.5	100
3	0.1	4.5	100
6	0.1	2.8	100
(Minimum LOS)	0.002 dB	0.6 dB	9.6 dB

SYSTEM WITH TIME - DELAYED ROTOR SIGNAL

0.5 dB		2.5%	26%
1		1.4	18.5
2		0.7	12.5
3		0.5	9.5
6		0.3	6

While the potential user of the traversing microphone system must decide whether his fan results are completely satisfactory, it is clear from Table 6-6 that use of a compensating time delay in the rotor reference signal results in a marked improvement of the results. The table also illustrates the large differences possible among fan rigs and engines.

Further development of the use of compensating time delays is beyond the scope of the current program. However, it is easy to appreciate, in the light of the large improvement produced by use of a single, common, time delay applied to all target modes, that a more elaborate compensation procedure that employs several compensating delays in sequence is worth further study. The results given above suggest that such a modification could probably be developed to give further significant improvement.

6.7 SUMMARY OF SYSTEM CHARACTERISTICS - VARIABLE SPEED

Analytical and computer-aided studies have been conducted to determine the effects of departures from normal, constant rotor and traverse speed operation. Major findings are summarized below.

- Significant variations in microphone traverse speed were found to have negligible effect upon the accuracy of the traversing microphone system outputs.

- For highly propagating modes, measured close to the source, so that propagation time delays are negligible, the effects of significant rotor speed variations are negligible.

- On the other hand, for modes nearer cutoff and/or measured farther from the source, rotor speed variations produce two effects that seriously affect measurement accuracy: (1) Attenuation of the target mode measured amplitude, called "loss of signal", (LOS), (2) "Contamination" of the target mode signal reading by neighboring, off-target modes.

- These two adverse effects were studied for a variety of types of speed variation, including linear drift, sawtooth wave variation, square wave and sinusoidal variations. The precise loss of signal and contamination depend on details of the variation, but in all cases are functions of the magnitude of the deviations from constant speed during the run and the modal time delay.

- It was found that contamination of the target signal by neighboring modes could be reduced to satisfactory levels by employing two procedures in the system: (1) Hamming weighting should be used in data processing to reduce system response to neighboring modes, (2) traverse speeds that are as high as convenient (without exceeding an upper bound discussed earlier) should be used to separate the modal frequencies so that frequency shifts due to varying speed do not intrude on the response function for the target mode.

- The above measures do not improve the loss of signal, however. In order to evaluate the severity of this LOS problem in practice, an analysis of how the loss of signal affects the different modes (from those near cutoff to highly propagating modes) was performed. The analysis centered on the modal time delay - the time between initiation of a speed change and its reception at the traversing microphone plane, and how the number of modes is distributed with respect to time delay.

- Knowing the modal distribution with respect to delay time, and how LOS is related to delay, the fraction of modes that will be subject to varying LOS was computed for three test vehicles: (1) the P&WA 10-inch fan rig, (2) the JT9D engine, (3) the 21-inch NASA-LeRC fan rig. Using information about speed variations for each of these machines, the fraction of modes that would undergo LOS greater than 0.5, 1, 2, 3, and 6dB was determined. Results range from satisfactory on the 10-inch rig to clearly unsatisfactory on the 21-inch rig, with the JT9D results being open to judgment depending on the use to which they would be put.

- It was found that a simple modification of the basic traversing microphone system could improve the results significantly. The modification consists of inserting a compensating time delay in the rotor reference signal during the data processing. It was found that if the reference delay is set equal to the time delay for a specific mode that the mode can be recovered with no loss of signal. In addition, all modes will have improved recovery if some compensating delay is employed. Further, by selecting several appropriate time delays, the fraction of modes exceeding allowable loss of signal can be reduced significantly, thus increasing the chances of obtaining satisfactory results on all three test vehicles.

- On the basis of these results it is reasonable to expect that a more elaborate modified method, using more than a single compensating delay, can be developed with further effort, so that accurate modal measurements can be made on rigs and engines having large speed fluctuations.

ORIGINAL PAGE IS
OF POOR QUALITY

7.0 PLAN FOR FURTHER DEVELOPMENT

Development of the traversing microphone concept into a workable system for mode measurement on a variety of engines and rigs was initially visualized as a three-phase program. The firs' 'hase, which is the subject of the current program, reported here, was intended to determine the feasibility of the basic method, and to uncover problems that were not known at the initiation of this phase of the program. It was known initially that speed variations could be a serious problem, but it was decided to defer development of suitable corrective modifications until the second phase of the overall program. Phase two was intended to develop, by analytical and computer-aided studies, the required system modifications to handle speed variation effects, and also to resolve other problems that were disclosed in the phase one program.

It was initially visualized that if the current phase one program turned up an unanticipated major problem with the basic traversing microphone method, for which no solution seemed forthcoming, the method would be judged unfeasible and the program would be terminated at that point. The initial plan contemplated proceeding with the second phase if the basic method was deemed feasible. If the results of the phase two study were satisfactory - that is, if a satisfactory modified procedure for handling reasonably large speed variations were to be developed, then phase three would be initiated. Phase three would cover extensive mode measurement tests on a suitable fan rig and would lead to operable instrumentation, traverse hardware, and detailed operating experience with this new system. At the conclusion of this three-phase program a complete, operational, checked-out, system would be available for use on a variety of full-scale engines and fan rigs.

In accordance with this three-phase program structure, it was made a part of the current first phase effort, reported here, to establish a plan for further development if the basic method was evaluated as feasible. Since current studies have failed to disclose any unresolvable, unforseen problems, and the results of analytical and computer-simulated studies have been satisfactory, further development of the traversing microphone system is clearly warranted.

Elements of the required further development effort are describe below. In formulating a specific program plan, a selection from these items will be influenced by additional considerations, such as time and cost schedules and the availabilty of suitable fan test rigs.

1. Compensation For Speed Variations

The effect of fan speed variation on mode measurement was recognized as a potentially serious problem before the current program began, and this was confirmed by results obtained and reported here. It was also found that use of a compensating time delay in the data processing reduced the impact of this problem significantly, thus suggesting that the problem could be satisfactorily overcome with further development. The extent of the problem varies among different fan configurations, and a modified method would allow mode measurements to be attempted with confidence on a range of engines and rigs.

The basic concept for modifying the current method is to use a plurality
of compensating time delays in the data reduction. Some of these delays
will optimize recovery of certain groups of modes; other delays will
handle modes with other ranges of modal delay time. It remains to develop
this concept into a working procedure, and this is by far the largest
analytical task required for further development of the traversing
microphone method. Some questions that this task will address are: How
many such delays are needed? What values of delay time should be used? How
will the best result be recognized? Will contamination from neighboring
modes with different delay times obscure the result? What quantitative
effect does the actual time history of speed variation during the data
acquisition of the run have upon the results, and how does this affect the
details of the optimum data processing procedure? These questions can be
addressed and the modified method can be developed and checked by
analytical and computer-simulation methods. At that point a complete,
efficient computer program can be written, incorporating the experience
gained in the studies.

2. Broadband Noise Suppression

Depending on signal-to-background ratio, broadband noise can affect the
accuracy of the modal coefficient determinations. This is a well-known
matter in the field of fan noise measurement and is handled by "signal
enhancement" methods. The traversing microphone method provides such
enhancement by use of time-averaging, which is the common basis of all
enhancement procedures. As was shown here, enhancement is increased by use
of longer time averages, but the manner of determining the time required
for obtaining mode coefficients to prescribed accuracy needs further
examination. It is expected that a satisfactory procedure can be developed
by analytical studies and computer-simulated tests. There is also the
possibility of using a modification of the traversing microphone method to
obtain estimates of the detailed spectral structure of fan broadband
noise. In addition to computer-simulated tests, refinement of the method
for suppressing broadband noise (and possibly estimating its spectral
structure) would benefit greatly from actual test experience on a fan rig
with real broadband noise. For this purpose, a vehicle having closely
constant fan speed characteristics, such as the P&WA 10-inch fan rig, is
highly desirable, since the complications due to speed variation would be
absent and would not affect the broadband noise investigation.

3. Radial Mode Determination

It was found here that fewer radial microphone locations are required for
a given accuracy when the rig annulus in which the traverse is made has a
comparatively high hub-tip ratio. For low hub-tip ratios, such as with no
spinner or inner body, a larger number of radial microphone locations is
needed. It may be possible to reduce this required number by optimizing
their distribution across the duct radius, and to thus make easier the
task not only of maintaining microphones, but also to reduce the digitizer
and recorder channel capacity requirements. Further investigation of
optimum radial microphone locations and algorithms for extracting the
radial mode components corresponding to the circumferential modes should
be a part of further program development effort.

It should be a part of the next phase of the development program to evolve detailed plans for test and evaluation of the modified method on a fan rig. Further, if a suitable fan rig and measurement equipment are available, it would be advisable to proceed with initial, exploratory tests before awaiting completion of the analytical and computer-simulated studies of items 1, 2, and 3, above are completed. The following items address this aspect of the development plan.

4.   Selection of Fan Rig For Evaluation of the Method

While the objective of the overall program is to develop a mode measurement system for use in a variety of rigs and full-scale engines (including, ultimately, flight test operation) there are obvious advantages to using a convenient, versatile, accurately controlable fan rig for the development phase of the traversing microphone system. Some important features of the test rig are listed below.

● In normal operation, the speed characteristic should be sufficiently constant so that the effects on mode measurement of its small variations can be confidently predicted by calculation to be negligible.

● The rig must also be suitable for obtaining mode measurements using conventional, fixed microphone methods, to provide a basis for comparing the traversing system results.

● There should be a means for deliberately varying rig speed to simulate larger speed variations that will be encountered in some other rig and engine applications. This controlled speed variation capability is desirable to evaluate the modified delay-compensated method that will be developed.

● If the selected fan test rig normally operates with significant speed variation, means for controlling operation to reduce speed fluctuation should be explored. Further, a procedure should be developed that will provide a check of the Traversing Microphone System results under these conditions.

● .ne r.. should have the operational flexibility to accommodate change. in mode-generating stator hardware in a convenient and inexpensive way, so that a variety of acoustic mode structures can be generated for measurement.

● It should be possible to vary coherent mode signal level by changing axial location of the stators. The rig should have comparatively low levels of fan broadband noise in its basic configuration, and it should be possible to raise these levels by inlet turbulence generators. These features are helpful in developing operating procedures for use of the traversing system that will ensure adequate signal enhancement over the broadband noise levels that will be encountered in practice.

● It would also be desirable to conduct some tests with the rig configured to both high and low hub-tip ratio annuli, to check out development of optimum microphone distributions across the annulus.

5. Test and Measurement Equipment

During the next phase of the development program, and after the fan rig has been selected, suitable traverse hardware and measurement system equipment must be provided. This phase will involve analytical design, to establish parameter requirements, followed by detailed design and procurement of traverse and rig hardware and selection of instrumentation items, such as microphones, shaft angle transducers, digitizers, and tape reccrder. The characteristics of the selected rig and the availability of instrumentation should be important considerations in design and selection of this equipment and instrumentation, since the program objective is to arrive at an experimental evaluation of the traversing system as expediently as possible.

6. Test Program

The last part of the Traversing Microphone System development program consists of evaluation of the method, and will be conducted after the fan rig equipment, the traverse system equipment, and the required measurement instrumentation have been installed and checked out. The test program should provide, if possible, for evaluation of the traversing system under both constant speed operation and with controlled speed variations. Mode measurement of some acoustic fields should be made by conventional fixed microphone methods to provide a check of the traverse system results. Several mode structures should be measured, some using two hub-tip ratio annuli to check optimum radial locations of the microphones. Broadband noise with several signal to noise ratios should be provided to allow evaluation of signal enhancement procedures.

It is believed that the Traversing Microphone System will be found to be an effective means for mode measurement, as a result of these tests. It is also considered essential that an experimental program of the general form described above be conducted prior to attempting measurements on a full-scale engine on which data are needed for specific application. Inevitably, during the course of the experimental evaluation, operating problems will come to light that were not predicted by analytical or computer-simulated studies. The purpose of the experimental evaluation is to disclose such problems, and solve them, before the system is needed for important engine test results.

The above description of items requiring further development is as complete as is possible to formulate at this time. It is clear that several combinations of these items may be used to formulate specific programs that are consistent with time, cost, and fan rig schedules that prevail when further work is initiated.

8.0 CONCLUSIONS

Development and an evaluation of the feasibility of the Traversing Microphone System has been made, using analytical methods and computer-simulated studies. Detailed conclusions about the system performance under constant speed operation are given at the end of Section 5. The effects of fan speed variation on the system, an important problem in all mode measurement methods, are summarized in detail at the end of Section 6. These detailed conclusions can be condensed as follows:

1. Under constant fan speed operation the Traversing Microphone System will perform satisfactorily. Mode coefficients can be obtained accurately and will not be affected by extraneous noise resulting from cutting of the traversing microphone wakes by the fan. The system also inherently provides for coherent signal enhancement to reduce the effects of broadband noise.

2. With variations of fan speed that could be encountered in some engines and fan rigs, the performance of the system could become unsatisfactory. Of three fan configurations evaluated one application of the method was satisfactory, one was completely unsatisfactory, and the other was marginally acceptable.

3. A simple modification of the basic Traversing Microphone System produced significant improvement in results when fan speed fluctuates. This modification involves using a time delay during the data processing of the microphone signal in order to match the average propagation delay time of the modes.

4. By further modifying the procedure to use a plurality of time delays it should be possible to approach the accuracy obtained under constant speed operation.

The overall conclusion of this analytical and computer-aided evaluation is that the Traversing Microphone System in its present form is suitable for use in some fan rig tests for the complete measurement of fan noise mode structure. Relatively minor refinements in the details of data processing should make the method satisfactory for use in essentially all full-scale engine and fan rig noise test programs. A plan for the required further development of the method has been prepared for guidance.

9.0 RECOMMENDATION

In view of the satisfactory results obtained in the evaluation of the
traversing microphone system, using analtyical and computer-simulated studies,
it is recommended that the system be developed for operational use in engine
and fan rig noise measurements. A plan for persuing development of the system
into a practical, experimentally verified procedure has been prepared for
guidance and is included in Section 7 of this report.

REFERENCES

1. Cicon, D. E., Sofrin, T. G., Mathews, D. C., "Improved Methods for Fan Sound Field Determination", NASA-CR-165188, January, 1981.

2. Pickett, G. F., Sofrin, T. G., Wells, R. A., "Method of Fan Sound Mode Structure Determination - Final Report", NASA-CR-135293, August 1977.

3. Gorton, R. E., "Facilities and Instrumentation for Aircraft Engine Noise Studies", ASME Paper No. 66-GT/N-41, March 1966.

4. Sofrin, T. G. and McCann, J. C., "Pratt & Whitney Aircraft Experience in Compressor Noise Reduction", Acoustical Soc. Amer. 72nd Meeting, Los Angeles, California, November 1966.

5. Mugridge, B. D., "The Measurement of Spinning Acoustic Modes Generated in an Axial Flow Fan", J. Sound and Vibration, 10(2), 1969, pp. 227-249.

6. Bolleter, U. and Chanaud, R. C., "Propagation of Fan Noise in Cylindrical Ducts", J. Acoustical Soc. Amer. Vol. 49, No. 3, (Part 1), 1971.

7. Moore, C. J. "In-Duct Investigation of Subsonic Fan 'Rotor Alone' Noise", J. Acoustical Soc. Amer., Vol. 51, No. 5, (Part 1), 1972.

8. Bolleter, U. and Crocker, M., "Theory and Measurement of Modal Spectra in Hardwall Cylindrical Ducts', J. Acoustical Soc. Amer., Vol. 51, No. 5 (Part 1), 1972.

9. Plumblee, H. E., Dean, P. D., Wynne, G. A., and Burrin, R. H., "Sound Propagation in and Radiation from Acoustically Lined Ducts: A Comparison of Experiment and Theory", NASA CR-2306, October 1973.

10. Kraft, R. E. and Posey, J. W., " A Preliminary In-Duct Measurement of Spinning Modes in the Inlet of a Rotating Vehicle", Acoustical Soc. Amer., 91st Meeting, Washington, D. C., April 1976.

11. Sofrin, T. G., "Some Modal-Frequency Spectra of Fan Noise", AIAA paper No. 81-1990 October, 1981.

12. Moore, C. J., "Measurement of Radial and Circumferential Modes in Annular and Circular Fan Ducts", Journal of Sound & Vibration, 62(2) p. 235-56, 1979.

13. Bendat, J. S., and Piersol, A. G., " Random Data: Analysis and Measurement Procedures", Wiley-Interscience, 1971.

14. Goldman, S., "Frequency Analysis, Modulation, and Noise", Dover, 1967.

15. Rice, E. J., "Modal Density Function and Number of Propagating Modes in Ducts", NASA TMX 73539, November, 1976.

16. Pickett, G. F., Sofrin, T. G., Wells, R. A., "Method of Fan Sound Mode Structure Determination Computer Program User's Manual Microphone Location Program," NASA-CR-135294, August 1977.

17. Pickett, G. F., Sofrin, T. G., Wells, R. A., "Method of Fan Sound Mode Structure Determination Computer Program User's Manual Modal Calculation Program," NASA-CR-135295, August 1977.

APPENDIX A - NOTATION

English Symbols

a	acceleration of fan (radians/sec^2) constant
a	inner radius of annular duct
a, b	coefficients of Mach number variation
B	number of fan blades
B^n	signal coefficient of microphone wake-rotor interaction noise
BPF	fan blade passage frequency
b	outer radius of annular duct
C_k	complex amplitude coefficient
C_{ℓ}^n	coefficient of microphone wake-rotor interaction pressure
C_M^N	coefficient of target mode, order N
C_m^n, $C_m^n(r_i)$	coefficient of m-mode, order n
$C_{m\mu}^n$	coefficient of (m,μ) circumferential-radial mode, order n
c	speed of sound
$D_{\zeta} N$	density function with respect to cuton ratio
$D_{\xi} N$	density function with respect to cutoff ratio
dif(z)	function defined by eq. (5-3)
diff(z)	function defined by eq. (5-4)
E(z)	expected value of z
$E_{m\mu}$, $E_{m\nu}$	radial mode eigenfunction
expi(z)	complex exponential function, e^{iz}
f	frequency (Hz)
f(t)	variable part of fan speed
Δf	frequency difference

117

English Symbols

$G(t)$ $\displaystyle\int_0^t g(t)\,dt$

q arbitrary multiple of fan speed

$g(t)$ variable part of microphone speed

$Ham(z)$ function defined by eq. (5-9d)

$Hamm(z)$ function defined by eq. (5-9b)

I number of microphone radial locations

i $\sqrt{-1}$

$J_m,\ J_q$ Bessel function of first kind, order m or q

k wave number ω/c

k index

$k_{m\mu},\ k_{m\nu}$ eigenvalue for (m,μ) mode

$k_x,\ k_{xm\mu}$ axial wave number for (m,μ) mode

L_0 extent of microphone traverse

LOS loss of target mode signal

ℓ number of cycles of speed variation/revolution

ℓ spatial harmonic of microphone wake

M target circumferential mode index

M_x axial Mach number of flow in duct

ΔM mode difference $(m-M)$

m circumferential mode index

N target order

N fraction of propagating modes

N_1 fan speed (rps)

N_ζ distribution function with respect to cuton ratio

English Symbols

N_ξ	distribution function with respect to cutoff ratio
n	order or multiple of fan speed
$P(t)$, $P(x,t)$	complex pressure
$p(t)$	acoustic pressure $= \mathrm{Re}\{P(t)\}$
$p^n(t)$	pressure of the nth harmonic
$p^n_\ell(t)$	pressure due to interaction of microphone wake with rotor
$p^N_m(t)$	pressure of mth circumferential mode, order N
$p^n_{m\mu}(t)$	pressure of (m,μ) mode, order n
Q	number of digitized points in run
$Q_{m\mu}$	eigenvalue for (m,μ) mode
R	number of revolutions of traversing microphone
Re	real part of
$R(\tau)$	autocorrelation function
r, r_i	microphone radial coordinate
$r(t)$, $r(t_q)$	random noise function
$S(m,\omega)$	modal power spectral density function of random noise field
$S(\omega')$	power spectral density of traversing microphone signal
T	run or analysis time
$Tr\{\}$	transform of quantity $\{\}$
t, t_q	time
Δt	$t_{q+1} - t_q$ time increment
Δt	T/Q
U	number of propagating radial modes
V, V_K, V^N_M	target signal

APPENDIX A - NOTATION (Cont'd)

English Symbols

$V_M^N(t)$	target signal
V_g, $V_{gm\mu}$	group velocity for (m,μ) mode
V_p, $V_{pm\mu}$	phase velocity for (m,μ) mode
W, $W(t)$	transform weighting function
x	axial distance from rotor to microphone plane
y, y_b, y_d, y_i	alternative designations for transform
Y_m	Bessel function of the second kind, order m

Greek Symbols

β	parameter $= \Delta fT$
Γ, $\Gamma(t)$,	microphone rotation speed (rad/sec)
Γ'	microphone rotation speed (revs/sec)
Γ_0	mean microphone speed
γ, $\gamma(t)$	fan shaft angle
ζ	cuton ratio $k_{m\mu}/k$
θ, $\theta(t)$	microphone angle
Λ	normalizing factor, defined by eq. (4-8)
μ	radial mode index
ν	target mode index
ν	circular frequency of fan speed variation
ν'	frequency of fan speed variation
ξ	cutoff ratio $k/k_{m\mu}$
τ	time delay
τ_c	time delay at sound speed
$\tau_{m\mu}^n$, $\tau_{m\mu}$	time delay for (m,μ) mode
ϕ	phase angle

APPENDIX A - NOTATION (Cont'd)

Greek Symbols

$\Delta\phi$	phase shift
$\psi_{m\mu}$	eigenfunction
$\Omega,\ \Omega(t)$	fan shaft speed
Ω_0	mean fan shaft speed
$\Delta\Omega$	amplitude of fan speed variation
ω	circular frequency = $2\pi f$
ω_0	mean frequency
ω'	frequency in rotating coordinate system
$\Delta\omega$	frequency difference
ω_m^n	frequency of m mode, nth order, in rotating coordinates

Indices

i

k

K

ℓ

m

n

q

μ

ν

Symbols

$\star$	complex conjugate

APPENDIX B

COMPUTER PROGRAM DESCRIPTION

While the development of computer programs was required to complete the objectives of this contract, delivery of these computer programs and associated user's manuals was not specifically requi.ed by the contract. For this reason no detailed Fortran listings or flow charts are provided in this report. This appendix was included, however, to describe the programs developed in sufficient detail to provide the interested reader with the basis for construction of his own programs.

The computing .ffort required under the contract was divided into four tasks for convenience:

1. simulation of circumferential mode coefficients, C_m^n, from assumed circumferential-radial mode coefficients, $C_{m\mu}^n$, for a set of radii, r_i;

2. reduction of the C_m^n (r_i) to retrieve the original set of $C_{m\mu}^n$ including the effects of deliberately introduced errors, if any;

3. simulation of the pressure-time history that would be measured by a circumferentially traversing microphone, from values of C_m^n which were given assumed values, usually $1 + i0 = 1\underline{/0^\circ}$, or values derived from 1. above;

4. reduction of the pressure-time history of 3. above, to retrieve the original input values of C_m^n including the effects of any deliberate errors.

The first two tasks were performed with separate but similar computer programs called "Radial Mode Program Simulation" and "Radial Mode Program - Reduction." The last two tasks were performed using a combined program called the "Circumferential Mode Program." The program descriptions which follow assume constant speed operation of both the traverse mechanism and rotor and also assume a rectangular weighting window for the discrete Fourier transform. In general, modifications were made to the Fortran code, as required, to study the various deviations from ideal operating conditions discussed in the main body of this report. The methods used for the various simulations should be clear from the text.

RADIAL MODE PROGRAM - SIMULATION

Algorithm

The algorithm used to obtain the circumferential mode coefficients was described in Section 3, eq (3-16) and (3-17);

$$C_m^n(r_i) = \sum_{\mu=0}^{U-1} C_{m\mu}^n \cdot E_{m\mu} (k_{m\mu} \cdot r_i)$$

and $\quad E_{m\mu} = J_m (k_{m\mu} \cdot r_i) + Q_{m\mu} Y_m (k_{m\mu} \cdot r_i)$

Here J_m and Y_m are Bessel functions of the first and second kinds and the $k_{m\mu}$ and $Q_{m\mu}$ are obtained by solving two simultaneous equations which require that the pressure function satisfy the hardwall boundary condition at the duct outer wall and also at the duct inner wall if there is one.

A series of computer subroutines to evaluate the E function was developed under contract NAS3-20047 and reported in Reference 2. A detailed description and listing of the computer programs which perform the evaluation is included in related References 16 and 17. Subroutines were taken from these references and a main program was written to read and write required parameters and initiate the computation. The subroutines and function subprograms taken from the references and used for the simulation program were BESJ, BESL1, BESL2, BESY, BLOCK DATA, EMUCAL, FALZIP, KMUCAL, and KQCAL.

Input

The following is a list of inputs used for the radial mode simulation program

    Number of Radii, NR
    Number of (m, μ) values (n must be constant for each run), ND
    Hub-Tip Ratio, σ
    Outer Wall Radius, b
    Vector of Radii where C_m is Desired, R_i i = 1 ... NR
    Circumferential Mode Number, m
    Vector of Radial Modes, μ_j, j = 1 ... ND

Output

The following is a list of outputs from the radial mode simulation program;

    Eigenvalues at each μ_j, $(k_{m\mu})_j$, $(Q_{m\mu})_j$
    $E_{m\mu}(r_i)$ i = 1 ... NR
    $C_m(r_i)$ i = 1 ... NR

This output can be used as input to the reduction part of the Radial Mode deck with or without modification to determine effects of errors of the circumferential mode coefficients C_m^n on the final circumferential-radial coefficients, $C_{m\mu}^n$. Optionally this output could also be used as input to the Circumferential Mode Program.

124

RADIAL MODE PROGRAM - REDUCTION

Algorithm

The algorithm used in the Radial Mode-Reduction program was based on Reference 12 and is discussed in the text of this report leading to eq. (4-10).

$$\sum_{i=1}^{I} C_m^n (r_i) \; r_i \; E_{m\nu} (k_{m\nu} \cdot r_i)$$

$$\sum_{\mu=0}^{U-1} c_{m\mu}^n \left[\sum_{i=1}^{I} r_i \; E_{m\mu}(k_{m\mu} \cdot r_i) \; E_{m\nu} (k_{m\nu} \cdot r_i) \right]$$

This equation can be written in the matrix form $y = Ax$ and is written out below for two radial modes, 0 and 1.

$$y = \begin{bmatrix} \sum_i C_m^n (r_i) \cdot r_i \cdot E_{m,0} (k_{m,0} \cdot r_i) \\ \sum_i C_m^n (r_i) \cdot r_i \cdot E_{m,1} (k_{m,1} \cdot r_i) \end{bmatrix}$$

$$A = \begin{bmatrix} \sum_i r_i \cdot E_{m,0} (k_{m,0} \cdot r_i) \cdot & \sum_i r_i \cdot E_{m,0} (k_{m,0} \cdot r_i) \cdot \\ E_{m,0} (k_{m,0} \cdot r_i) & E_{m,1} (k_{m,1} \cdot r_i) \\ \hline \sum_i r_i \cdot E_{m,1} (k_{m,1} \cdot r_i) \cdot & \sum_i r_i \cdot E_{m,1} (k_{m,1} \cdot r_i) \cdot \\ E_{m,0} (k_{m,0} \cdot r_i) & E_{m,1} (k_{m,1} \cdot r_2) \end{bmatrix}$$

$$x = \begin{bmatrix} c_{m,0}^n \\ c_{m,1}^n \end{bmatrix}$$

Subroutines discussed in the previous section were used to solve for the E-functions. Vector and matrix elements were then formed by summations as indicated above. The system of simultaneous equations was then solved using SIMEQC of Reference 17. This subroutine was based on an IBM subroutine which solves the equations using Gaussian elimination, but was modified to include complex variables.

A calculation was performed to evaluate the sensitivity of the solution of a set of simultaneous equations to errors in its elements. The resulting measure, called the condition number, is described in Reference 2. This number is the ratio of maximum to minimum eigenvalue of the system of equations and required for its calculation use of the following subroutines; EIGCC, EBALAC, EHESSC, ELRH1C, ELRH2C, EBBCKC, AND UERTEST. These routines are the property of International Mathematical and Statistical Libraries, Inc. of Houston, Texas (IMSL). These rented routines, however, were not required for any other portion of the programming and can be omitted if the condition number calculation is not required.

Input

Number of Radii, NR
Number of (m, μ) Diads, ND
Hub-Tip Ratio, σ
Outer Radius of Duct, b
Vector of Radii Values, R_i, i = 1 ... NR
Circumferential Mode Number, m
Vector of Radial Mode Numbers, μ_j, j = 1 ... ND

Vector of Complex Circumferential Mode Coefficients, $(C_m^n)_i$, i = 1 ... NR

Output

In order to checkout the computations, values of $k_{m\mu}$, $Q_{m\mu}$, $E_{m\mu}$, elements of the A matrix and the y vector were printed. The main result of interest, however, was the vector of $C_{m\mu}^n$ for the various values of μ , and the condition number, CN, which indicated the sensitivity of the computation to input or computer roundoff errors.

CIRCUMFERENTIAL MODE PROGRAM - SIMULATION

Algorithm

The equation used to simulate the pressure at a typical microphone location was based on eq. (4-11). The double summation over n and m indicated in the equation was replaced by a single sum over j where j is an index denoting a particular input m, n pair. With this change the simulation equation became;

$$p_i = \text{Re}\left\{\sum_j (C_m^n)_j \text{ expi } [m_j \theta_i - n_j \gamma(t - \tau_j)]\right\} + A \cdot N_i$$

where τ_j is an assumed time delay for the jth (m, n) pair (usually assumed to be zero), N is the output of a random noise generation subroutine with input standard deviation, A.

The random noise was obtained from an IBM subroutine, GAUSS, which generated a random number sequence with mean value of zero and a Guassian distribution. The subroutine is reported to produce $2^{29}/12$ or approximately 44,700,000 values before repeating.

Microphone traverse angle and rotor angle were simulated by the equations:

$$\theta_i = T t_i$$

$$\gamma_i = \Omega t_i$$

where T and Ω are the constant angular velocities of the traverse and rotor, respectively, and i is the time index.

The programming of these equations was very straight forward. Within an outer loop indexed by time there was an inner loop within which was summed the contributions of each mode. The results of the computation were a string of sets $\{ p_i, \theta_i, \gamma_i \}$ which can be thought of as going to a disk or tape which represents the simulated result of a test program. Since the use of the additional disk or tape units was not desirable for this computer study, the pressure and angle sets were processed by the reduction part of the program, described in the next section, at each instant within the outer time loop. Because of roundoff error accumulation it was found necessary to program this and the reduction portion of the Circumferential Mode Program in double precision.

Input

    Number of Time Increments, IMAX
    Number of Input (m, n) Diads, JMAX
    Time Increment Between Samples; Δt - sec
    Random Noise Standard Deviation
    Angular Velocity of Microphone
    Angular Velocity of Rotor
    Vector of Circumferential Mode Numbers, m_j, j = 1, 2 ... JMAX
    Vector of Shaft Orders, n_j, j = 1, 2, ... JMAX
    Vector of Time Delays $(\tau_m^n)_j$, j = 1, 2, ... JMAX

    Vector of Amplitudes, $(C_m^n)_j$, j = 1, 2, ... JMAX

Output

    Pressure at Each Instant of Time, p_i
    Traverse Angle at Each Instant of Time, θ_i
    Rotor Angle at Each Instant of Time, γ_i

CIRCUMFERENTIAL MODE PROGRAM - REDUCTION

Algorithm

From eq. (4-2) and (3-15) the circumferential mode coefficients were obtained by;

$$(C_M^N)_k = \frac{2}{i_{max}} \sum_i p_i \, \text{expi} \, [-M_k \theta_i + N_k \gamma_i]$$

where i is the time index and k is the index for a particular target (M, N) set.

Input

Input to this portion of the program consists of the microphone pressure at each instant of time, p_i, rotor angle at each instant of time γ_i and traverse angle at each instant of time, θ_i. A list of target (M, N) sets is also required.

Output

The output of this portion of the program consists a list of target (M, N) sets and the computed complex mode amplitudes, C_M^N. To help check out various modifications to the program values of p_i, θ_i, γ_i, $(C_m^n)_i$ were printed for various times.